NTNU – Trondheim
Norwegian University of
Science and Technology

Measurements of Harmonic Distortion in Maritime Power Systems

Runar Lahti

Master of Energy Use and Energy Planning
Submission date: June 2015
Supervisor: Lars Einar Norum, ELKRAFT

Norwegian University of Science and Technology
Department of Electric Power Engineering

Abstract

Harmonic voltage distortion is a problem becoming more and more common in maritime power systems because of the increasing use of power electronics; especially in relation to VFDs. To avoid the possibility of damage and malfunction of the components in the power system international standards and regulative organs like DNV, ABS and Bureau Veritas has defined limits for the harmonic distortion levels in the maritime power system.

This study is conducted to design a measurement system for harmonics, suitable for measurements in an offshore and maritime power system environment. The measurement system then has to be small and portable, and the requirements in the international standards IEC 61000-4-7 and IEC 61000-4-30 should be met to obtain reliable results from the measurements. The chosen measurement system is the compactDAQ system delivered by National Instruments, with processing of the measurements handled by LabVIEW, a programmable software for analysis, also delivered by National Instruments.

For the sake of interest, a method for identification of the harmonic contribution from different loads connected to the power system is proposed and applied for further analysis of the results obtained from the measurement system tests. The method tested in the study is the harmonic voltage component method. This method is applied for both voltage and current measurement analysis.

An active harmonic filter is suggested for mitigation of harmonic distortion. This filter is connected to the laboratory test system used in the study to verify the filtering effect of the filter.

All the testing is conducted on a laboratory test system. Four configurations are defined to achieve variable harmonic levels for various testing

Sammendrag

Harmonisk spenningsforvrengning er et problem som blir mer og mer vanlig i maritime kraftsystemer på grunn av den økende bruken av kraftelektronikk; spesielt i forbindelse frekvensomformere. For å unngå sannsynligheten for skade og funksjonssvikt hos komponentene i kraftsystemet har internasjonale standarder og regulative organer som DNV, ABS og Bureau Veritas definert grenser for de harmoniske forvrengningsnivåene i det maritime kraftsystemet.

Dette studiet er gjennomført for å utforme et målesystem for harmoniske egnet for målinger i offshore og maritime kraftsystemomgivelser. Målesystemet må være lite og portabelt, og kravene i de internasjonale standardene IEC 61000-4-7 og IEC 61000-4-30 bør være oppfylt for å få pålitelige resultater fra målingene. Løsningen for målesystemet er et CompactDAQ-system levert av National Instruments, hvor behandlingen av målingene håndteres av LabVIEW, en programmerbar programvare for analyse, også levert av National Instruments.

Av interesse er en fremgangsmåte for identifisering av det harmoniske bidraget fra forskjellige laster tilkoblet kraftsystem foreslått og anvendt for de oppnådde resultatene fra måletestingen. Metoden testet i studien er den harmoniske spenningskomponentmetoden. Metoden er anvendt for både spennings- og strømmålinger.

Et aktiv harmonisk filter er foreslått for reduksjon av den harmoniske forvrengningen. Filteret blir koblet til testsystemet i laboratoriumet som er anvendt i studiet for å verifisere filtrets virkning.

All testingen er utført på et testsystem i laboratorium. Fire konfigurasjoner er definert for ulike testforhold, og variasjonen i de harmoniske nivåer fra lastene.

Preface

This is my Master's thesis in Electrical Power Engineering. It concludes my 2-year education at Norwegian University of Science and Technology (NTNU) in Energy Use and Energy Planning, a MSc programme in Energy and Environmental Engineering. It also marks the end of a total of five years studying and living in Trondheim, the number 1 student city in Norway for a reason.

I want to thank my supervisor, Lars Einar Norum, for support and guidance. He was also the one introducing me to the topic of harmonic components in the electric power system at HiST during my BSc study.

Thanks to "Gullrekka" and all my other friends in Trondheim for making the stay unforgettable and probably some of the best years of my life.

Thanks to my family for helping me with motivation, guidance and other necessaries during all my years of education.

At last I want to thank Kongsberg Maritime Engineering, especially Cato Strandin, for providing me with support for my thesis work and giving me real work and experience during the education and also after the education is finished.

Runar Lahti

Trondheim, June 2015

Table of Contents

Abstract ..... **I**

Sammendrag ..... **III**

Preface ..... **V**

Table of Contents ..... **VII**

List of Figures ..... **XI**

List of Tables ..... **XIII**

Abbreviations ..... **XV**

1 Introduction **1**
1.1 Background 1
1.2 Problem description 2
1.3 Problem limitations 2

2 Harmonic distortion **3**
2.1 Definition of harmonics 3
2.2 Harmonic sources 7
2.3 Harmonic consequences 10
2.3.1 Harmonic power loss 10
2.3.2 Component malfunction 12
2.3.3 Resonance 13

3 Mitigation of harmonics **16**
3.1 Filtering 16
3.2 Active harmonic filters 19

4 Measurement system **26**
4.1 Data acquisition 26
4.1.1 Measurement categories 26
4.1.2 Isolation 28
4.1.3 Sampling theory 37
4.1.4 How to measure current and voltage 43

5 International measuring standards **47**
5.1 IEC 61000-4-7:2009 47
5.1.1 The instrument 47
5.1.2 Current input 49
5.1.3 Voltage input 49

5.2 IEC 61000-4-30:2015 49
5.2.1 Classes of measurements 49
5.2.2 Organisation of measurements 52

6 Identifying harmonic sources 52
6.1 The harmonic voltage component method 52
6.2 FIS method 56

7 Laboratory testing 59
7.1 Testing conditions 59
7.2 NI compactDAQ hardware 59
7.3 NI LabVIEW software 62
7.4 Laboratory set-up and testing procedure 67

8 Measurement results 71

9 Analysis 77
9.1 Harmonic voltage component method 77
9.2 Measurements accuracy 82
9.3 Harmonic filtering 83

10 Discussion 84
10.1 Harmonic voltage component method 84
10.1.1 Configuration 2 84
10.1.2 Configuration 3 84
10.1.3 Configuration 4 85
10.2 Harmonic current component method 85
10.2.1 Configuration 2 85
10.2.2 Configuration 3 86
10.2.3 Configuration 4 86
10.3 Measurement accuracy 87
10.4 Testing conditions 87
10.5 Harmonic filtering 89

11 Conclusion 90
11.1 Harmonic source detection method 90
11.2 Measurement accuracy 91
11.3 Harmonic filtering 91

12 Further work 92

13 Bibliography 93

Appendix A – VI front panel for configuration 1 97

Appendix B – VI front panel for configuration 2 101

Appendix C – VI front panel for configuration 3 105

Appendix D – VI front panel for configuration 4 109

List of Figures

Figure 2.1 - 3rd harmonic distortion [1] 4
Figure 2.2 - Harmonic distortion resulting in a square wave [3] 4
Figure 2.3 - Square wave with harmonic components [4] 5
Figure 2.4 - VFD equivalent circuit [1] 7
Figure 2.5 - Diode rectifier input current waveform for one phase [1] 8
Figure 2.6 - Voltage distortion due to current distortion in power system [5] 8
Figure 2.7 - Half period magnetization of transformer [6] 9
Figure 2.8 – Magnetization current of a transformer [7] 10
Figure 2.9 - Series resonant circuit 14
Figure 2.10 - Parallel resonant circuit 14
Figure 2.11 - Series resonant circuit impedance vs. frequency [1] 15
Figure 3.1 - Active filter block diagram [1] 17
Figure 3.2 - THDi levels for AC PWM drive with/without active filter [1] 17
Figure 3.3 - Parallel single tuned filters [1] 18
Figure 3.4 - Without AHF [9] 20
Figure 3.5 - With AHF [9] 20
Figure 3.6 - Shunt coupled active filter [8] 21
Figure 3.7 - Series coupled active filter [8] 21
Figure 3.8 - Single-line system of a three-phase active filter [8] 22
Figure 3.9 – 480V pure active filter [8] 23
Figure 3.10 - 480V pure active filter control system [8] 24
Figure 4.1 - Measurement categories [9] 27
Figure 4.2 - Bank-isolated analog input circuitry [12] 29
Figure 4.3 - Channel-to-earth isolation [12] 30
Figure 4.4 - Bank (channel-to-bus) isolation 31
Figure 4.5 - Channel-to-channel isolation 31
Figure 4.6 - Optical isolation [13] 33

Figure 4.7 - Capacitive isolation [13] 33
Figure 4.8 - Inductive coupling isolation [13] 34
Figure 4.9 - Analog isolation [13] 35
Figure 4.10 - Digital isolation [13] 35
Figure 4.11 - Isolation amplifier [13] 36
Figure 4.12 - Sampling of a signal [14] 37
Figure 4.13 - 2 kHz and 10 kHz sampling of 1 kHz sine wave [16] 38
Figure 4.14 - Sampled signal [16] 39
Figure 4.15 - 3-bit and 16-bit resolution [16] 39
Figure 4.16 - Aliasing [17] 41
Figure 4.17 - Sampled signal components [17] 41
Figure 4.18 - Sampled signal components and aliased components [17] 42
Figure 4.19 - Current transducer with voltage output [21] 44
Figure 4.20 - Solid core CTs [20] 45
Figure 4.21 - Split core CTs [20] 45
Figure 5.1 - Organisation of measurement 52
Figure 7.1 - National Instruments DAQ system [24] 60
Figure 7.2 - NI cDAQ-9174 [25] 60
Figure 7.3 - NI 9225 voltage module [26] 61
Figure 7.4 - NI 9227 current module [25] 61
Figure 7.5 - LabVIEW program for harmonic analysis 64
Figure 7.6 - Measurement, data storage and graphical window blocks 64
Figure 7.7 - Harmonic Distortion Analyser block 65
Figure 7.8 - Voltage and Current RMS measurements 66
Figure 7.9 - Read from Measurement File 66
Figure 7.10 - SLD of laboratory set-up 67
Figure 7.11 - Pictures from the laboratory set-up 69
Figure 7.12 - Parallel AHF arrangement [36] 70

List of Tables

Table 4.1 - Isolation type overview [13] 34
Table 5.1 - Accuracy requirements 48
Table 6.1 - Voltage values of harmonic components [22] 54
Table 6.2 - Harmonic current injected by nonlinear loads [22] 55
Table 7.1 - Module specifications 61
Table 7.2 - AHF technical details [36] 70
Table 8.1 - IHDv magnitudes for configuration 1 71
Table 8.2 - IHDv magnitudes for configuration 2 72
Table 8.3 - IHDv magnitudes for configuration 3 72
Table 8.4 - IHDv magnitudes for configuration 4 73
Table 8.5 - IHDi magnitudes for configuration 1 73
Table 8.6 - IHDi magnitudes for configuration 2 74
Table 8.7 - IHDi magnitudes for configuration 3 74
Table 8.8 - IHDi magnitudes for configuration 4 75
Table 8.9 - THDv for the configurations 75
Table 8.10 - THDi for the configurations 76
Table 8.11 - THD measurements with an AHF at PCC 76
Table 9.1 - Voltage and current components change for configuration 2 77
Table 9.2 - Voltage and current components change for configuration 3 78
Table 9.3 - Voltage and current components change for configuration 4 79
Table 9.4 - Voltage and current THD for each load individually 81
Table 9.5 - Voltage and current components for each load related to configuration 1 82

Abbreviations

NTNU	Norwegian University of Science and Technology
HiST	Sør-Trøndelag University College
VFD	Variable Frequency Drive
DNV	Det Norske Veritas
ABS	American Bureau of Shipping
IEC	International Electrotechnical Commission
DAQ	Data Acquisition
THD	Total Harmonic Distortion
THDv	Total Harmonic Voltage Distortion
THDi	Total Harmonic Current Distortion
IHD	Individual Harmonic Distortion
IHDv	Individual Harmonic Voltage Distortion
IHDi	Individual Harmonic Current Distortion
IGBT	Insulated-Gate Bipolar Transistor
AC	Alternating Current
DC	Direct Current
AFE	Active Front End
SPWM	Sinus Pulse-Width Modulation
RMS	Root-Mean-Square
AVR	Automatic Voltage Regulator
PF	Power Factor
EMI	Electromagnetic Interference
BV	Bureau Veritas
AHF	Active Harmonic Filter
PCC	Point of Common Coupling

PWM	Pulse-Width Modulation
FPGA	Field-Programmable Gate Array
ASD	Adjustable Speed Drive
NI	National Instruments
LED	Light Emitting Diode
I/O	Input/Output
ADC	Analog-to-Digital Converter
CT	Current Transformer/Transducer
ANSI	American National Standards Institute
A/D	Analog-to-Digital
FFT	Fast Fourier Transform
DFT	Discrete Fourier Transform
FIS	Fuzzy Inference System
PC	Personal Computer
USB	Universal Serial Bus
Wi-Fi	Wireless Fidelity
VI	Virtual Instrument
PQA	Power Quality Analyser

1 Introduction

1.1 Background

Maritime power systems are small, island operated systems. This makes these power systems sensitive to power quality indices, like harmonic distortion of the voltage. This is caused by an increasing use of power electronics; especially in relation to VFDs. The weak power system combined with the high rated loads utilizing the VFDs causes a high distorting effect on the voltage quality. With too high levels of harmonic voltage distortion unfavourable incidents for the equipment installed in the power system may occur. Due to this the international standards and regulation organs have regulated the harmonic distortion levels.

The levels of harmonic distortion in a power system are not always easy to calculate when a power system is designed. For projects where a redesign of the power systems is done and some old equipment is kept from the old power system, the levels of harmonics are even harder to foresee. This is the case for retrofit projects, where typically leased vessels are redesigned for different purposes between the projects they are leased for.

When the new power system is designed with old motors and other old loads, injecting unknown levels of harmonics into the maritime power system, the harmonic limits set by regulative organs can be exceeded. Due to this, equipment can be damaged, additional power loss occurs and significant functions such as navigation and communication can be affected. To avoid these problems filtering techniques can be applied. Harmonic filtering is a way of limiting the harmonic distortion, making sure the power system will work without any problems addressed to harmonic distortion, keeping the harmonic levels within the limits set by the regulation organs.

To limit the cost of the harmonic filter in a case with too high harmonic distortion measuring and identifying the harmonic contribution from the re-used and new equipment at different troubled points in the power system must be done. This way one can find the largest contributors to the harmonic distortion and limit the influence to the rest of the power system by installing a harmonic filter at the most significant harmonic source or point in the power system instead of installing larger filters at a location where it isn’t really necessary, potentially giving higher costs and taking more physical space.

1.2 Problem description

To measure and identify the harmonic injections from the different loads in the maritime power system a small and portable measurement system is needed. Analysis methods are also necessary for identifying the points in the power system where the distortion limits are exceeded and identifying the sources of the distortion.

The main purpose of this thesis is to design a measurement system for harmonic distortion that may be applied in maritime power systems, and to find a way of identifying the sources of the harmonic distortion.

1.3 Problem limitations

The measurement system will be designed for measuring the harmonic distortion levels in a maritime power system, and shall satisfy the standards for measurement instruments for this purpose.

A method for identifying the harmonic contribution from different loads connected to the system will be tested and the results analysed.

The effect of a harmonic filter will be documented to verify the filters harmonic mitigation.

All testing will be done on a laboratory test system.

2 Harmonic distortion

Harmonic distortion is in general distortion caused by non-linear loads, drawing non-sinusoidal currents and voltages from the power system. This phenomenon is an increasing problem in most power systems due to the increasing use of power electronics. The presents of too much harmonic distortion can cause equipment to malfunction or even break. Additional power losses and decreased lifetime of system components are also some of the common consequences caused by harmonic distortion [1].

2.1 Definition of harmonics

When talking about harmonic components the distorted waveform is typically seen as several individual waveforms added together to one wave. The harmonic components are sinusoidal signals with different frequency and amplitude. From (Eq. 2.1) the frequency of a harmonic component can be found. The different harmonic components of a distorted signal can be seen in Figure 2.1, where a distorted signal is divided into the fundamental signal and a third harmonic component.

$$f_n = n \cdot f_1 \qquad \text{(Eq. 2.1)}$$

$f_n = harmonic\ frequency$

$n = order\ of\ harmonic$

$f_1 = fundamental\ frequency$

The magnitudes of the harmonic components are usually lower than the fundamental component's magnitude and typically they are decreasing with the order of the components. When adding several harmonic components to each other, the resulting signal can be much distorted from the pure sinusoidal fundamental one wish to find in the power system. Figure 2.2 shows how odd numbered harmonic components from the 3rd harmonic to the 15th harmonic distort the sinusoidal fundamental component to become more like a square wave signal [2].

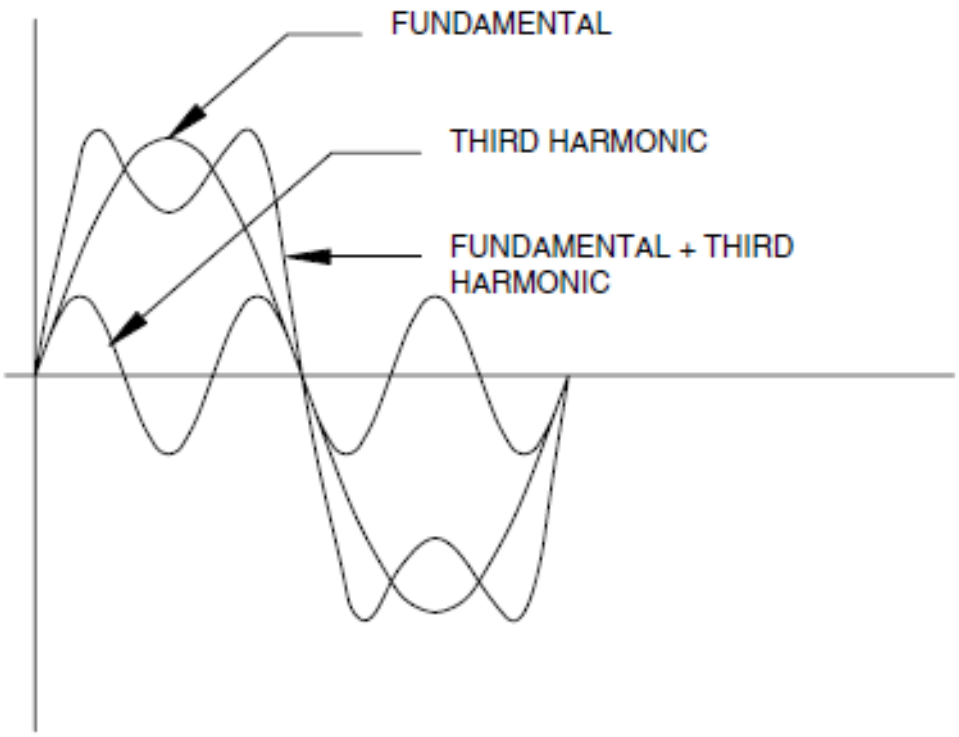

Figure 2.1 - 3rd harmonic distortion [1]

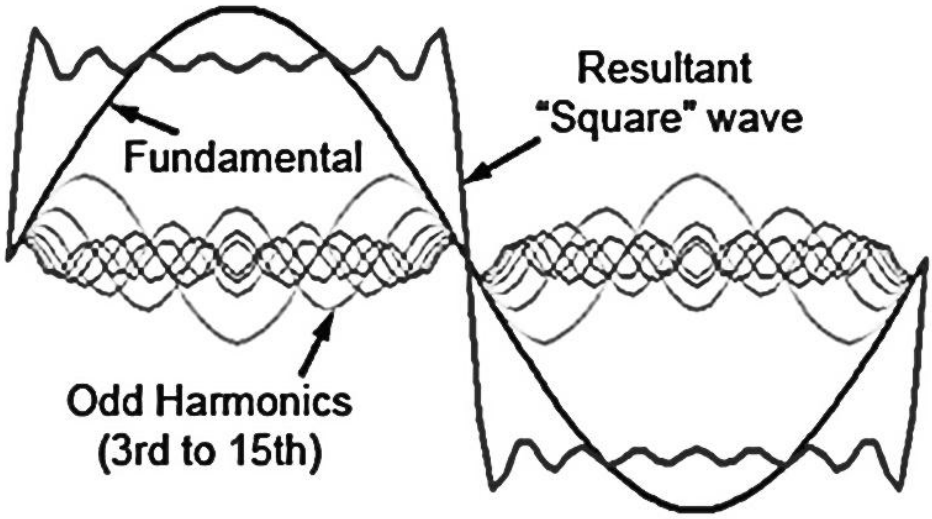

Figure 2.2 - Harmonic distortion resulting in a square wave [3]

Mathematically this division is done by the Fourier analysis of a signal, dividing a resultant signal into several smaller components. This can be seen in (Eq. 2.3), where a Fourier series has been developed for the square wave signal seen in Figure 2.3, over a period of 2L, from 0 to 2L [4].

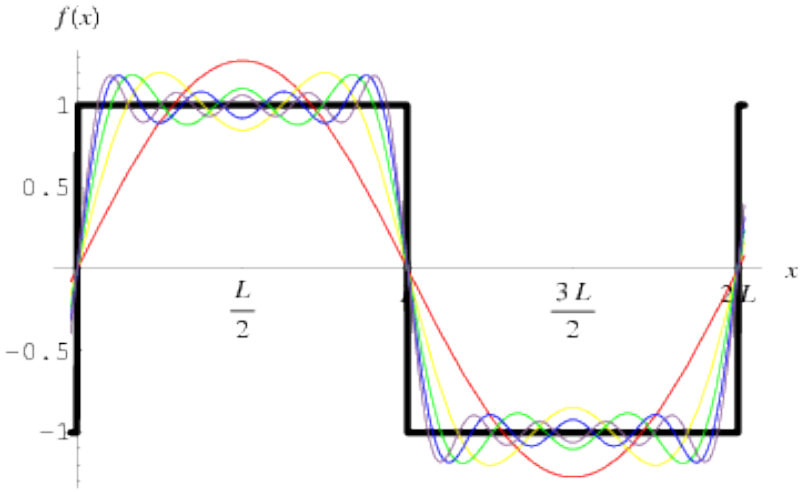

Figure 2.3 - Square wave with harmonic components [4]

Since the function is unsymmetrical round the y-axis it is an odd function. This means that

$$a_0 = a_n = 0 \qquad \text{(Eq. 2.2)}$$

$$b_n = \frac{1}{L}\int_0^{2L} f(x)\sin\left(\frac{n\pi x}{L}\right)dx \qquad \text{(Eq. 2.3)}$$

$$= \frac{2}{L}\int_0^{L} f(x)\sin\left(\frac{n\pi x}{L}\right)dx \qquad \text{(Eq. 2.4)}$$

$$= \frac{4}{n\pi}sin^2\left(\frac{1}{2}n\pi\right) \qquad \text{(Eq. 2.5)}$$

$$= \frac{2}{n\pi}[1-(-1)^n] \qquad \text{(Eq. 2.6)}$$

$$= \frac{4}{n\pi}\begin{cases}0, & n = even\\ 1, & n = odd\end{cases} \qquad \text{(Eq. 2.7)}$$

$$f(x) = \frac{4}{\pi}\sum_{n=1,3,5,\ldots}^{\infty}\frac{1}{n}\sin\left(\frac{n\pi x}{L}\right) \qquad \text{(Eq. 2.8)}$$

Harmonic components can have different frequencies. The most common ones are odd integer harmonics with a frequency higher than the fundamental frequency. Even harmonics can also occur. Harmonics with a frequency lower than the fundamental also exist, and these are known as sub-harmonics. Harmonics with a frequency that is not an integer multiple of the fundamental frequency are known as interharmonics [5].

When harmonic distortion is measured in power system the values are given in total harmonic distortion (THD) and individual harmonic distortion (IHD). The THD is the square root of all the harmonic components squared and added together, then divided by the fundamental component. This can be seen in (Eq. 2.9) and (Eq. 2.10). The IHD is one single harmonic component divided by the fundamental component as seen in (Eq. 2.11).

$$I_{H,RMS} = \sqrt{\sum_{n=2}^{\infty} I_n^2} \qquad \text{(Eq. 2.9)}$$

$I_{H,RMS} = RMS\ value\ of\ harmonic\ currents$

$I_n = n^{th}\ harmonic\ current$

$$THDi = \frac{I_{H,RMS}}{I_{1,RMS}} \cdot 100\% \qquad \text{(Eq. 2.10)}$$

To be able to find the THDv the same formulas as above can be applied, just change the current components with voltage components.

For individual harmonic components (Eq. 2.11) is used. Same as for THD, both voltage and current can be found by this formula.

$$IHD_n = \frac{I_n}{I_1} \cdot 100\% \qquad \text{(Eq. 2.11)}$$

$IHD_n = n^{th}\ harmonic\ individual\ harmonic\ distortion$

The IHD is used to tell which harmonic components that are contributing the most to the distortion of the waveform, and the THD tells how distorted the waveform is referred to the fundamental component [1].

2.2 Harmonic sources

In maritime vessels the use of power electronic converters in form of variable frequency drives (VFDs) has become very popular for motor control. This helps to regulate the motor's power input and thereby helps the vessel to become more fuel efficient, and thereby more economic and environmental friendly. The power electronics also isolates the motor's short circuit contribution reducing the transient current levels in case of a short circuit.

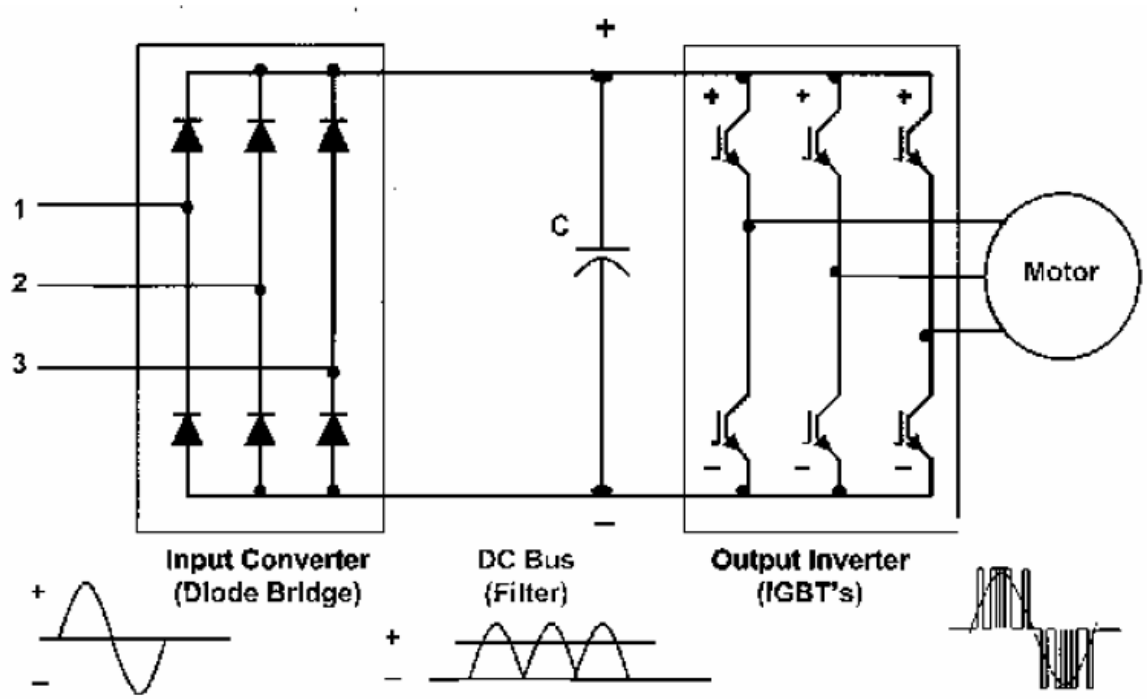

Figure 2.4 - VFD equivalent circuit [1]

A common VFD configuration is the diode bridge rectifier. This is shown in Figure 2.4. At the system side a 6-pulse diode bridge rectifier is located. In the middle there is a capacitive filter for DC smoothening, and at the output an IGBT inverter is located, controlling the motor's power consumption and the frequency.

The part of this VFD affecting the system the most is the diode bridge rectifier at the front end of the VFD. As the diodes for a 6-pulse diode bridge rectifier leads current in pulses of 60° at

a time the input current for each phase becomes as shown in Figure 2.5. This current waveform contains large magnitudes of harmonic component.

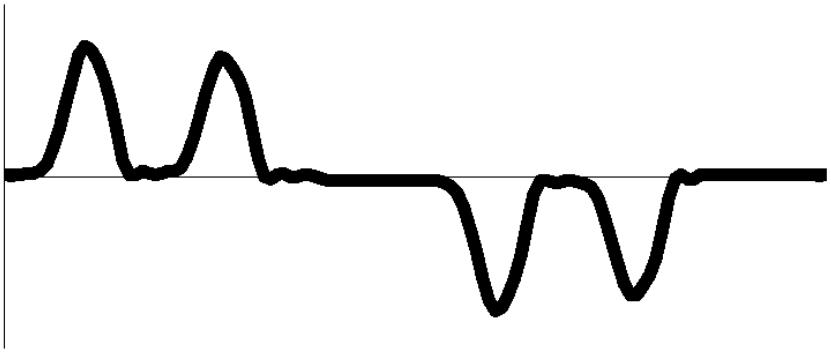

Figure 2.5 - Diode rectifier input current waveform for one phase [1]

The harmonic current components will affect the voltage waveform as well as the current waveform. As the distorted current spreads through the system it will react with the impedances found in the power system. This transmits the current distortion to the voltage as voltage drops occur. The problem is most common in the area around the harmonic source as the harmonic current components will be attenuated as they spread further away from the harmonic source. This is illustrated in Figure 2.6.

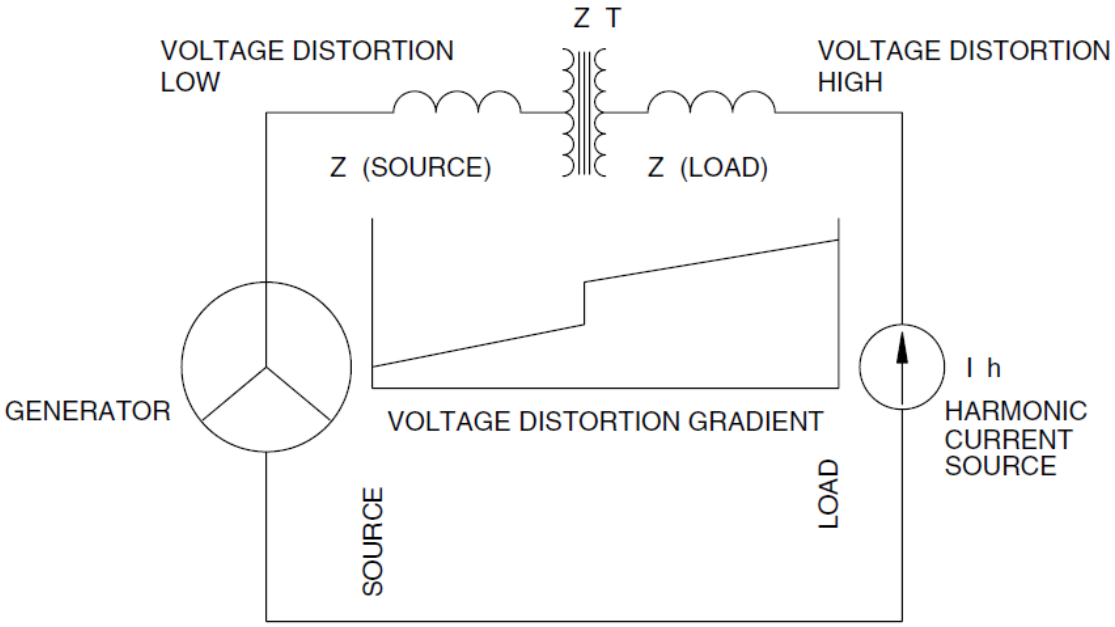

Figure 2.6 - Voltage distortion due to current distortion in power system [5]

Other harmonic sources are in general other non-linear loads. VFDs with an IGBT input bridge, known as active front end (AFE) converters, is one example. Here the harmonic components produced got a frequency around the switching frequency of the IGBTs. The advantage of using IGBTs instead of diodes regarding produces harmonics is that the IHD of the harmonic components produced by an AFE are much lower than the ones produces by a diode bridge rectifier and the low order harmonic components related to the power quality are almost none existent. An exception is if the modulation ratio for a SPWM controlled IGBT rectifier becomes greater than 1. This results in an output signal looking more and more squared as the modulation ratio increases beyond 1.

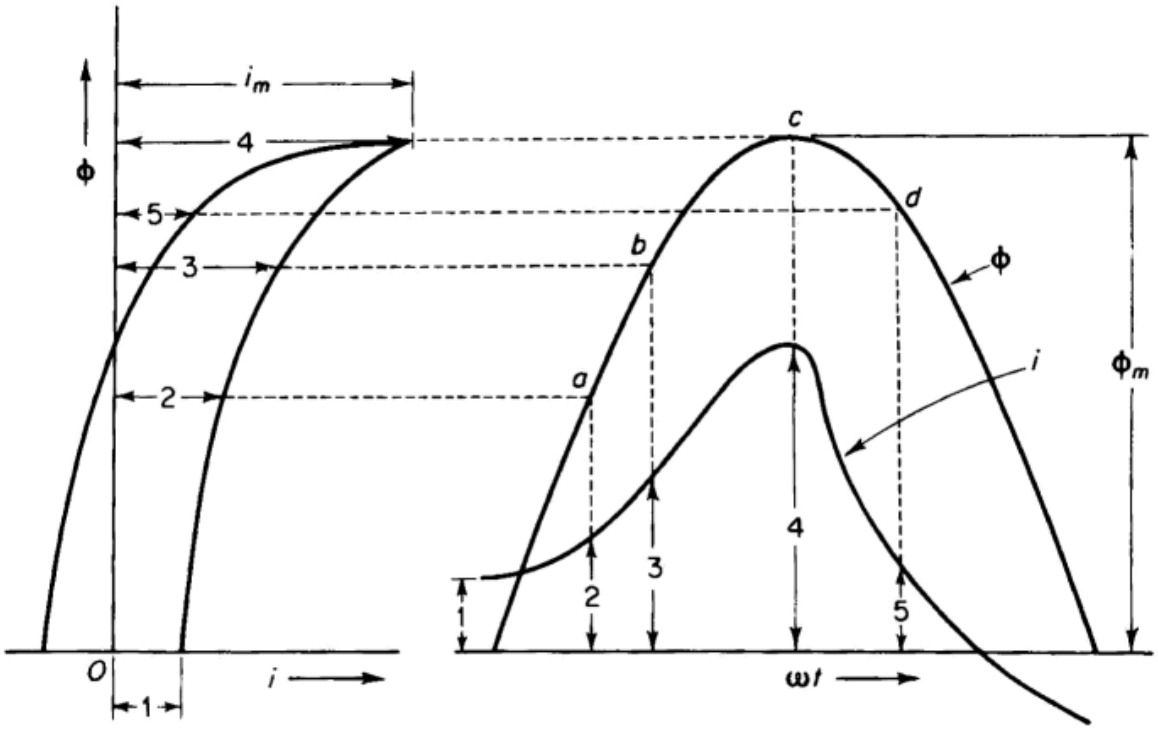

Figure 2.7 - Half period magnetization of transformer [6]

Transformers are also contributing to harmonic distortion as the magnetization current of a transformer is non-linear. This is because of the excitation characteristics of the transformer core. This can be seen in Figure 2.7, where the left side represents the current/flux relationship for a typical transformer. The right side represents the resulting current drawn from the primary side of the transformer. From Figure 2.8 one can see the most significant harmonics in the current drawn by a transformer. These are typically the 3rd and 5th harmonics [5].

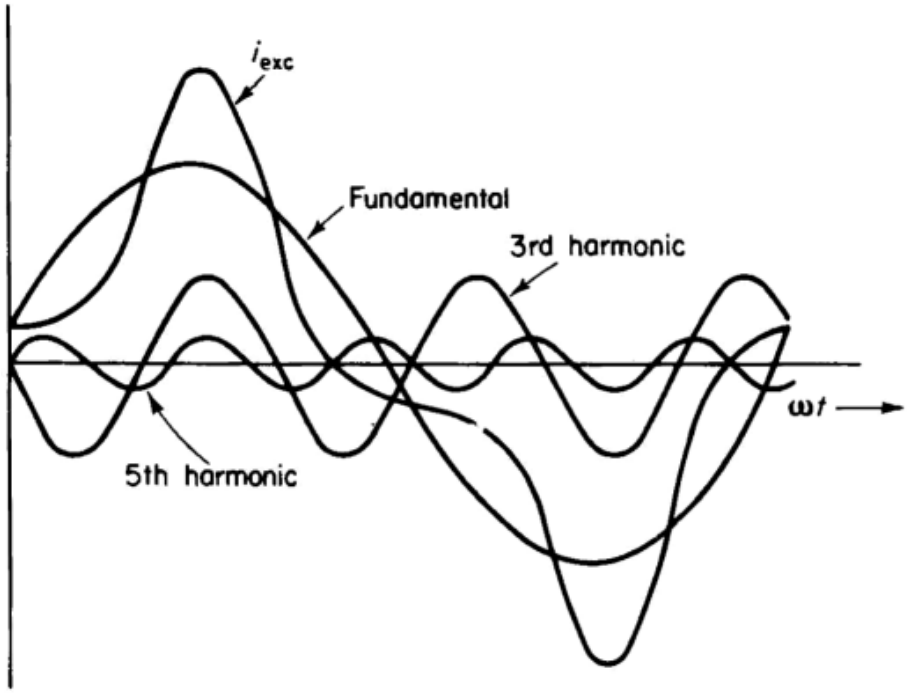

Figure 2.8 – Magnetization current of a transformer [7]

2.3 Harmonic consequences

Harmonic distortion can affect the power system and the components in the system in many different ways. As mentioned, harmonic power loss, malfunction or breaking of components and reduced lifetime expectancy for components are some of the unwanted consequences that can be caused by too much harmonic distortion.

2.3.1 Harmonic power loss

With high levels of harmonic distortion, the RMS value of current and voltage will increase. Reacting with impedances in the power system this will contribute to increased power loss, as seen from (Eq. 2.12). This problem is found in cables and the windings of generators, transformers and AC machines.

$$P_{loss} = I_{RMS}^2 R_{system} \quad \text{(Eq. 2.12)}$$

$P_{loss} = Copper\ losses$

$I_{RMS} = current\ RMS$

$R_{cable} = System\ resistance$

For AC systems the frequency will also affect the leading cross-section of the cables. Due to the skin effect the high frequency of harmonic components will decrease the leading cross-section of the cables, as seen from (Eq. 2.13).

$$\delta = \sqrt{\frac{2\rho}{\omega\mu_0\mu_r}} \qquad \text{(Eq. 2.13)}$$

$\delta = skin\ depth$

$\rho = resestivity\ of\ the\ conductor$

$\omega = angular\ frequency\ of\ current\ (2\pi f)$

$\mu_0 = permability\ of\ free\ space$

$\mu_r = relative\ permability\ of\ conductor$

Eddy current losses can increase in machines such as generators, transformers and other AC machines. These losses are caused by circulating currents induced in the conductors by the leakage flux. High order harmonics especially contribute to the losses caused by increased eddy currents. The increase of eddy current losses is proportional to $I_H^2 \cdot n^2$, where I_H is the nth harmonic RMS current and n is the order of the harmonic component. These eddy current losses can increase the winding temperature significantly. The total eddy current losses are shown in (Eq. 2.14) [1].

$$P_{EC} = P_{EF} \sum_{n=1}^{\infty} I_{H,n}^2 \cdot n^2 \qquad \text{(Eq. 2.14)}$$

$P_{EC} = Eddy\ current\ losses$

$P_{EF} = Eddy\ current\ losses\ at\ full\ load\ at\ fundamental\ frequency$

$I_{H,n} = n^{th}\ harmonic\ RMS\ current$

$n = harmonic\ current\ order$

2.3.2 Component malfunction

As mentioned, harmonic distortion may cause malfunction or even breakdown of components in the power system. The harmonic power loss causes additional heat production in the components in question. For cables, generators, transformers and other AC machines this means accelerated ageing. Cable insulation will with ageing be exposed to electrical breakdowns causing short circuits as the insulation breaks down as it is exposed to electrical distress over time.

For control systems that are relying on readings of the RMS values or zero crossing of voltage or current the control system may be misreading the distorted signals and malfunction. Generators with electronic AVRs may cause oscillations in the generator's power output. Power electronic devices with control systems may also have problems reading the reference signals, causing misfiring of IGBTs or even breaking of the power electronics. Protective devices rely on reading RMS values, peak values and the heat production from loss in the protection device. These devices may trip prematurely due to the increased RMS values caused by harmonic distortion. Peaks may be higher or lower for a distorted signal causing a protective device to trip either to late or too soon if it depends on the peak value of either current or voltage. The heat caused by increased RMS values will cause devices with heat sensors to trip prematurely.

Measurement equipment reading the RMS values of either current or voltage will also be affected by the distorted waveforms, giving inaccurate or false readings.

$$Peak\ factor = \frac{Peak\ value}{Rms\ value}$$

$$Form\ factor = \frac{RMS\ value}{Mean\ value}$$

The most conventional meters are using a method called *Average reading, RMS calibrated*. This method is measuring the peak values of a signal and calculates the average (0.636 times peak value) and multiplies it with the sinusoidal form factor (1.11). The final result is 0.707 times the peak, which is the square root of two, meaning that the final value is the RMS value of a sinusoidal signal. This means that this method only gives accurate measurements for purely sinusoidal signals. For distorted signals a method named *True RMS* gives an accurate measurement of the signals RMS.

One of the potentially most critical consequences caused by harmonic components is electromagnetic interference (EMI). The high order harmonics, typically produced by IGBTs, set up magnetic fields inducing interfering and distorting signals in nearby cables. If these signals are in the same frequency range as navigation, communication, visual or control system signal frequency the consequences can be huge.

For AC motors harmonic components will affect the performance and accelerate the ageing process. The harmonic components induce currents revolving in different directions in the rotor. This gives torsional oscillations to the motor shaft with a higher frequency than the fundamental frequency. If the induced oscillations should have the same frequency as the natural frequency of any motor parts the damage to the motor could be severe due to resonance. Additional heat losses occur due to the harmonic components, and this affects the insulating material in the motors. Together with the torsional oscillations the lifetime of the AC motors decrease due to the harmonic distortion [1].

2.3.3 Resonance

Resonance is a phenomenon that occurs due to interaction between the inductance and the capacitance in a power system. The reactances of these are changing inversely to each other relevant to frequency of an AC signal. This can be seen in (Eq. 2.15) and (Eq. 2.16).

$$X_L = \omega L = 2\pi f L \qquad \text{(Eq. 2.15)}$$

$X_L = Inductance\ reactance$

$\omega = Angular\ frequency$

$L = Inductance\ [Henry]$

$f = Frequency$

$$X_C = \frac{1}{\omega C} = \frac{1}{2\pi f C} \qquad \text{(Eq. 2.16)}$$

$X_C = Capacitance\ reactance$

$C = Capacitance\ [Farad]$

There are two kinds of resonances: Parallel and series resonance. For series resonance the impedance will be very low as the inductance and capacitance cancels each other out for a certain frequency. The impedance is in series with the resonant circuit, as seen in Figure 2.9 This results in high currents.

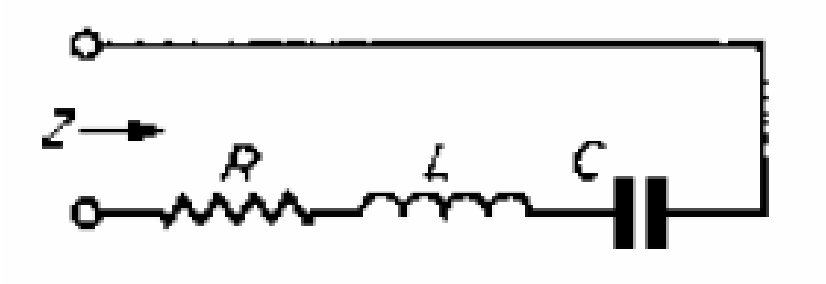

Figure 2.9 - Series resonant circuit

Parallel resonance gives high impedance, causing huge voltages at the location of the resonance. In the case of parallel resonance the impedance causing the problem is coupled in parallel with the resonant circuit as seen in Figure 2.10.

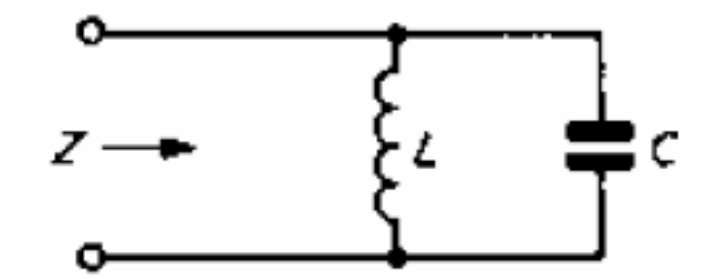

Figure 2.10 - Parallel resonant circuit

Figure 2.11 shows the impedance magnitude in a series resonant circuit. Here both parallel and series resonance occurs, with parallel resonance at a lower frequency. This is quite normal for series resonant circuits due to resonance with the source impedance which will be in parallel [1].

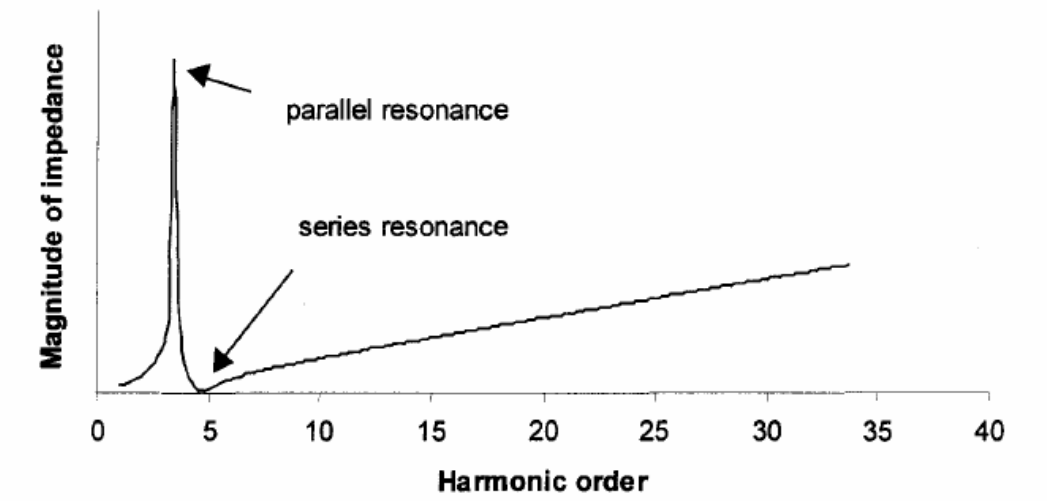

Figure 2.11 - Series resonant circuit impedance vs. frequency [1]

3 Mitigation of harmonics

As a result of the possible consequences caused by too much harmonic distortion in power systems the classification societies such as DNV, Bureau Veritas and ABS have set limits on THD and IHD for voltage limits. The reason for not limiting the current harmonic distortion levels is that in order to keep the voltage harmonic levels within the limits mitigation of the current harmonic distortion levels is one of the ways to limit the voltage distortion levels as well as the current affects the voltage (see 2.2).

The regulations from the different societies are mostly the same. IEC 61000-2-4 Class 2 is a common standard, implying the THDv shall not exceed 8%, and in addition, no IHD shall exceed 5%. If all customers and equipment affected by the harmonic distortion can be documented to withstand higher levels of harmonic distortion the levels may be exceeded. BV's regulations are stricter and say that THDv shall not exceed 5% and no IHD may exceed 3% of the nominal voltage. If the system is intended to be fed by static converters the IHDv up to the 15^{th} harmonic may not exceed 5%, decreasing to 1% for the 100^{th} harmonic component. The THDv may not exceed 10%. Also for BV the levels may be exceeded if all electrical devices operate correctly.

3.1 Filtering

For power systems with a large number of non-linear loads the harmonic distortion levels are expected to exceed the limits set by the classification societies. One way of handling the excessive harmonic distortion is by harmonic filtering. This will help smoothening the distorted voltage and current signals in the power system and prevent non-linear loads from affecting the upstream power system.

The active harmonic filter (AHF) is the most effective filtering technique. It utilizes IGBTs controlled by a measuring device and a control system to generate a counter signal for the harmonic components. Thereby it almost completely eliminates all the harmonic components. The AHF is normally placed in points of common coupling (PCC) for areas that produce too much harmonic distortion and affect the rest of the power system. The AHF then measures the distorted signal at the PCC and produces the counter signal to the harmonic components. One way of visualising this is by picturing that the power system provides the non-linear loads with the sinusoidal fundamental signal and the AHF supplies the harmonic components that

the non-linear loads draw. Figure 3.1 illustrates the basic function of the AHF, where it is connected at the input of a non-linear load.

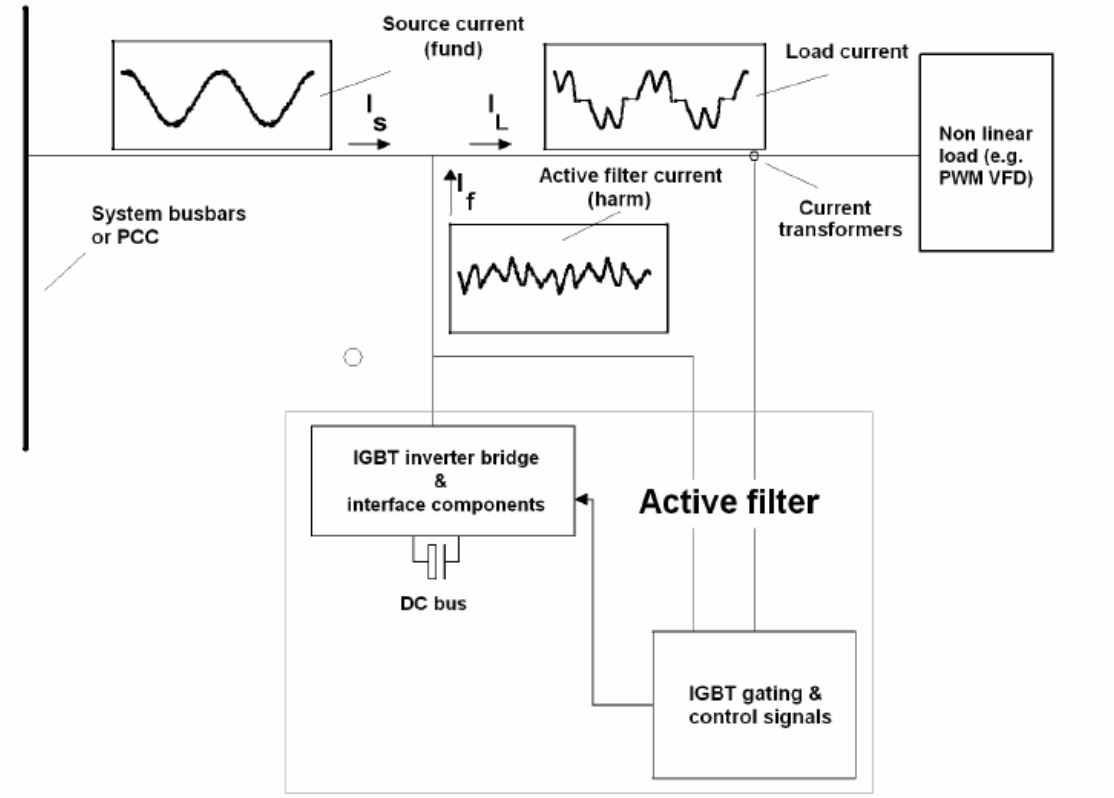

Figure 3.1 - Active filter block diagram [1]

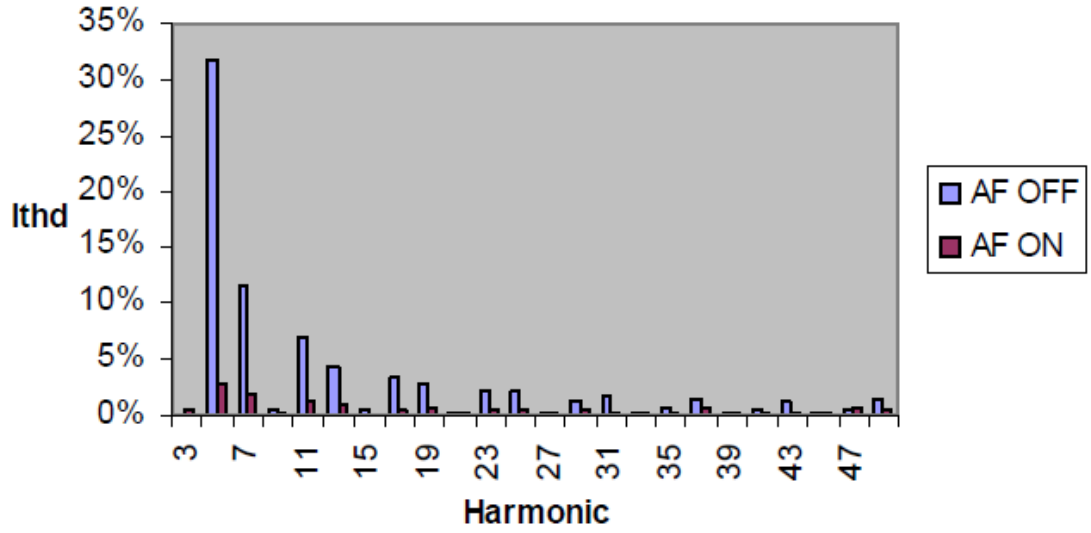

Figure 3.2 - THDi levels for AC PWM drive with/without active filter [1]

Since the AHF uses IGBTs and commonly SPWM or other complicated control systems the maintenance and repair is demanding professional expertise. This means that if an AHF installed in a maritime power system was to experience malfunction, a service engineer would most likely be required to come help out. This can be both time demanding and expensive.

Another filtering technology is passive harmonic filters. These filters are made of passive components. Mostly inductors and capacitors are used, but resistors appear in some configurations as well.

These filters are tuned to introduce a low impedance path for specific harmonic frequencies leading them away from the power system. As seen from (Eq. 2.15) and (Eq. 2.16) the impedance of a capacitor and an inductor are inverse according to the frequency, meaning that if they are coupled in series, a certain frequency will make them cancel each other out for the signal or harmonic component with the specific frequency the filter is tuned for. In this way the passive harmonic filters can be tuned to filter out a specific harmonic component by introducing a low impedance path for the harmonic component away from the power system.

To filter out a wider spectrum of harmonic components the passive harmonic filters have to be coupled in parallel to each other as seen in Figure 3.3. Another way is by using special configurations made for a wider spectrum, but this makes the design and installation more complicated and the filters become physically larger.

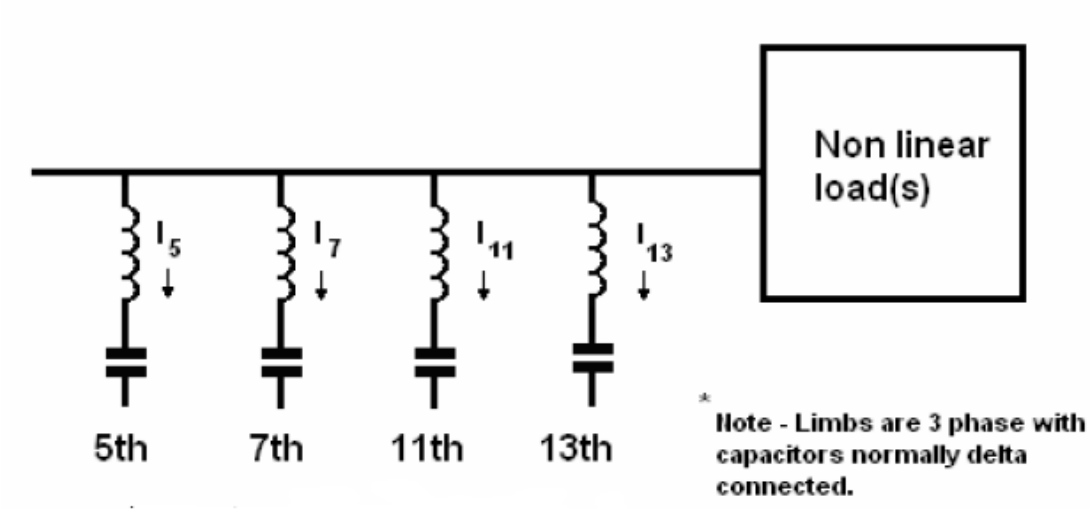

Figure 3.3 - Parallel single tuned filters [1]

A drawback with the passive harmonic filters is the potential of resonance. When installing a passive harmonic filter one needs to make a deep analysis of the power system, evaluating the risk of resonance to occur. Also, the passive harmonic filters tend to behave like a drain for harmonics, attracting harmonic components from other parts of the system. This can make the filter saturate, which can damage the filter components and cause malfunction [1].

3.2 Active harmonic filters

The operating principles for the AHFs were established in the 1970s. Since then there has been a revolution for components and technology used in AHF applications. IGBTs and other power electronics have improved performance and lowered power loss and cost. Digital signal processors are much better and cheaper. FPGAs, analog-to-digital converters and hall-effect current and voltage sensors have also improved greatly in performance, size and cost.

The improvements in technology used in active harmonic filters have made it superior compared to the passive harmonic filter. Better performance, smaller size and more flexible in applications are all reasons for the superiority. Still, the active harmonic filter is more expensive and got larger power loss and usage than the passive harmonic filters.

The pure active harmonic filter can either be a voltage source PWM controlled filter with a DC capacitor or a current source PWM controlled filter with a DC inductor. The voltage source solution is the one preferred the most due to performance, cost and physical size as the DC capacitor is smaller than the DC inductor [8].

The harmonic current emitted from a diode rectifier is decided by the natural diode commutation process, and the magnitude is depending on the size of the load. When a higher current is drawn by the load, the amplitude of the harmonic currents emitted by the diode rectifier's front end becomes larger. Without any filter installed, the harmonics have no other paths than through the upstream power system. This can be seen in Figure 3.4. With an AHF installed, and assuming total harmonic current mitigation, the harmonic current components would flow through the filter and the fundamental component alone would flow through the upstream power system as seen in Figure 3.5. Ideally for the load's power supply the harmonic components are supplied by the AHF and the fundamental component alone is supplied by the upstream power system, avoiding that the harmonic distortion injected by the load spreads to the upstream power system [9].

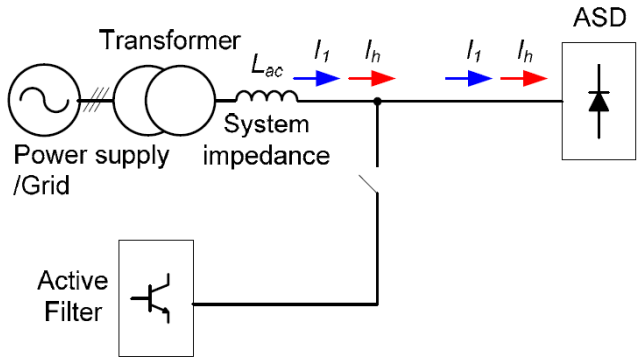

Figure 3.4 - Without AHF [9]

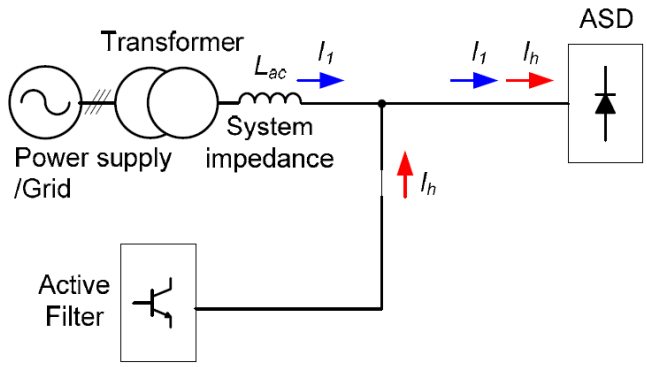

Figure 3.5 - With AHF [9]

The active harmonic filter can be either coupled in shunt or in series. The shunt coupled harmonic filter is the preferable solution for power correction usage, while the series coupled harmonic filter is used more for harmonic filtering.

Figure 3.6 shows a shunt coupled active harmonic filter for harmonic current filtering connected at the input of a 6-pulse diode rectifier. The filter in the figure is coupled in parallel with the non-linear load through a transformer, but it may also be coupled directly to the power system. It works by three simple steps:

1. The controller measures the instantaneous load current, i_L
2. The fundamental component is removed from the sampled signal by the digital signal processing unit
3. The active filter draws the compensating current i_F (=-i_{Lh}) from the utility supply voltage v_S to cancel out the harmonic current i_{Lh}

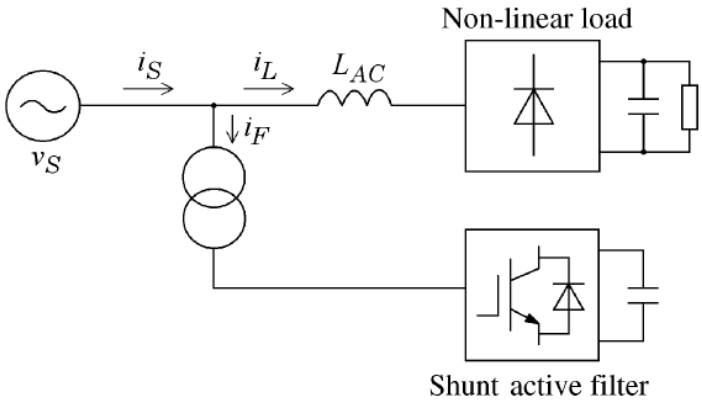

Figure 3.6 - Shunt coupled active filter [8]

For stable and proper control of the active harmonic filter, an AC inductor, L_{AC}, is placed at the AC side of the diode rectifier.

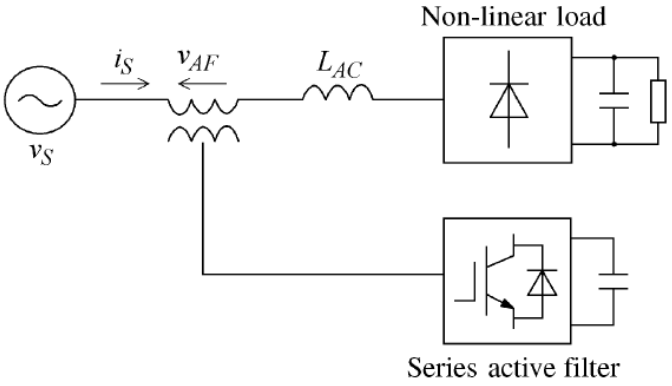

Figure 3.7 - Series coupled active filter [8]

Figure 3.7 shows a series coupled active harmonic filter for harmonic voltage filtering connected at the input of a 6-pulse diode rectifier. The filter is coupled in series with the utility supply voltage through a transformer. The series filter works by these three steps:

1. The controller measures the instantaneous supply current i_S
2. The fundamental component is removed from the sampled signal by the digital signal processing unit
3. The active filter applies the compensating voltage v_{AF} (=-Ki_{Sh}) to the utility supply through the transformer. This greatly reduces the supply harmonic current i_{Sh} if the feedback gain constant K is set to correct value.

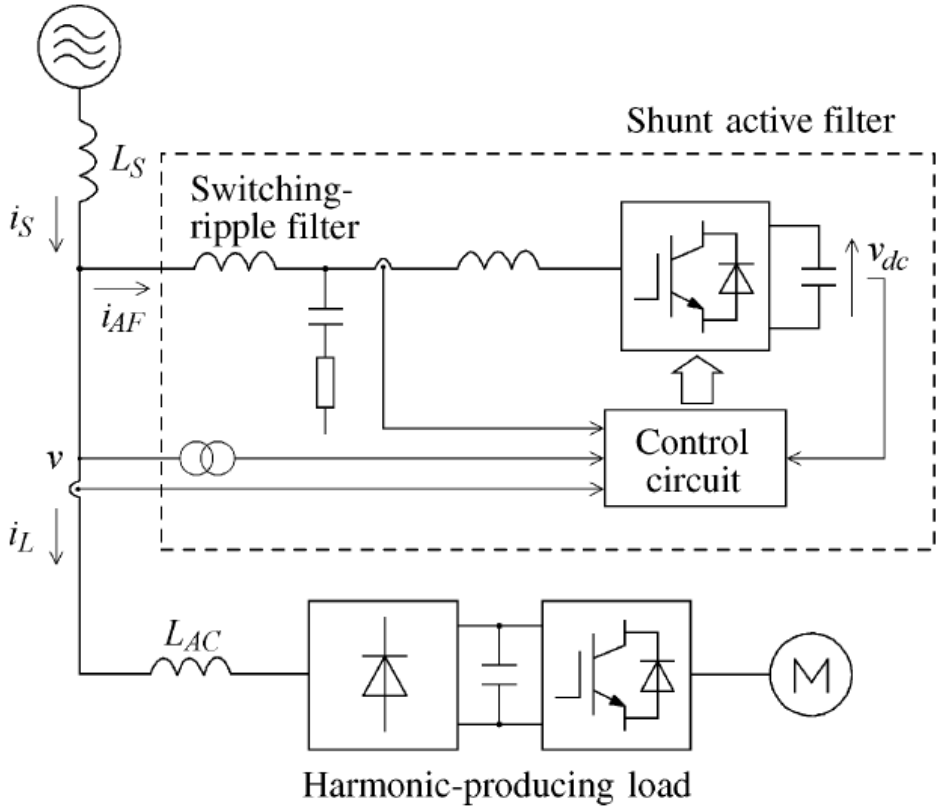

Figure 3.8 - Single-line system of a three-phase active filter [8]

Figure 3.8 shows a three-phase shunt active harmonic filter voltage source PWM converter with a DC capacitor. It is built up of three main parts: a three-phase voltage-source PWM converter with a DC capacitor, a control circuit consisting of digital signal processors, FPGAs, analog-to-digital converters, operational and isolation amplifiers and hall-effect current and voltage sensors, and a switching frequency ripple filter. Each part of the filter is supposed to do following tasks:

- The voltage-source PWM converter is generating and controlling the compensating current i_{AF} with a frequency bandwidth up to 1 kHz. This eliminates harmonics in the range from the typical 5^{th} harmonic produced by a 6-pulse diode rectifier up to the 25^{th} harmonic component.
- The control circuit is sensing the current waveform i_L drawn by the non-linear load and extracts the harmonic components, i_{Lh} from the waveform. This has to be done as precise as possible in term of amplitude and phase for both steady state operation and transient incidents.

- The switching-ripple filter is smoothing the filters compensating current i_F generated by the voltage-source PWM converter. This filter is placed in parallel as close to the converter as possible.

This filter is a pure active filter, even though there is a small passive filter in the configuration. As the passive filter is meant for smoothing of the compensating current, and not for the power system currents the filter is still considered purely active.

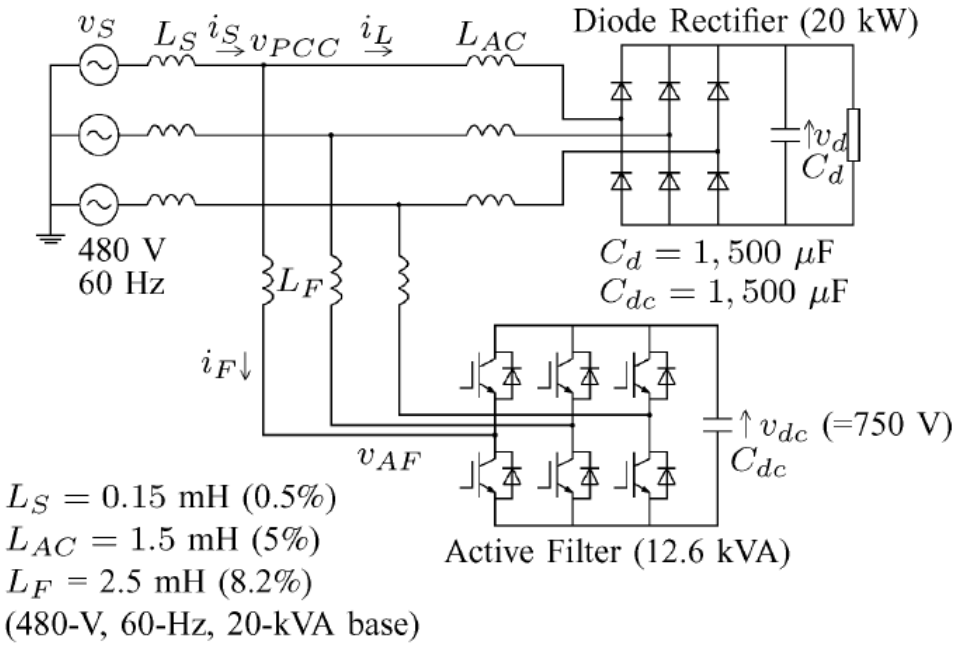

Figure 3.9 – 480V pure active filter [8]

An example from [8] shows the performance of a 480V pure active filter which can be seen in Figure 3.9. A 20 kW 6-pulse diode rectifier with a resistor and a capacitor in parallel at the DC side is connected as load. The rating of the filter is 12.6 kVA which is quite high. The DC voltage over the active filters capacitor is 750V, requiring large rated IGBTs. The filter requires 1.2kV or higher IGBTs as a power device. The formula for calculating the power rating of the filter is shown in (Eq. 3.1), where maximum filter current is given as 19.4 amperes [8].

$$P_{HF} = \sqrt{3} \cdot \frac{V_{DC}}{\sqrt{2}} \cdot \frac{I_{Fmax}}{\sqrt{2}} \qquad \text{(Eq. 3.1)}$$

$V_{DC} = DC\ voltage\ of\ active\ filter$

$I_{Fmax} = Maximum\ filter\ current$

In Figure 3.10 the control system for the 480V pure active filter is shown. It is divided into three different control functions: the feedback control, DC voltage control and feedforward control. The tasks of the different control functions are as follows:

- The feedback control leads all the harmonic components from the load current i_L into the pure active filter. It also avoids leading harmonic components from the source into the pure active filter, meaning the rating of the filter can be reduced and reduces the chance of overloading the filter.
- The DC voltage control regulates the pure active filter's DC capacitor voltage by itself by a PI regulator. This means that no external power supply is necessary.
- The feedforward control forces the 5th harmonic current components in the load current i_L to flow into the filter.

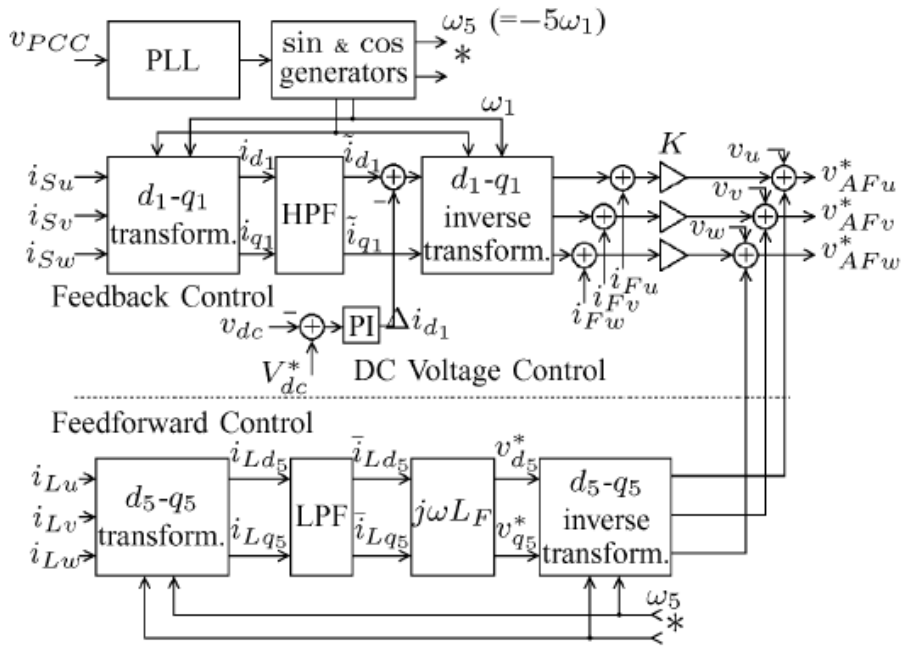

Figure 3.10 - 480V pure active filter control system [8]

The components in the AHF require some power themselves, and contributes to additional power loss. These losses depend on the efficiency of the filter and the filter's power rating.

$$P_{loss} = (1 - \eta_{AF}) \cdot \frac{S_{AF}}{S_{ASD}} \quad \text{(Eq. 3.2)}$$

$\eta_{AF} = Effiency\ of\ the\ AHF$

$S_{AF} = AHF\ power\ rating\ [kVA]$

$S_{ASD} = ASD\ power\ consumption\ [kVA]$

With a typical loss of 3% (η=0.97) for the AHF and a rating of 50% of the ASD's power consumption the additional losses would become 3% · 0.5 = 1.5%.

By applying an AHF in the power system, the demanded harmonic component levels increases. For the load, the impedance seen upstream is lowered when the AHF is installed as it decouples the grid impedance. The natural commutation behaviour of the diode rectifier is then changed. The raised magnitude of the harmonics then results in an increased demand for compensating harmonic current from the AHF.

If the AHF is compensating the whole amount of harmonic components by itself the systems AC impedance is as mentioned decoupled as seen from the load. This makes the AC impedance practically zero for the ASD coupled to the load. This means that the harmonic current components are less damped by AC impedance, resulting in higher levels at the ASD front end. To compensate for the lowered AC impedance seen by the load an AC choke has to be installed at the input of the ASD. The additional AC choke is giving additional losses of typically 0.7-1.0%.

For a 6-pulse diode bridge rectifier with an AHF the losses of the AHF are typically of 2.2-2.7%. The harmonic mitigation is very good, with THDi levels lower than 5%. Also the power factor and main current balance can be controlled and corrected with an AHF. The drawbacks of the AHF compared to other solutions are the AC choke which is required and the large rating of the filter itself [9].

4 Measurement system

When a harmonic measurement is made several factors has to be taken into account, and different solutions are available for solving the task. When the measurement system is put together the way the measurements are taken, what signals that are measured and which equipment that is going to be used are some of the things that has to be taken into account.

This chapter will come up with some sampling theory that that should be considered when designing a measurement system and also describe a solution delivered by National Instruments (NI).

4.1 Data acquisition

When planning how to make harmonic measurements, some of the most basic and important things to consider are the equipment's ratings with regard to voltage and current levels in this project. For small electronic equipment and control circuits the voltage levels are quite low and the same for the current. Here low voltage and current rated modules are sufficient and cheaper. For measurements of a distribution power system other voltages and current levels are present, requiring equipment capable of these levels of energy.

4.1.1 Measurement categories

There are three different measurement categories defined by the IEC 61010-1 standard. These categories are a method to classify measurement equipment for different energy levels to make sure that the measurements can be conducted safely, both with regard to equipment safety and human safety.

The four categories are described as follows:

- *"CAT I is applicable to instruments and equipment, which are not intended to be connected to the mains supply.*

  Because the available energy is very limited, this category is normally not marked on the equipment - instead simply rated voltages and currents are stated (e.g. in multimeters).

  Examples: low voltage electronic circuits, load circuits of bench power supplies, etc."

- *"CAT II defines circuits which are intended for direct connection into mains sockets or similar points. The energy in such installations should be limited to below 100 A continuously (or below 500 A for voltages not exceeding 150 V).*

  The maximum available continuous power must be limited (for instance by a circuit breaker) to not more than 22 000 VA.

  Example: a device connected to a 240 V mains socket with 13 A fuse (energy limited to 3100 VA)."

- *"CAT III is for circuits which can be connected to the mains installation of a building. Energy is limited by circuit breakers to less than 110 000 VA with the current not exceeding 11 000 A.*

  Example: 110/240 V distribution boards, busbars, or equipment permanently connected to the 3-phase power supply (e.g. electric motors)."

- *"CAT IV includes circuits which are connected directly to the source of power for a given building. There are very high levels of available energy (e.g. limited only by the power transformer) and arc flash can occur.*

  Example: measurements on a cable connecting the power transformer and a building (i.e. before the circuit breakers in the building)."

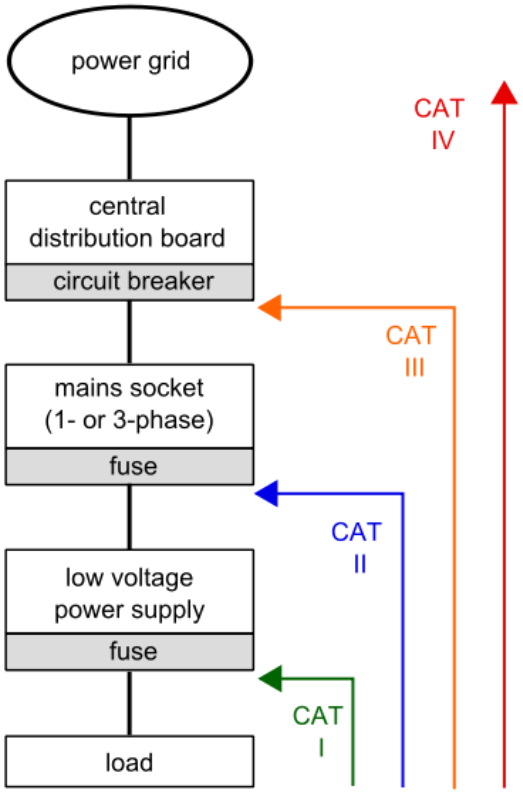

Figure 4.1 - Measurement categories [9]

These categories take into account the total continuous energy available at the different points in the power system clearance and the impulsive voltage levels that can occur. Equipment is for instance marked as "CAT III, 150V" or "CAT IV, 1000V", giving the limitations

regarding insulation of the equipment and impulsive voltages where the given voltage is the designated voltage level for the equipment.

Clearance of the equipment relates to the electrical insulation and the risk of an arc flash to occur between different parts of the equipment, either between energized parts or between live and grounded parts. The higher the voltage, the higher the clearance is required. The clearance values may vary from 0.04 mm for single insulation CAT II, 50V, to 28 mm for double insulation CAT IV, 1000V. The IEC 61010-20-030 standard gives the exact clearance values for the different categories and voltages.

The impulse withstand voltage which as mentioned takes voltage impulses into account for the measurement equipment also varies as the clearance values. For CAT II, 50V rated equipment the impulse withstand voltage is 500V, while it is 12000V for CAT IV, 1000V rated equipment [10].

4.1.2 Isolation

Isolation is necessary for applications where hazardous voltages, transient signals, common-mode voltage or fluctuating ground potential is present or likely to occur. These phenomenons can potentially damage measurement equipment or ruin measurement accuracy. To deal with this electrical isolation is used for analog measurement systems [11].

Electrical isolation got many benefits for measurements:

- It electrically separates the sensor signals with potentially hazardous voltages from low-voltage backplane measurement equipment.
- It protects expensive equipment, the user of the equipment and sampled data from transient voltages.
- With isolation the measurement system is more immune to noise interference.
- Ground-loops are removed.
- Common-mode voltages are rejected much better.

Ground loops which is one of the most common sources of noise in a data acquisition system occurs when different terminals in a circuit are connected to different ground potentials. This causes a voltage potential between the two points, which again causes current to flow as well. The measurement error caused by ground loops can be calculated by (Eq. 4.1).

$$V_m = V_s + \Delta V_g \quad \text{(Eq. 4.1)}$$

$V_m = Measured\ voltage$

$V_s = Signal\ voltage$

$\Delta V_g = Voltage\ difference\ between\ signal\ source\ ground\ and\ instrument\ ground$

The ground planes of the sensor front end signals and the measurement backplane signals are separated, so the sensor measurements are separated from the rest of the system. The ground potential of the front end signal is a floating pin, capable of operating at a different potential than the earth ground. This can be seen in Figure 4.2, where an analog voltage measurement device is illustrated. Common-mode voltage between the sensor ground and measurement ground is rejected, which prevents ground-loops and removes noise on the sensor lines.

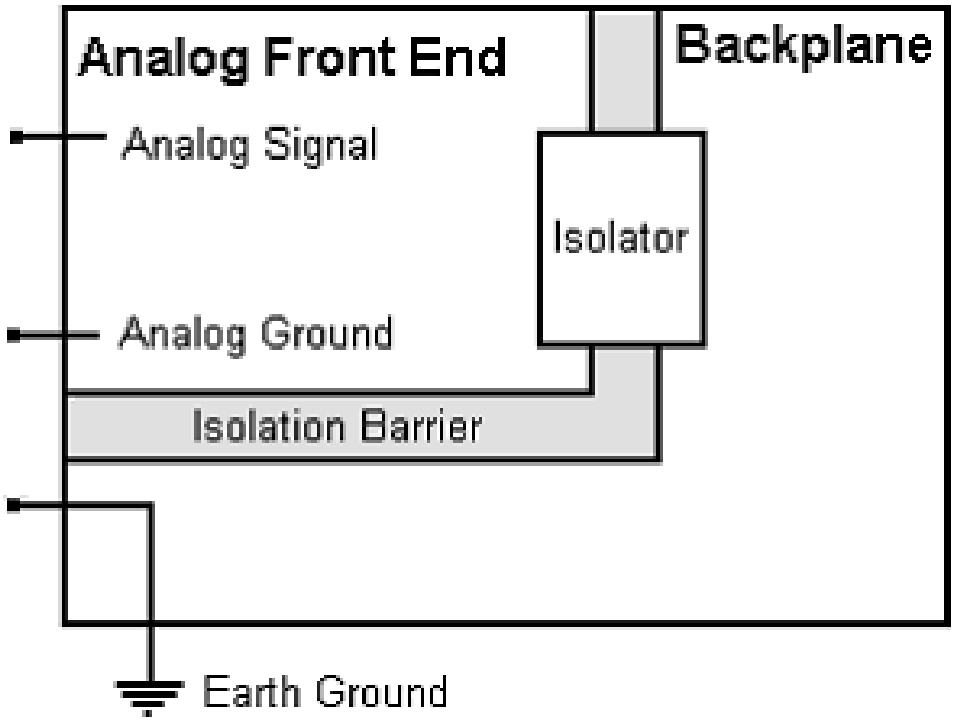

Figure 4.2 - Bank-isolated analog input circuitry [12]

Different isolation topologies exist, where there are three in general. These have different levels of protection. From low to high protection, they are respectively:

- Channel-to-earth isolation.
- Bank (channel-to-bus) isolation.
- Channel-to-channel isolation.

Channel-to-earth isolation isolates the front end from the earth ground. The analog inputs are not isolated from each other, meaning that a current at one input can induce a voltage at another input as they are not isolated from each other.

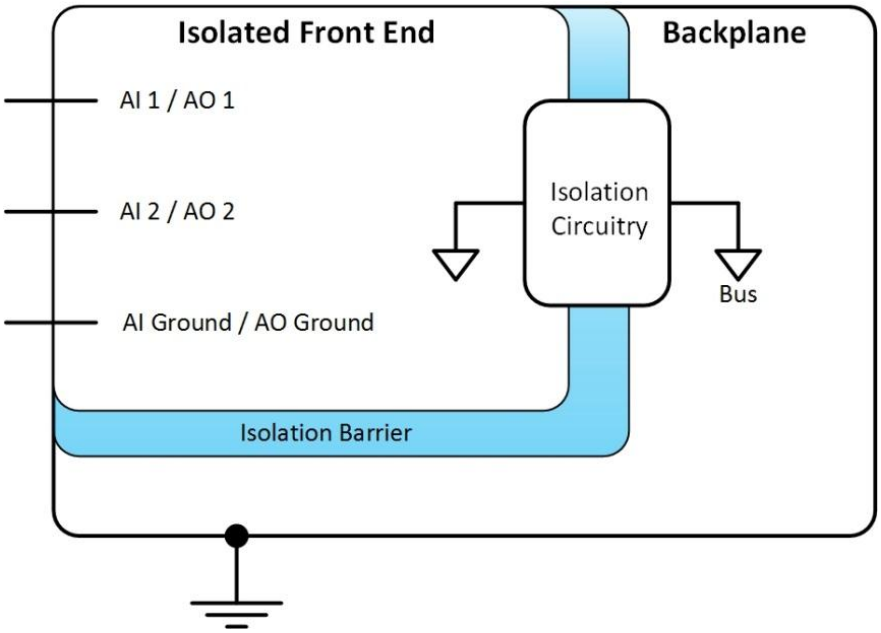

Figure 4.3 - Channel-to-earth isolation [12]

Bank (channel-to-bus) isolation got several physical lines grouped together into banks. This topology provides high ground loop protection as there are isolation barriers between the banks. However, within a bank, the signals can still affect each other.

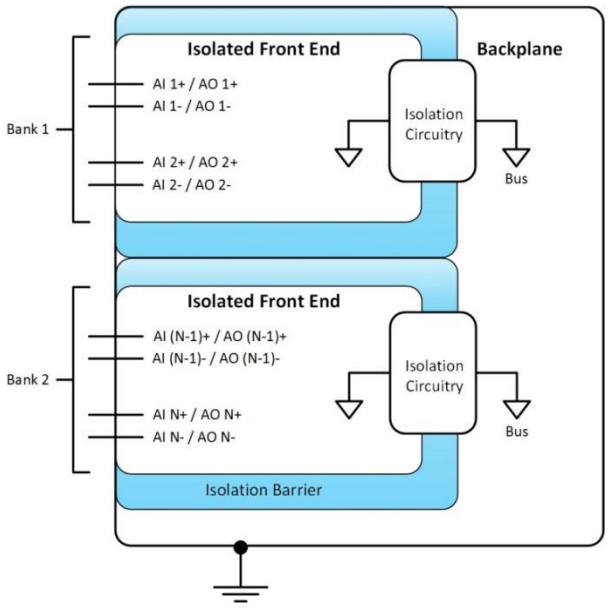

Figure 4.4 - Bank (channel-to-bus) isolation

Channel-to-channel isolation is the best isolation topology as all channels are isolated from ground and from all other channels. This means that the protection from ground loops and interference from other channels is very high [12].

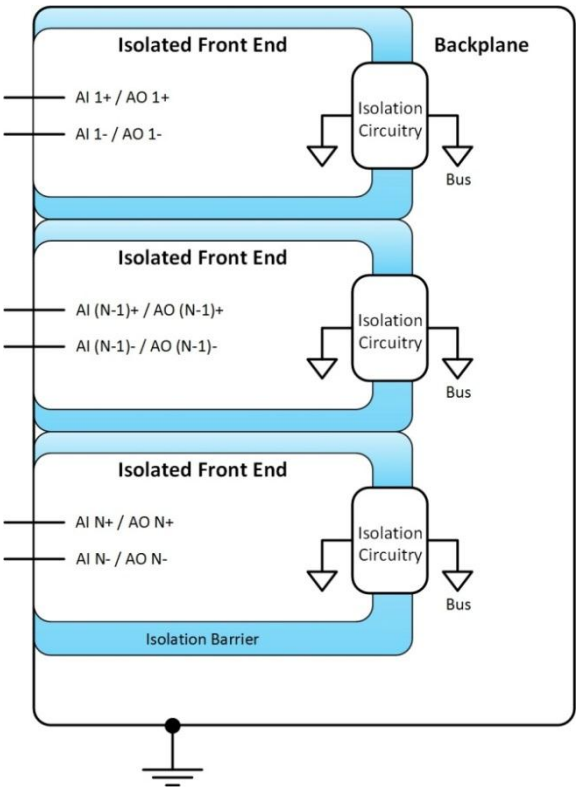

Figure 4.5 - Channel-to-channel isolation

Isolation should in general be considered for applications with one or more of these cases:

- Close proximity to hazardous voltages.
- Environments with the risk of transient voltages to occur.
- Environments with common-mode voltage or fluctuating ground potential.
- Environments with electrical noise such as those with industrial motors.
- Transient-sensitive applications where it is crucial to prevent voltage spikes from being transmitted through the measurement system.

For industrial or similar applications with large voltages, high transient voltage, common-mode voltage and electrical noise electrical isolation is preferable. This improves the measurements and makes them more reliable in these harsh environments.

Electrical isolation requires the transmittal of a signal over a isolation barrier without any direct electric contact. Some of the most commonly used solutions involve LEDs, capacitors or inductors. These three represent three different techniques: optical, capacitive and inductive coupling.

Optical isolation involves the transmission of a light signal over the isolation barrier. This can involve a LED which emits light when voltage is applied over the LED. On the other side of the isolation barrier a photodetector detects the transmitted light and converts it into the original signal.

This is as mentioned one of the most common isolation techniques. Some reasons to this are that the utilization of light makes this solution immune to electric and magnetic noise from the environment. A drawback with the optical isolation is the low transmission speed restricted by the LED’s switching speed. High-power dissipation, and LED wear are other weak sides to this solution.

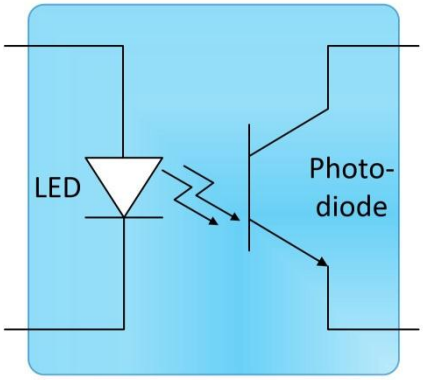

Figure 4.6 - Optical isolation [13]

Capacitive isolation is based on electrical fields. The electric field in a capacitor changes with the charge at the capacitive plates. Charge built up on the sensor side of the capacitive isolation is detected across the isolation barrier. The charge is proportional to the sensed signal, and the detected signal is the same.

The capacitive isolation is immune to magnetic noise. Compared to the optical isolation the data transmission goes much faster as there are no LEDs that need switching. The utilization of electric field for data transmission makes the capacitive isolation sensitive to interference from other external electric fields.

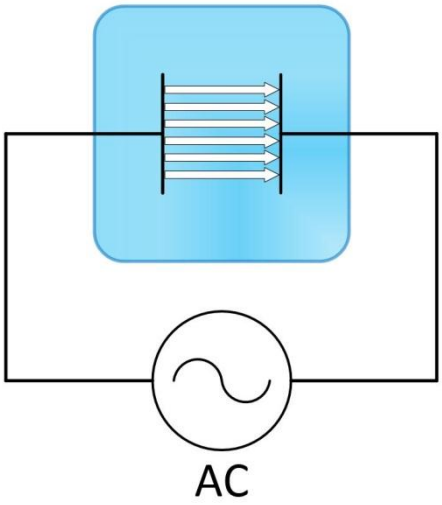

Figure 4.7 - Capacitive isolation [13]

Inductive coupling isolation is based on the principle of mutual induction. This is when changing current in a coil sets up a magnetic field, which again induces a similar current in a

secondary coil. The voltage and current induced in the secondary coil depends on the number of windings relationship between the two coils.

The two coils in an inductive isolation is separated by a thin insulation layer which prevents any physical signal transmission. The varying signal measured induces a secondary, similarly shaped signal across the insulation barrier on the secondary side of the inductive isolation. The inductive isolation allows high-speed transmission of signals in the same way as the capacitive isolation. Also, the utilization of magnetic field makes the inductive isolation technology susceptible to interference from external magnetic fields.

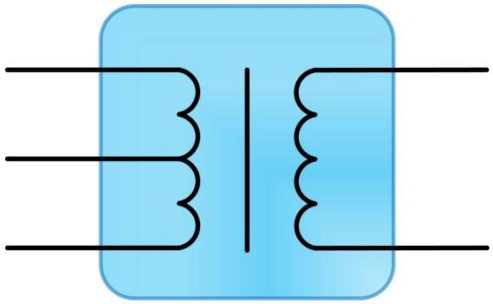

Figure 4.8 - Inductive coupling isolation [13]

Table 4.1 - Isolation type overview [13]

Isolation type	Advantages	Disadvantages
Capacitive	• Fast data transmission rate • Magnetic field interference immunity	• Susceptible to electric field interference
Inductive	• Fast data transmission rate • Magnetic field interference immunity	• Susceptible to electric field interference
Optical	• Electric field interference immunity • Magnetic field interference immunity	• Slower data transmission rates • Relatively high power dissipation

Products today that are typically off-the-shelf components uses mostly one of the above mentioned isolation technologies. For analog I/O-channels this isolation can be implemented in both the digital and the analog part of the component. Either before the analog-to-digital converter has digitalized the measured signal, known as analog isolation, or after the analog-to-digital converter has digitalized the measured signal, known as digital isolation.

These two solutions are illustrated in Figure 4.9 and Figure 4.10. When choosing which isolation solution needed for a data acquisition system the performance, cost and physical requirements should be considered before a decision is made.

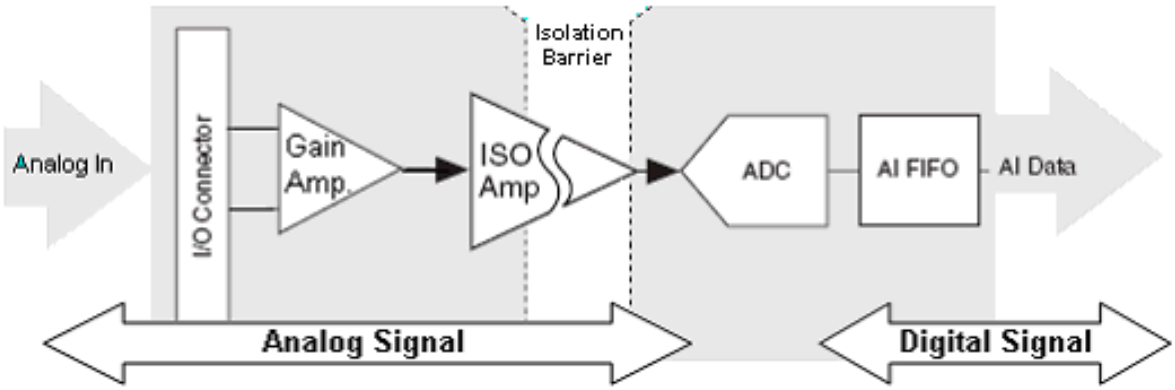

Figure 4.9 - Analog isolation [13]

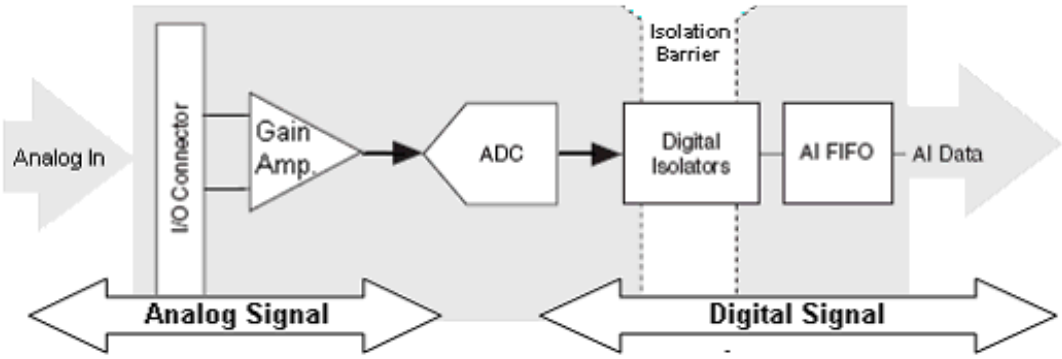

Figure 4.10 - Digital isolation [13]

As seen in Figure 4.9 the analog isolation uses an “ISO Amp”. For most analog circuit this is the first components in the analog circuitry. The analog signal from the sensor is sent to the isolation amplifier which provides isolation and transmits the analog signal over the isolation barrier. The signal is then sent on to the ADC circuitry. The transmission method used in analog isolation is one of the previously mentioned methods: optical, capacitive or inductive. In Figure 4.11 the “isolation” part represents the transmission method.

For an ideal analog isolation the output signal is similar to the input sensor signal. To get a good output signal the isolation amplifier is built up of three main parts. First is the modulator, which prepares the senor signal for the isolation circuitry. For optical method transfer the signal must be digitized for varying light intensity. Capacitive and inductive methods require an electric or magnetic field signal for transmittal. Second comes the

isolation part with the transfer of the signal over the isolation barrier. The last part is the demodulator which converts the signal back to the initial analog signal.

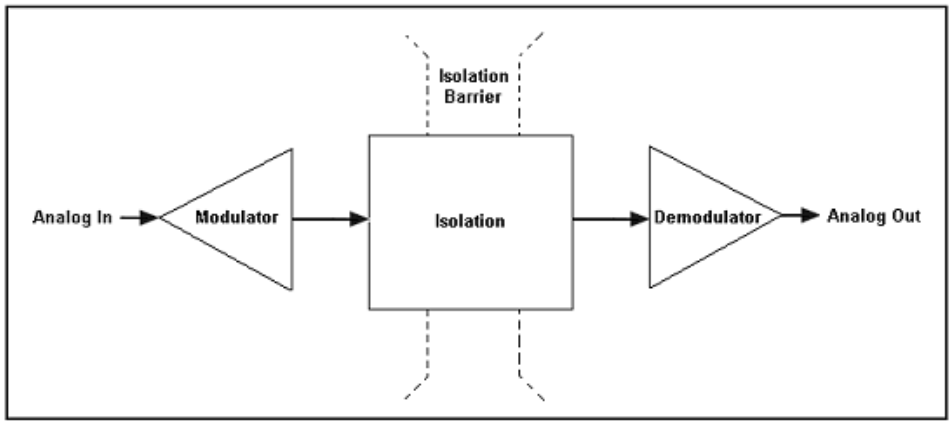

Figure 4.11 - Isolation amplifier [13]

The analog isolation provides some benefits regarding flexibility of data acquisition systems. The isolation before the digitizing of the signal is beneficial for non-isolated data acquisition devices. The non-isolated data acquisition device is responsible for the analog-to-digital conversion, while the external isolation circuitry provides the isolation. This allows vendors to combine different isolation and data acquisition devices. For different measurements the same data acquisition device can be used, while the external analog isolation circuitry can be changed out to fit the new specifications.

In a data acquisition system the ADC is one of the most important components in digital-to-analog conversion. For this reason the ADC's input signal should be as close to the real, measured signal as possible. Analog isolation before the ADC can cause distortion and errors such as gain, nonlinearity and offset in the sensor signal, causing an inaccurate input signal for the ACD.

Analog isolation components are expensive. The use of this technology was previously popular due to the protection of the even more expensive ADC. However, since 1990 the cost of the ADC has been reduced by over 50% reducing the need of protection caused by the cost.

The digital isolation has due to cost and performance become the most preferred solution for most vendors. The performance is better since the isolation is done after the analog-to-digital conversion, reducing the probability of errors before the digitizing. The digital isolation also has higher data transfer speeds. For designers of a data acquisition system the design of the

analog measurement front end is more flexible, allowing possibly better configurations. Voltage and current limiting circuits are responsible for the voltage and current protection of the ADC in digital isolation solutions. The basis for the digital isolation is the same as for the analog: optical, capacitive and inductive [13].

4.1.3 Sampling theory

When a periodic function or signal is being sampled it is being reduced to a discrete signal. A set of samples, which are a value or a set of values at a point in time and/or space, are gathered with a put sampling interval, *T*, between each sample. The sampling frequency or sampling rate, f_s, is the inverse of the sampling interval and given in samples per second. Figure 4.12 below shows a sampled function (S(t)), where the vertical, blue bars represent the sampling points with the sampling interval between them [14].

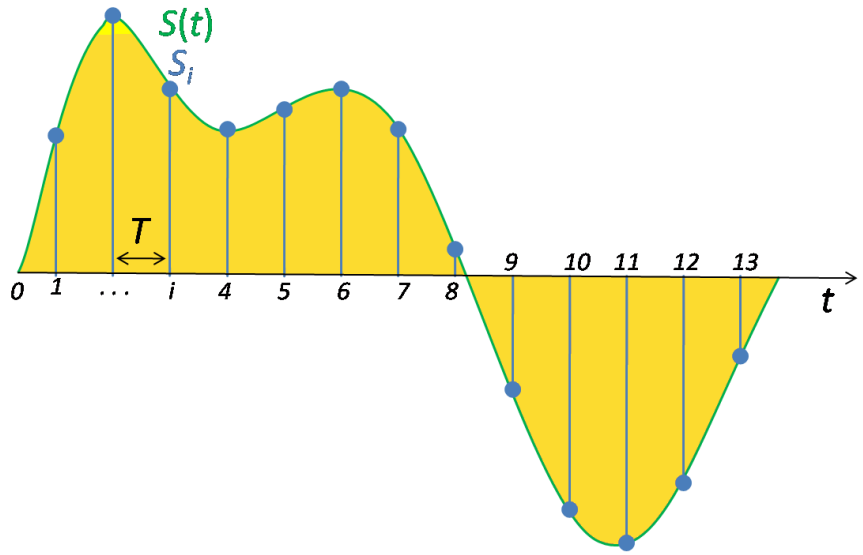

Figure 4.12 - Sampling of a signal [14]

When the discrete signals sampled from the continuous signal are seen alone they create a unclear picture of the continuous signal. Due to the sampling interval, the continuity in the signal is lost, and the instantaneous value for each sample is held until the next sample [15].

This makes the sampling rate one of the most important factors for data acquisition. The Nyquist theorem (Eq. 4.2) states that a signal can be accurately reconstructed with a sampling frequency of two times the frequency of the highest component of interest. In practice the sampling frequency is normally chosen to at least 10 times the frequency of the highest component of interest.

$$f_s \geq 2 \cdot f \qquad \text{(Eq. 4.2)}$$

$f_s = Sampling\ frequncy$

$f = Frequency\ of\ highest\ component\ of\ interest$

The reason for choosing a higher sampling frequency than recommended by the Nyquist theorem can be seen in Figure 4.13, where a sine wave with a frequency of 1 kHz has been sampled with 2 kHz sampling frequency, as stated by the Nyquist theorem, and also with a 10 kHz sampling rate as in common practice. The 2 kHz sampling frequency signal becomes a triangular wave, and not sine, as the measured signal really is. The 10 kHz sampled signal gives a better reconstruction of the measured sine wave.

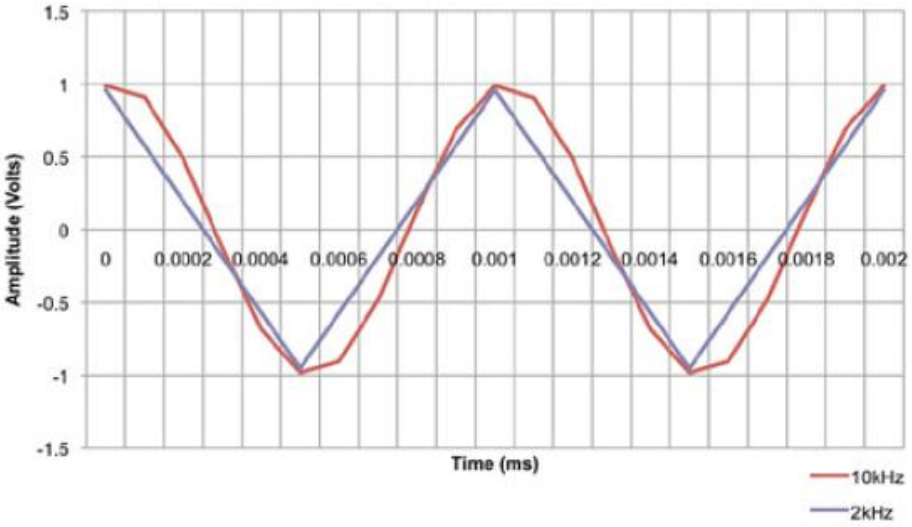

Figure 4.13 - 2 kHz and 10 kHz sampling of 1 kHz sine wave [16]

When a signal is measured, the discrete sampled signal is converted to a digital signal by the ADC, known as analog-to-digital conversion. This digital signal is then supposed to be similar to the continuous, measured signal. This is however difficult as the sampled signal is discrete. The discrete signal has to be replaced by values selected from a given discrete set and is often done by rounding, which can be seen in Figure 4.14. This process is known as quantization. The process loses information, which means that the discrete signal is only an approximation of the continuous signal as there is not enough information in the digital signal to perfectly recreate the initial analog measured signal [16].

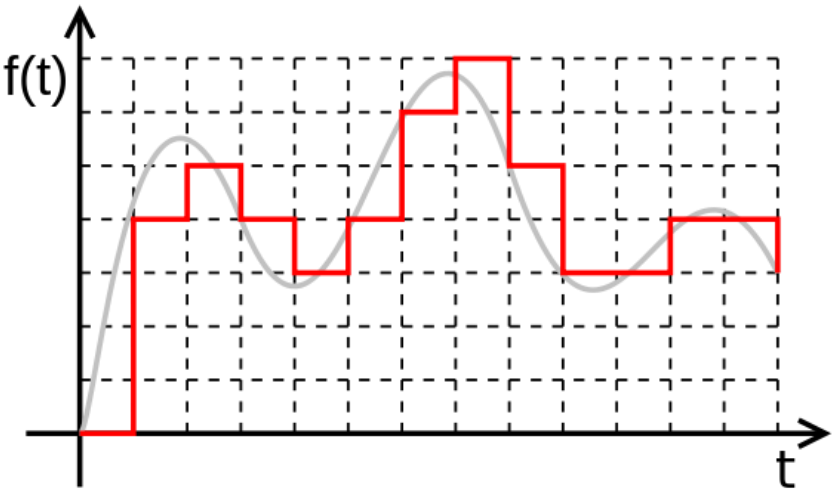

Figure 4.14 - Sampled signal [16]

The levels of lost information due to the quantization depend on the resolution, or number of bits, in the ADC. The values the discrete absolute measurements can be approximated as are several evenly distributed values. The values depend on the resolution of the ADC and the input range of the measurement device. In Figure 4.15 a measurement with an input range of 10V has measured a signal varying between 0-10V. The blue line is the digitized signal from a 3-bit ADC, and the red line is the digitized signal from a 16-bit ADC. It is clear that the 16-bit ADC gives a much better representation of the measured signal. This is because of the higher number of approximate evenly distributed values available in the quantization process.

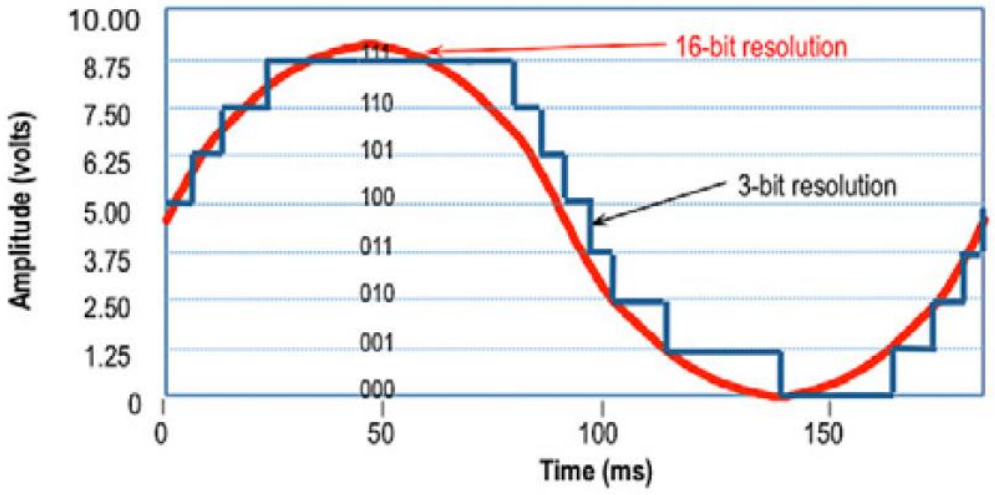

Figure 4.15 - 3-bit and 16-bit resolution [16]

The number of evenly distributed values related to the bit rate is shown in (Eq. 4.3). From the formula one can calculate that a 3-bit resolution gives eight evenly distributed levels. These can be seen in Figure 4.13, where each level is marked with its binary value. A 16-bit resolution gives as much as 65,536 discrete voltage levels.

$$\Delta V_n = 2^n \qquad \text{(Eq. 4.3)}$$

$\Delta V_n = Number\ of\ evenly\ distributed\ voltage\ levels$

$n = Number\ of\ bits$

The smallest detectable change in the measured signal can be calculated on basis of the ADC's bit resolution and the input range of the measurement device. See (Eq. 4.4). From the equation, a +/- 10V measurement device with a 16-bit ADC resolution will be able to detect a signal change of 300µV. This is an accuracy of 0.0015% relative to the input range, which should be sufficient for most measurements. Higher resolutions can be required for measurements where small signals are measured with measurement devices with a large input range [16].

$$\Delta V_{det} = \frac{V_{in}}{\Delta V_n} \qquad \text{(Eq. 4.4)}$$

$\Delta V_{det} = Smallest\ detectable\ voltage\ change$

$V_{in} = Voltage\ input\ range$

A problem associated to sampling frequency in data acquisition is aliasing. This is a phenomenon that occurs due to undersampling of a signal. Aliasing provides poor recreation of the analog measured signal and gives a false picture in spectral representation. This is because aliasing causes false lower frequency components to appear in the sampled measurement signal.

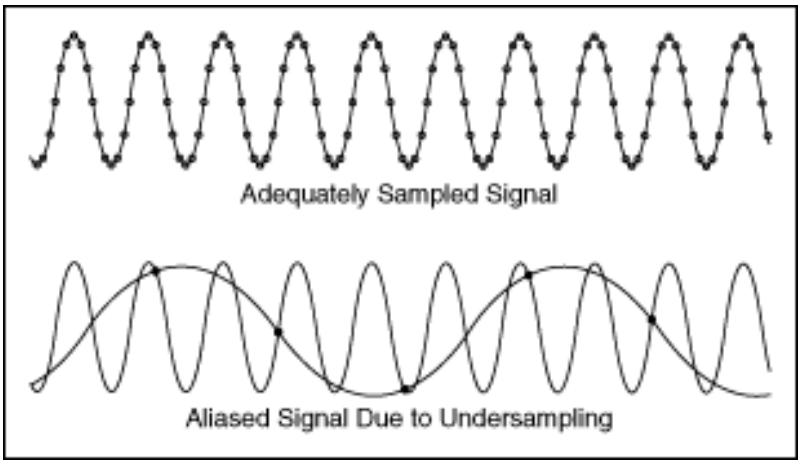

Figure 4.16 - Aliasing [17]

In general, aliasing appears for frequencies above the Nyquist frequency, seen in (Eq. 4.5). The aliased signal appears with a frequency between DC and the Nyquist frequency. For components with a frequency below the Nyquist frequency aliasing is no problem. In Figure 4.16 an undersampled signal is presented. The recreation of this undersampled signal clearly has a lower frequency than the original signal itself, causing a false lower frequency component to appear in the measured signal data acquisition.

$$f_{nq} = \frac{f_s}{2} \qquad \text{(Eq. 4.5)}$$

$f_{nq} = Nyquist\ frequency$

In Figure 4.17 some sampled signals are presented in a graph. These are the component measured in a signal, with a sampling frequency of 100 Hz, and the Nyquist frequency of half the sampling frequency, 50 Hz. In Figure 4.18 the aliased signals of the components with a frequency above the Nyquist frequency is also represented in the graph.

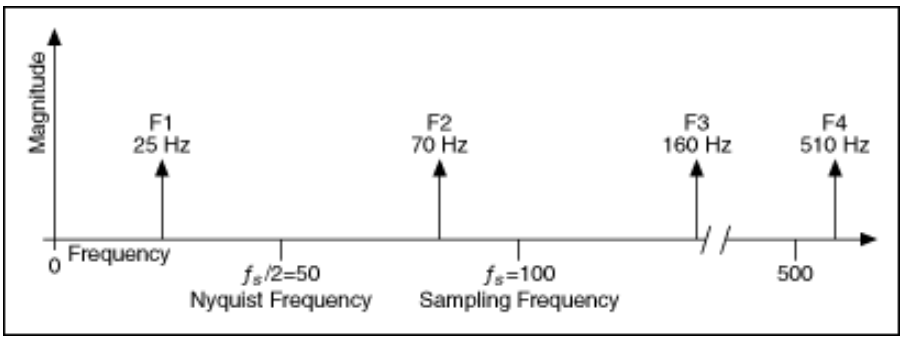

Figure 4.17 - Sampled signal components [17]

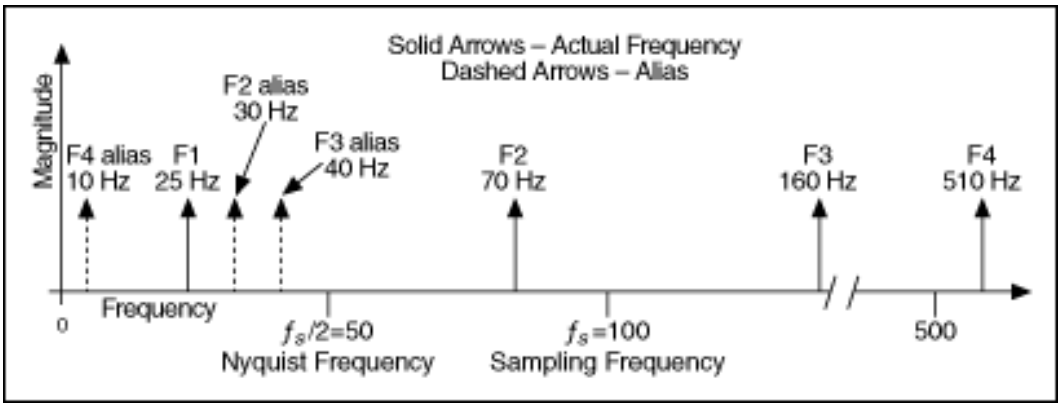

Figure 4.18 - Sampled signal components and aliased components [17]

The frequency of the aliased signals is the absolute value of the closest integer multiple of the sampling frequency minus the input frequency of the component that causes the aliasing. This is seen in (Eq. 4.6). From Figure 4.18 the aliased signal F2 alias is 30 Hz as |100-70|=30 Hz. For F4 alias, the closest integer multiple is 5, giving |5·100-510|=10 Hz [17].

$$f_a = |Z \cdot f_s - f_n| \qquad \text{(Eq. 4.6)}$$

$f_a = Frequency\ of\ aliased\ component$

$Z = Integer\ value$

$f_n = Frequency\ of\ component\ above\ Nyquist\ frequency$

To cope with aliasing and avoiding this problem an anti-alias filter can be applied. Before this topic is brought up, an important factor for a successful filtering operation will be the subject: the sampling rate, again. The highest frequency component of interest usually sets the sampling rate to 10 times the components frequency, as mentioned. When a filter is applied the cut-off frequency of the filter can be very close to the DC or the Nyquist frequency, and might have a slow convergence. To avoid this, the sampling rate can be increased if the cut-off frequency is too close to the Nyquist frequency. If the cut-off is too close to the DC the sampling rate can be decreased. In general, adjustments to the sampling frequency should be made only if problems are encountered [18].

The anti-alias filter is typically a low-pass filter used before the signal sampler. This is done to limit the bandwidth of the sampled signal to approximately or completely keep the bandwidth within the limit of the Nyquist frequency. In this way it is made sure there are no components in the measured signal that can cause problems regarding aliasing.

An anti-alias filter in practice is not ideal and will not be cutting the bandwidth exactly at the Nyquist frequency. It will either permit some aliasing to occur, or attenuate some frequencies close to the Nyquist frequency. To avoid both of these problems, oversampling is typically used for sampling of analog signals. In this way one can attenuate frequencies that actually are outside the band of interest, leaving the band of interest untouched. Problems regarding aliasing are also avoided. Another advantage with this is that oversampling can help reducing the filters rating as the components filtered out are better sampled, relaxing the filter demands which limits the filter cost [19].

4.1.4 How to measure current and voltage

To measure current and voltage signals in a power system a data acquisition system has to be designed for this specific purpose. Data acquisition is when the measured signal is gathered from the source and then digitized for storage and prepared for analysis and presentation. This is done for testing, measuring and automation applications. A complete data acquisition system consists of roughly five parts: transducers/sensors, signals, signal conditioning, hardware and software.

The data acquisition starts with measurements of the physical phenomenon that is going to be analysed. In this case where alternating voltage and current harmonics are the physical phenomenons, the signals are analog signals where the frequency is of importance. This means that the sampling rate is of importance for the results of the measurements. The levels of the measured signals are also of importance, as the magnitudes of the signals are used for calculation of THD and IHD. For harmonic components that are measured, they are added the total signal, meaning they are not measured as pure sinusoidal waveforms, symmetrical around the x-axis. This makes the shape important as well, as the harmonic components are seen with a voltage offset.

For most measurements a transducer is necessary for conversion of the physical phenomenon into a measurable signal. For current and voltage the measured signals are already readable for the data acquisition system. Transducers are commonly used for adjustments of the signal

magnitudes to fit within the input range of the measurement system. Another important attribute with the use of transducers for current measurements is safety. When large currents are measured, direct measurements can be dangerous to humans and measurement equipment. By adjusting the current level by using a current transducer this safety risk can be limited. Further, for systems with a settled mounting, for examples cables that are hard to dismount and connect directly to the measurement system, transducers/sensors which are clipped on around cables makes the installation of the measurement system very simple and easy [20].

For current sensors there are two types of output signals. Either a current output or a voltage output can be chosen for a current transducer, depending on which of the two the measurement system uses as input. The output signal is proportional to the measured signal on the transducers primary side. The relationship between the primary input signal and the secondary output is often given as 0.1V per ampere for voltage output transducers, and 500:5 CT for current output transformers.

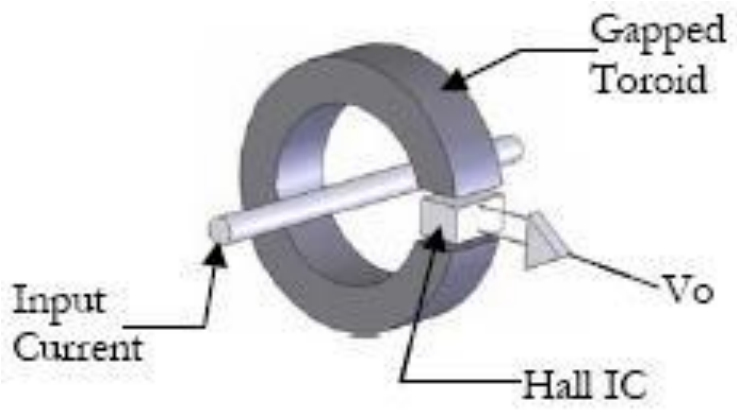

Figure 4.19 - Current transducer with voltage output [21]

For current transducers with a voltage output signal the sensors typically contain a precise burden resistor internally which allows the output to be a voltage signal. This makes current measurements very easy and flexible as the transducer can be connected to most measurement equipment as long as the voltage is within the equipment's voltage rating. Regarding safety, the voltage output signal is a low energy signal, and can safely be used by the user. Connecting and disconnecting the sensors won't damage them. However, due to the low energy, the signal is sensitive to interference from the outside, and connections via long cables are not recommended.

For the current output current transducer, known as a current transformer, the current output is a high energy signal that can cause damage to equipment and is hazardous for the user. The standard output is typically of 5A or 1A and cannot be connected directly to most equipment as it would cause damage. If the sensors are connected to an open circuit, the voltage occurring can be very high, permanently damaging the sensors. For this reason fuses are not used on the secondary side of a current transformer.

When choosing a transducer for a measurement system, one can choose between split core and open core CTs. For existing installations the split core CT is a good choice as it is easy to install in any system. The split core CT is more expensive than the solid core, but if rewiring of an existing system is difficult this is often the best choice. The solid core CT is cheaper than the split core, and also gives better readings. For measurements that require the best measurements this is the best solution, and also for testing of temporary lab set-ups the solid core is preferable due to cost and performance.

Figure 4.21 - Split core CTs [20]

Figure 4.20 - Solid core CTs [20]

After measurements are made the acquired data must be analysed, virtualized in a good way and stored if necessary. This is done with computer software programs. When choosing a data acquisition software there are some things one need to consider. The time it takes to learn the software, integration time of the software, performance and opportunities that comes with the software, available help like customer support, online communities/forums and available courses, and the stability, reliability and reputation of the software.

The data acquisition software can be ready-to-run software, where the measurement device can be plugged in and then a run button is pressed to get measurement results. This is very specific task solution good for specific tasks at that exact moment. Programmable software on the other hand allows more flexibility in the usage. It can be programmed to fit a larger range of measurement devices and it can be used for several specific tasks. The trade-off with programmable software is the time spent learning the programming and designing the programs for the different measurements.

The programming language must then be taken into account when programming software is chosen. The ANSI C/C++ for examples can be difficult and time consuming to learn. Easier programming like the graphical programming makes it easier and quicker to learn the software as it is more intuitive and built in a way that is more in the direction of an engineer's way of thinking.

To avoid much extra work the software must be able to communicate directly with the data acquisition hardware. This is to avoid work related to import and export of acquired data between the software and hardware. Post processing, analysis and storage are made less complicated by choosing software and hardware capable of communicating directly with each other.

The software of choice needs a good way of visualization and presentation of the results acquired. A good and easy presentation helps speeding up the analysis process and the understanding of the results from the measurements don't need any deeper analysis to get the information needed [21].

5 International measuring standards

For the measurements conducted in this project the following standards are applicable:

- IEC 61000-4-7:2009
- IEC 61000-4-30:2015

The IEC 61000-4-7 standard is a general guide on harmonics and interharmonics measurements and instrumentation. It is applicable for instrumentation intended for measuring spectral components in the frequency range up to 9 kHz and defines the measurement instrumentation intended for testing of equipment in accordance with emission limits given in certain standards (IEC 61000-3-2) as well as the measurement of harmonic currents and voltages in actual power systems.

The IEC 61000-4-30 standard is made for power quality measurement methods. It defines methods for measurement and interpretation of results for power quality parameters in AC power systems with a frequency of 50 Hz and 60 Hz. The parameters measured in this project; magnitude of supply voltage, voltage harmonics and current measurements are all covered by this standard.

5.1 IEC 61000-4-7:2009

5.1.1 The instrument

For the instrument, IEC 61000-4-7 specifies that the instrument should have following features:

- Input circuits with anti-aliasing filter
- A/D-converter including sample-and-hold unit
- Synchronization and window-shaping unit if necessary
- DFT-processor providing the Fourier coefficients a_k and b_k (“OUT 1”)

A test observation period, long enough to obtain successive measurement results that are within acceptable tolerance levels, is specified. This period is set to 200ms. For a 50Hz system this is 10 periods, while for a 60Hz system it is 12 periods.

Two classes are used for to define the measurement accuracy; class I and class II. Class II is a low-cost instrument, consistent with the requirements of the application. For emission tests

the class I instruments are required for harmonic levels near the limited values of harmonic distortion. These are the best and most accurate instruments. The accuracy can be seen in Table 5.1.

Table 5.1 - Accuracy requirements

Class	Measurement	Conditions	Maximum error
I	Voltage	$U_m \geq 1\%\ U_{nom}$	$\pm 5\%\ U_m$
		$U_m < 1\%\ U_{nom}$	$\pm 0.05\%\ U_{nom}$
	Current	$I_m \geq 3\%\ I_{nom}$	$\pm 5\%\ I_m$
		$I_m < 3\%\ I_{nom}$	$\pm 0.15\%\ I_{nom}$
	Power	$P_m \geq 150W$	$\pm 1\%\ P_m$
		$P_m < 150W$	$\pm 1.5W$
II	Voltage	$U_m \geq 3\%\ U_{nom}$	$\pm 5\%\ U_m$
		$U_m < 3\%\ U_{nom}$	$\pm 0.15\%\ U_{nom}$
	Current	$I_m \geq 10\%\ I_{nom}$	$\pm 5\%\ I_m$
		$I_m < 10\%\ I_{nom}$	$\pm 0.5\%\ I_{nom}$

$\boldsymbol{I_{nom} = Nominal\ current\ range\ of\ the\ measurement\ instrument}$
$\boldsymbol{U_{nom} = Nominal\ voltage\ range\ of\ the\ measurement\ instrument}$
$\boldsymbol{U_m, I_m\ and\ P_m = Measured\ values}$

The class I instruments are recommended for precise measurements. This is for examples to verify that the harmonic levels are within the regulations. Two different instruments of class I connected to the same signal will provide the same measurement results, indicating harmonic levels within and exceeding the levels allowed by the standards and regulations. The allowed phase shift between individual channels for a class I instrument should be smaller than $h \cdot 1°$.

The class II instruments are mainly recommended for survey measurements, but can also be used for emission measurements if the levels of harmonic distortion are of such level that the uncertainty won't affect the results. This means that the levels won't be exceeded, even if the uncertainty of the class II instrument is taken into account. In practice, this means that the measured values of harmonics should be lower than 90% of the allowed limits.

5.1.2 Current input

The current input circuit shall be suitable for the currents to be analysed, and the measurements shall be made directly. In case of the use of a current transformer the voltage input sensitivity range should be within 0.1V to 10V, where 0.1V is preferred. For direct current measurements with current input the preferred input ranges are 0.1A, 0.2A, 0.5A, 1A, 2A, 5A, 10A, 20A, 50A or 20A.

The current input circuits shall individually not excess 3VA for class II instrumentation. For class I instrumentation the voltage drop of the input shall not exceed $0.15V_{RMS}$. The current withstand should continuously be$1.2 \cdot I_{nom}$, and the 1 sec stress current of $10 \cdot I_{nom}$ shall not lead to any damage to the instrument. Regarding crest factor the instrument shall be able to handle a factor of 4 for current ranges up to $5A_{RMS}$, 3.5 for the $10A_{RMS}$ range and 2.5 for higher ranges. Further an overload indication is required.

5.1.3 Voltage input

The voltage input circuitry shall be suitable to the measured voltage. This goes for maximum voltage levels and the measured frequency. The accuracy of the measurements shall be kept up to $1.2 \cdot maximum\ voltage$ and the crest factor shall be at least 1.5 to provide sufficient measurements. Exception to this crest factor is for highly distorted voltages in industrial networks. Here a crest factor of at least 2 may be necessary. When overloaded, the instrument shall in any case give an indication of this.

The power absorption of the instrument's voltage input circuit shall not exceed 0.5VA at 230V. For high-sensitive inputs for voltages lower than 50V the channel's input resistance shall at least be 10kΩ/V.

The 1 sec stress input of AC voltage shall be of at least four times the input voltage setting or $1kV_{RMS}$, whichever is less, shall not lead to any damage to the instrument.

5.2 IEC 61000-4-30:2015

5.2.1 Classes of measurements

For each parameter covered by this standard there are two classes of measurements; A and S. The class A category is defined as follows:

"*This class is used where precise measurements are necessary, for example, for contractual applications that may require resolving disputes, verifying compliance with standards, etc. Any measurements of a parameter carried out with two different instruments complying with the requirements of Class A, when measuring the same signals, will produce matching results within the specified uncertainty for that parameter."*

The class S category is defined as follows:

"*This class is used for statistical applications such as surveys or power quality assessment, possibly with a limited subset of parameters. Although is uses equivalent intervals of measurement as Class A, the Class S processing requirements are much lower. Some surveys may assess power quality parameters of several measurement sites on a network; other surveys assess power quality parameters at a single site over a period of time, or at locations within a building or even within a single large piece of equipment."*

For an instrument that measures some or all of the parameters covered by the IEC 61000-4-30 it is preferable that the same class is used for all parameter measurements.

5.2.1.1 Measuring magnitude of the supply voltage

When the voltage of supplied is measured the measurement method is the same for both Class A and Class S measurements. Following description is given in the standard:

"The measurements shall be the RMS value of the voltage magnitude over a 10-cycle time interval for a 50 Hz power system or a 12-cycle time interval for a 60 Hz power system. Every 10/12-cycle interval shall be contiguous and not overlapping with adjacent 10/12-cycle intervals…"

For measurement uncertainty and measuring range following requirements are set for Class A and Class S:

- Class A: "*The measurement uncertainty shall not exceed ±0,1 % of U_{din}, over the range of 10 % to 150 % of U_{din}.*"
- Class S: "*The measurement uncertainty shall not exceed ±0,5 % of U_{din}, over the range of 20 % to 120 % of U_{din}.*"

5.2.1.2 Measuring voltage harmonics

Class A and Class B measurements are by the IEC 61000-4-30 standard set as the same requirements as Class I and Class II respectively, from the IEC 61000-4-7 standard.
See Table 5.1 for requirements.

In addition, measurements shall be made at least up to the 50^{th} harmonic component for Class I, and 40^{th} harmonic component for Class II.

For measurement uncertainty and measuring range, Class A has the same maximum uncertainty requirements as Class I from IEC 61000-4-7. The measuring range shall be 10 % to 200 % of Class 3 electromagnetic environment in IEC 61000-2-4.

Class S measurements shall have maximum uncertainty of twice the levels specified in IEC 61000-4-7 Class II. The anti-aliasing low-pass filter specified in IEC 61000-4-7 shall be optional.

5.2.1.3 Measuring current

"*Linked with voltage harmonics and interharmonics, the current harmonics and interharmonics can be useful to characterize the load connected to the network.*"

The measuring instrument for current measurements shall specify a full-scale RMS current, taking into account a crest factor of minimum 3.0.

For Class A measurements the measurement shall be made over the same period as for the voltage measurement in 5.2.1.1. For Class S measurements the manufacturer shall specify the RMS measurement method and the time interval used.

Measurement uncertainty for Class A shall not exceed ± 1 % of reading in the range of 10 % to 100 % of the specified full-scale RMS current. For Class S the measurement uncertainty shall not exceed ± 2 % of reading in the range of 10 % to 100 % of the specified full-scale RMS current.

For harmonic current measurement IEC 61000-4-7 is used for Class A. Class S measurements requires that the manufacturer shall specify measurement and aggregation methods.

5.2.2 Organisation of measurements

"The electrical quantity to be measured may be either directly accessible, as is generally the case in low-voltage systems, or accessible via measurement transducers."

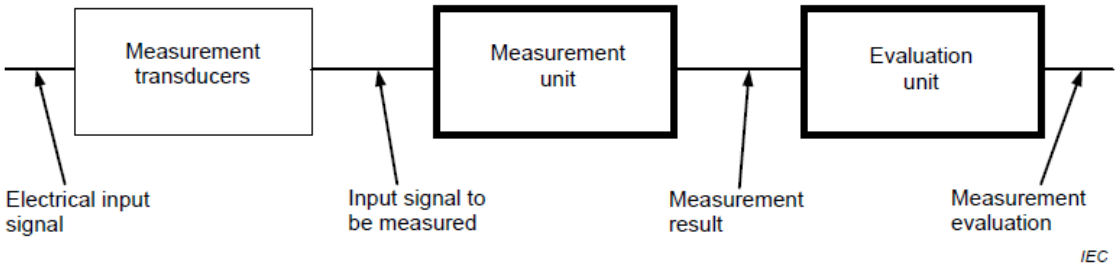

Figure 5.1 - Organisation of measurement

6 Identifying harmonic sources

As the data acquisition and analysis of the measured signal was the topic of the previous chapter, further calculations regarding identification of the harmonic injection from different sources and loads will be discussed in this chapter.

Several different methods have been proposed in previous literature. However, many of the methods have not included measurement uncertainty. Therefore [22] has taken the task of analysing some methods proposed including the uncertainty that comes with the methods. The results show that many of the methods have difficulties to identify which harmonic source is injecting specific components, but two methods seem to be quite accurate.

6.1 The harmonic voltage component method

The harmonic voltage component is one of the best methods. It is easy to apply and the results can be quite accurate. Some of the uncertainty tied to this method is related to low levels of harmonic components or the uncertainty of the systems Thevénin equivalent impedance. This will be seen later.

The method is based on analysing the harmonic component levels in a PCC for different cases. The base case is when the system is operating in normal mode, with all loads running. Next, a load is disconnected from the PCC then coupled to the system again while the next load is decoupled. By analysing the change in the harmonic component levels at PCC for each case it should be possible to identify the harmonic injection from the different loads connected to the PCC.

$$\Delta V_m(h) = |V_{PCC}(h)| - |V_{m0}(h)| \quad \text{(Eq. 6.1)}$$

$m = The\ disconnected\ load$

$h = Harmonic\ order$

$\Delta V_m(h) = Voltage\ change\ due\ to\ disconnection\ of\ load\ m\ for\ component\ h$

$V_{PCC}(h) = Voltage\ at\ PCC\ before\ disconnection\ of\ load$

$V_{m0}(h) = Voltage\ of\ component\ h\ at\ PCC\ after\ load\ m\ disconnection$

From (Eq. 6.1) it should be possible to define the harmonic contribution for the loads connected to the PCC. The contribution is then analysed for each harmonic component at a time. If $\Delta V_m(h)$ is positive, the load injects the specific harmonic component *h*. If $\Delta V_m(h)$ is negative, the load consumes the harmonic component, meaning it helps reducing the voltage distortion for the specific harmonic component in the PCC.

As an example, the test results from [22] are presented in Table 6.1. The 5^{th}, 7^{th}, 11^{th} and 13^{th} harmonic components are measured and set up in the table for four different buses in the test system, with the different loads connected to them. Also two different scenarios are considered, where configuration A, considering only one uncontrolled rectifier operating at rated power. Configuration B considers two rectifiers simultaneously connected to the PCC. One of the rectifiers in configuration B is an uncontrolled rectifier, and the other a controlled rectifier with a firing angle of 67.5°.

From Table 6.1 it can be read that for configuration A, bus 1 where the uncontrolled rectifier is located has higher values for all the harmonic components considered in the analysis. The positive values indicate that the load is injecting these components and the conclusion from the table is that the load at bus 1 is the main harmonic source.

Table 6.1 - Voltage values of harmonic components [22]

Bus	**1**	**2**	**3**	**4**
		Configuration A		
$\boldsymbol{\Delta V_m(5)}$	85.00	-3.97	-0.95	-2.81
$\boldsymbol{\Delta V_m(7)}$	656.00	9.69	-4.33	1.74
$\boldsymbol{\Delta V_m(11)}$	18.28	-1.19	-0.27	-0.86
$\boldsymbol{\Delta V_m(13)}$	9.10	-0.73	-0.16	-0.52
		Configuration B		
$\boldsymbol{\Delta V_m(5)}$	12..40	135.64	-3.70	-9.94
$\boldsymbol{\Delta V_m(7)}$	127.29	380.96	3.84	23.35
$\boldsymbol{\Delta V_m(11)}$	3.67	13.45	-0.22	-0.57
$\boldsymbol{\Delta V_m(13)}$	2.46	2.33	-0.12	-0.27

For configuration B, where the uncontrolled rectifier is located at bus 1, and the controlled rectifier is located at bus 2, it is clear that the values for bus 2 is much higher than for the other buses. Furthermore, the levels for bus 1 are still of positive value and higher than the values found at bus 3 and bus 4. This indicates that bus 2 is the main contributor to the harmonic injection, while bus 1 also contributes with harmonic injection, but not as much as bus 2.

The study measured the harmonic currents injected by the different nonlinear loads for the two configurations to compare the results of the test. The measured levels are shown in Table 6.2. Comparing the two tables to one another it can be concluded that the test results in Table 6.1 are valid.

Table 6.2 - Harmonic current injected by nonlinear loads [22]

Bus	**1**	**2**
	Configuration A	
$\|\boldsymbol{I_h(5)}\|$	8%	-
$\|\boldsymbol{I_h(7)}\|$	5%	-
$\|\boldsymbol{I_h(11)}\|$	2%	-
	Configuration B	
$\|\boldsymbol{I_h(5)}\|$	8%	25%
$\|\boldsymbol{I_h(7)}\|$	5%	7%
$\|\boldsymbol{I_h(11)}\|$	2%	3%

As mentioned, low levels of harmonic components can increase the uncertainty of the results. This is because of the uncertainty in the measurement equipment and other factors affecting the measurements. With small levels of harmonic voltages and currents the uncertainty of the measurements will be of greater significance, making the results more inaccurate, possibly resulting in wrong conclusions. Further, the system impedance was also mentioned as a factor causing uncertainty to the results of this method. This is when (Eq. 6.1) is rewritten to (Eq. 6.2), where the load harmonic voltage contribution, $\Delta V_m(h)$, is substituted with the harmonic current contribution $I_m(h)$ multiplied with the power system equivalent impedance [22].

$$V_{m0}(h) = V_{PCC}(h) + I_m(h)Z_m(h) \qquad \text{(Eq. 6.2)}$$

$I_m(h) = Current\ of\ load\ m$

$Z_m(h) = Power\ system\ equivalent\ impedance$

6.2 FIS method

FIS is short for fuzzy inference system. The FIS method is the method analysed in [22] which gave the best and most accurate results, with uncertainty taken into account. The method takes ground in several factors and equations. Still, some of these require deeper analysis of the measurements, making the requirements to the analysis software higher than for the harmonic voltage component method.

(Eq. 6.3) shows the calculation for the supply and loading quality index. Seen from the equation the calculation of this index requires input of the total three-phase active power and also the three-phase active power associated with the fundamental positive sequence component of voltage and current measured. For values where ξ_{slq}<1 the distortion is most likely injected by the load, while if ξ_{slq}>1, the load most likely consumes harmonic components.

$$\xi_{slq} = \frac{P_{\Sigma}}{P_{\Sigma+1}} \qquad \text{(Eq. 6.3)}$$

$\xi_{slq} = Supply\ and\ loading\ quality\ index$

$P_{\Sigma} = Total\ three - phase\ active\ power$

$P_{\Sigma+1} = Three - phase\ active\ power\ of\ positive\ sequence\ fundamental\ components$

Another factor used in the FIS method is the load and supply injected currents. This is used to define the harmonic global index. (Eq. 6.4) and (Eq. 6.5) show the calculations for the load and supply injected currents.

$$\left||I_{\Sigma_L}|\right|^2 = \sum_{h|P_{\Sigma h<0}} I_h^2 \qquad \text{(Eq. 6.4)}$$

$I_{\Sigma_L} = Active\ harmonic\ current\ injected\ by\ the\ load$

$P_{\Sigma h} = Active\ power\ of\ harmonic\ component\ h$

$I_h = Harmonic\ current\ component\ h$

$$\left||I_{\Sigma_S}|\right|^2 = \sum_{h|P_{\Sigma h>0, h\neq+1}} I_h^2 \qquad \text{(Eq. 6.5)}$$

$I_{\Sigma_S} = Active\ harmonic\ current\ injected\ by\ the\ source\ to\ the\ load$

For (Eq. 6.4), if $\left||I_{\Sigma_L}|\right|^2$ is greater than zero, the indication is that the load is injecting harmonic components to the PCC. Also, for (Eq. 6.5), if $\left||I_{\Sigma_S}|\right|^2$ is greater than zero, the indication is that the source is injecting harmonic components to the load. The greater these values are, the greater the levels of the injected harmonics.

The last index of interest in the FIS method is the ratio of the global THD factors of currents and voltages, i.e.

$$\eta^+ = \frac{GTHD_{I+}}{GTHD_{U+}} \qquad \text{(Eq. 6.6)}$$

where

$$GTHD_{I+} = \sqrt{\frac{I_\Sigma^2}{I_{\Sigma+1}^2 - 1}} \qquad GTHD_{U+} = \sqrt{\frac{U_\Sigma^2}{U_{\Sigma+1}^2} - 1} \qquad \text{(Eq. 6.7)}$$

$U_\Sigma = Collective\ RMS\ values\ of\ voltage$

$I_\Sigma = Collective\ RMS\ values\ of\ current$

$U_{\Sigma+1} = Collective\ RMS\ values\ of\ fundamental\ positive\ sequence\ voltages$

$I_{\Sigma+1} = Collective\ RMS\ values\ of\ fundamental\ positive\ sequence\ currents$

The calculations of (Eq. 6.6) can be problematic when the value of the distortion is low in (Eq. 6.7), and the factors are close to zero. Also, with uncertainty taken into account the values under the square root may become negative, giving problems with the calculations. For these reasons [23] has proposed alternative indices seen in (Eq. 6.8) and (Eq. 6.9).

$$GTHD_{I+}{}^2 + 1 = \frac{I_\Sigma^2}{I_{\Sigma+1}^2} \qquad GTHD_{U+}{}^2 + 1 = \frac{U_\Sigma^2}{U_{\Sigma+1}^2} \tag{Eq. 6.8}$$

and their ratio

$$\eta^{+^2} = \frac{I_\Sigma^2}{U_\Sigma^2} \cdot \frac{U_{\Sigma+1}^2}{I_{\Sigma+1}^2} \tag{Eq. 6.9}$$

Each of the indices that are defined in (Eq. 6.3), (Eq. 6.4), (Eq. 6.5) and (Eq. 6.6) are not capable of identifying the sources injecting the harmonic components by themselves. To be able to identify the sources injecting the harmonic components the indices must be evaluated together. Their global analysis allows with deeper evaluation of the results identification of the sources injecting harmonic distortion and those suffering from the harmonic distortion. The level of the distortion, either injected or suffered, can also be found with this method [23].

The further analysis of the indices is in [23] done with the Mamdani method, and the mentioned indices are used as input variables to the implemented FIS. This is as mentioned the method of harmonic injection detection that came out the best in [22], but the method is also demanding in term of input values and the analysis of the obtained results compared to the harmonic voltage component method. Due to this the FIS method will in this project only be described for information. The demands of the method were not fulfilled due to lack of time. Therefore the FIS method is not considered any further in this project, but the provided theory is included as inspiration for further work.

7 Laboratory testing

7.1 Testing conditions

For testing of the data acquisition system and the harmonic source identification methods described in 6.1 a laboratory testing set-up is put together. The system consists of three different loads with different harmonic footprints. A linear load with a resistor coupled in series with an inductor for each phase, star connected between the three phases. Two non-linear loads are connected for harmonic pollution to the system. One is a 6-pulse diode bridge rectifier, and another one is a 6-pulse thyristor bridge rectifier with adjustable firing angle.

The three loads are connected to a PCC, supplied with power from a 50 Hz, 230V stiff three-phase power system.

This set-up allows testing of the data acquisition system at several points and the three loads with different harmonic footprint allows the harmonic source identification methods to be tested.

7.2 NI compactDAQ hardware

National Instruments is a supplier of measurements systems. In general they supply data acquisition solutions, including different hardware solutions and software for further analysis of the sampled data.

For data acquisition and logging National Instruments offers a data acquisition system named compactDAQ, where DAQ is short for data acquisition. This is a very reliable PC based measuring hardware unit that can be adjusted to fit different measurements. The system is built up by three different main units: sensors for making the measured signals readable for the system, DAQ device for gathering the measurements through signal conditioning and analog-to-digital conversion, and at last a computer with driver software and application software for storage, presentation and analysis of the measurement.

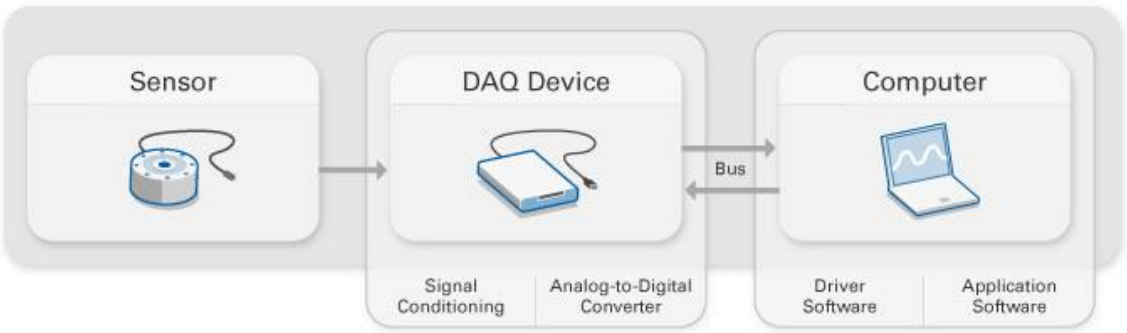

Figure 7.1 - National Instruments DAQ system [24]

The compactDAQ system consists of a chassis, NI C-series I/O modules and software. The chassis is connected to a computer through a USB cable, Ethernet, Wi-Fi or as stand-alone with an internal controller. The system is made to fit all kind of electrical or sensor based measurement systems [24].

For the laboratory testing system requirements a 4-slot cDAQ-9174 USB chassis is used. This chassis is designed to be small and portable. It can be used for several purposes, depending on the I/O modules used. It has four 32-bit general-purpose counter/timers built in which can be accessed through the NI C series modules that are used together with the chassis [25].

Figure 7.2 - NI cDAQ-9174 [25]

For current measurements a NI 9227 C series module is used. This module is designed for measurements up to $5A_{RMS}$ continuous measurement, with a peak tolerance of 14A. The isolation is channel-to-channel. Sampling frequency is up to 50 kS/s per channel, and sampling can be done simultaneous for all the four input channels without reducing the sampling frequency for the channels. ADC resolution is 24-bit, which is very good, allowing

accurate measurements for basically all current magnitudes. The isolation is CAT II, and the measurement range is $250V_{RMS}$ channel-to-channel. Regarding aliasing, the NI 9227 has an inbuilt anti-aliasing filter for the input channels [26].

Figure 7.4 - NI 9227 current module [25]

Figure 7.3 - NI 9225 voltage module [26]

For voltage measurements a NI 9225 C series module is used. This module is designed for measurements up to $300V_{RMS}$ phase-to-phase. The isolation is CAT II, with a $600V_{RMS}$ channel-to-channel withstand. There are three input channels, each with a sampling rate of 50 kS/s, and a 24-bit ADC resolution, giving very accurate measurements. To avoid aliasing, each channel has a built-in anti-alias filter for this module as well [27].

Table 7.1 - Module specifications

	NI 9225	**NI 9227**
Signal	Voltage	Current
Range	$5A_{RMS}$, $14A_{peak}$	$300V_{RMS}$
Channels	4	3
Resolution	24-bit	24-bit
Sampling rate	50 kS/s pr. channel	50 kS/s pr. channel
Isolation	$250V_{RMS}$ ch-to-ch, CAT II	$600V_{RMS}$ ch-to-ch, CAT II
Anti-alias filter	Yes	Yes

For the laboratory test system these two modules are within the requirements for harmonic analysis, satisfying the requirements from the standards (see 5). The 50 kS/s sampling rate

gives measurements up to approximately the 500th harmonic component. Also, both voltage and current levels are within the respective magnitudes in the test system as long as the system's load currents are kept under a total demand of $5A_{RMS}$. This allows direct measurements as the CAT II isolation also is satisfying for the test systems levels. The 24-bit resolution makes sure that even small voltage and current levels can be accurately measured for each load and the PCC.

For measurements on power systems with higher voltage and current levels National Instruments delivers more modules that can be applied for these systems. The highest voltage rating for a NI voltage module is $400V_{RMS}$ phase-to-phase and $800V_{RMS}$ phase-to-neutral. This is the NI 9244 module with three input channels, with the same specifications as the NI 9225 voltage module, just with a higher voltage input range. For current measurements the NI 9227 module is the module with the highest current input range. For measurements of currents above $5A_{RMS}$ it is therefore necessary with current transducers. This allows the use of voltage input modules as well as current input modules for current measurements, depending on the current transducer's output signal. For this purpose the NI 9227 current module is still relevant. For voltage output current transducers there are several modules to choose from. The mentioned voltage modules (NI 9225 and NI 9244) are some examples, and also the NI 9239 module with a ±10V input range with four input channels is sufficient. The specifications are all the same for the mentioned modules except from the CAT III isolation for the NI 9244 module and the input ranges [28] [29].

7.3 NI LabVIEW software

LabVIEW is a software for programming delivered by National Instruments. The programming is performed on a graphical platform, making it more intuitive and easier to understand, and predefined building blocks for different purposes which are dragged and dropped into place makes the programming quick and simple [30].

Together with LabVIEW a number of templates and sample projects are included. As there are examples for almost all kind of measurements one can study different solutions for different applications, giving more ideas to how to solve one owns programming challenges. National Instruments got online self-paced courses where different parts of the programming is made step by step. Furthermore, assignments are given for each part of the online course,

giving the user the opportunity to use and test what was learned from the course. Online forums and help from National Instruments are available if further help is needed.

As National Instruments also is the provider of the hardware, the communication and integration between software and hardware is no problem. With the compactDAQ measurement system it is just to plug in the USB cable from the chassis to a computer with LabVIEW installed. With LabVIEW's own block for sampling from communicating with the DAQ system, all needed for sampling are some inputs in the blocks, and then it's just to press "play" and the sampling is done.

For presentation of the measured and processed sampled data, LabVIEW got its own front panel where input values can be set and output, like waveform, harmonic spectrum, power values, phasors etc. can be presented. This front panel can be set up in the way the user wishes, depending on what information is crucial and of interest.

For this project, measuring harmonic components for current and voltage, a custom made program has been designed in LabVIEW. The block diagram can be seen in Figure 7.5. The blocks used for measuring both current and voltage inputs are the same. This is because the digital signal analysed by LabVIEW is equal for all kinds of measured signals. The input range of the blocks in LabVIEW has no limits, meaning the input signal is only limited by the hardware ratings.

The program works from left to right. It starts with the blocks named *DAQ Assistant*, which are the blocks communicating with the DAQ hardware. Here the signal type and channels of the measurement modules are specified. For the measurements in this project all voltage channels are in use, as the NI 9225 voltage module got only three input channels. This is configured in the top DAQ Assistant block in Figure 7.5. For the NI 9227 current module the three first channels are used for the three phase measurements, configured in the lower DAQ Assistant block in Figure 7.5. Further, sampling rate and number of samples is set in these blocks [31].

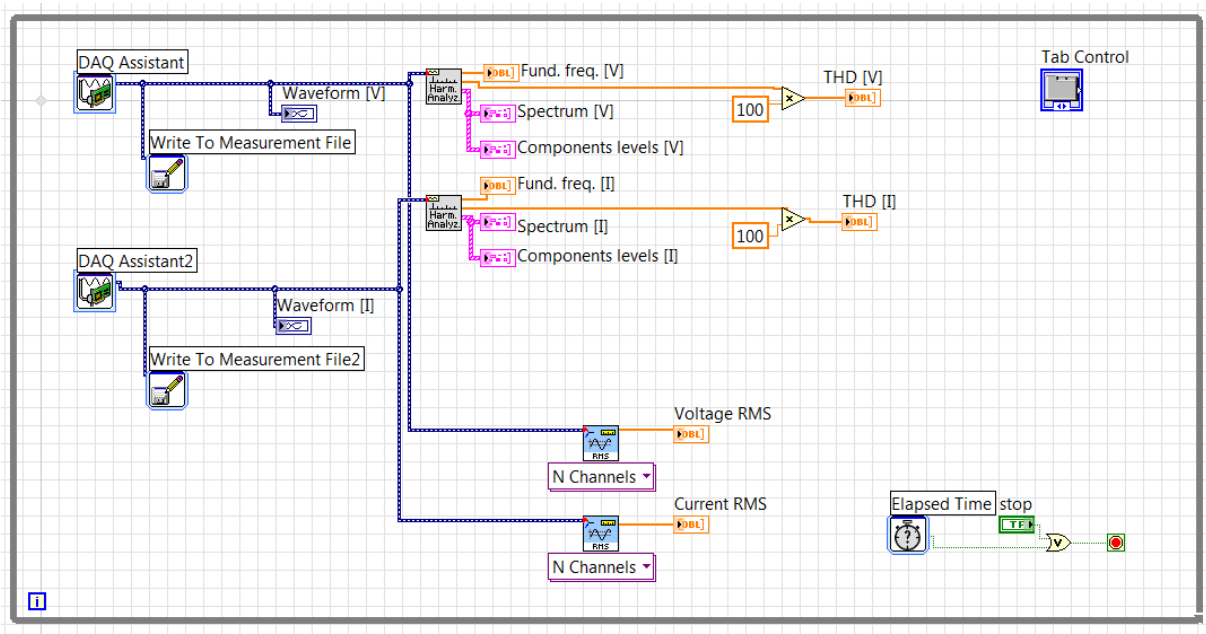

Figure 7.5 - LabVIEW program for harmonic analysis

The sampling rate is set to the maximum, 50,000 Hz, and the number of samples is set to 25.000, meaning a measuring time of 0.5 seconds for a 50 Hz system. The number of periods is then 30. This is higher than the measurement window specified in the IEC 61000-4-7 standard, but as the measurements are made for a steady state system without any transients or fluctuating currents or voltages this won't affect the measurements. If any, the measurements will be more accurate.

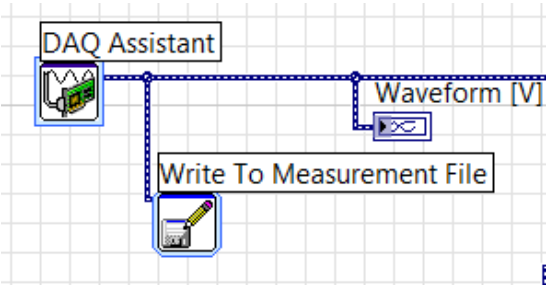

Figure 7.6 - Measurement, data storage and graphical window blocks

The VI block *Write To Measurement File* is a block used for saving the measured data. It takes the measured signals as an input and then creates a text file (.lvm), a binary file (.tdm/.tdms) or a Microsoft excel file (.xlms), which can be chosen by the user. The storage name and the storage location on the hard drive can be specified in the block. In this way the measured signals is saved for later analysis without having the compactDAQ system running and connected [32].

The *Waveform Graphs* VI is a block used for graphical display of one or more measured signals. It plots only single-valued functions, as in $y = f(x)$, with points evenly distributed along the x-axis, such as the time-varying current and voltage waveforms. The data output from the *DAQ Assistant* is a dynamic data signal which carries the start time and a delta *t*. The *Waveform Graph* block uses this information to build the waveform in a graphical output window on the front panel of the LabVIEW VI. An example output graph can be seen in Figure 7.6, named "Waveform [V]" as it displays the voltage waveform at the front panel.

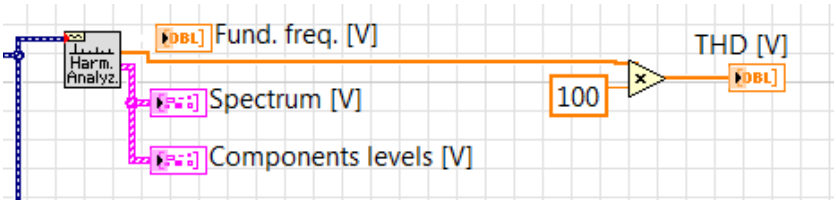

Figure 7.7 - Harmonic Distortion Analyser block

For the harmonic analysis of the measured signals a *Harmonic Distortion Analyser* VI block is used, as seen in Figure 7.7. The outputs from this block are of great interest for this project. The provided information is THD, detected fundamental frequency and all harmonic amplitude levels [33].

The input can be either a single channel measurement or as in this case a multichannel measurement. The dynamic data from the DAQ Assistant is automatic converted into an array of input time-domain signals at the block's signal input. This can be seen by the red dot at the input in Figure 7.7. The block analyses the signals by fast Fourier transformation (FFT). The spectrum output is achieved by discrete Fourier Transformation (DFT), a method that converts the digitized signal in the time domain into a frequency domain signal, giving the magnitudes of the different harmonic components related to their frequency. The THD is calculated by (Eq. 2.10).

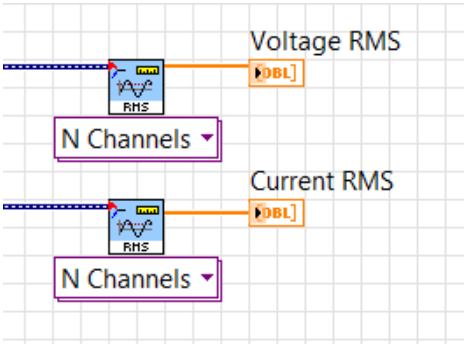

Figure 7.8 - Voltage and Current RMS measurements

The RMS measurements are mainly used for information on the measured magnitudes in the power system. This is for safety of the equipment, making sure the RMS values are within the levels the equipment is designed for.

The *RMS* VI block seen in Figure 7.8 takes in the three phase signal from the DAQ Assistant and converts in into a waveform signal containing the start time, t0, the time interval between the data points in the waveform, dt, and the data values of the waveform, Y. The RMS is calculated with the true RMS method, giving the exact RMS value of the signals measured. Further in the figure a numerical indicator is connected to the RMS output of the RMS block. This block displays the RMS values of the measured signals in the front panel of the VI [34].

Down in the right corner in Figure 7.5 an *Elapsed Time* VI block can be seen together with a stop button, connected to the loop condition of the while loop represented by the grey frame. This is to make sure the VI can be stopped, either automatically by the time set in the elapsed time block, or by the stop button shown on the front panel. The time set for the while loop represented by the grey frame is the same as the sampling time: 0.5 seconds.

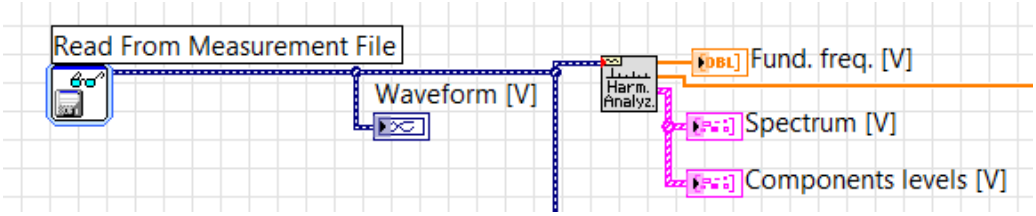

Figure 7.9 - Read from Measurement File

For analysis of the measurements that were saved, the DAQ Assistant VI block is replaced by the *Read From Measurement File* VI block. In this block the files saved from other measurements can be selected and used again in further analysis is required. This allows

analysis of the measurements outside the laboratory and without the DAQ system hardware connected to the computer [35].

7.4 Laboratory set-up and testing procedure

For testing of the measurement equipment and the harmonic injection identification methods described in 6.1, a system with following specifications has been set up in the laboratory:

- Three phase, 230V_{RMS}, 50Hz stiff network main feed
- Three different loads
    - RL series load
        - Star connection
        - Z_{ph}=90+j54 [Ω]
    - 6-pulse diode bridge rectifier with resistive DC load
        - R_{DC}=253Ω
    - 6-pulse thyristor rectifier with resistive DC load
        - Firing angle set to 20°
        - R_{DC}=221Ω

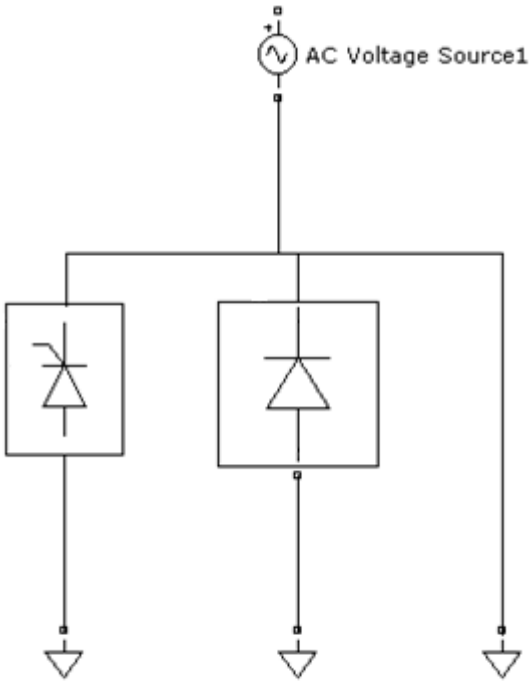

Figure 7.10 - SLD of laboratory set-up

The three loads are connected to a PCC. Measurements are in general made at this point for the analysis to be made later. The NI 9225 voltage module is coupled in parallel with the loads at the PCC. The measured voltage is phase-to-phase voltage. Channel 1 is measuring between phase A and phase B. Channel 2 measured between phase B and phase C. Channel 3 measures between phase C and phase A. The first mentioned phase is the positive input, and the second mentioned phase is the negative input at the measurement module, respectively.

The NI 9227 current module is connected in series with the loads, where the channels are measuring the phase currents. The connection is made between the AC voltage source and the PCC with the AC voltage source side as the positive input and the PCC side connected to the negative input on the current module channels. Channel 1 is connected in series to phase A, channel 2 to phase B and channel 3 to phase C.

The testing must have enough configurations for the harmonic voltage component method to be tested. A total of four measurements configurations are defined for this project. These are:

1. All loads running
2. Disconnected RL load, other loads running
3. Disconnected diode bridge load, other loads running
4. Disconnected thyristor bridge, other loads running

In addition to these four configurations each load is also measured individually where all other loads are disconnected. This is to have reference harmonic levels for comparison between test results and real individual harmonic magnitudes to see the accuracy and validity of the analysis results.

The range of harmonics to be measured and analysed will be limited. Due to the laboratory test systems limitations regarding power rating of the loads, no high order harmonic sources and the stiff AC voltage source, the harmonic levels considered in this project is limited to the 17^{th} harmonic. For the voltage harmonic distortion levels the stiff AC voltage source will limit the impact of the non-linear loads, making the evaluation of higher order components meaningless due to the low levels.

At last an active harmonic filter is connected to the PCC to measure the effect of the filter. Due to differences between an actual maritime power system and the laboratory test system, the measured effects can be hard to measure and see. Therefore only the effect of the filter will be documented in this project without any further analysis of the filters performance.

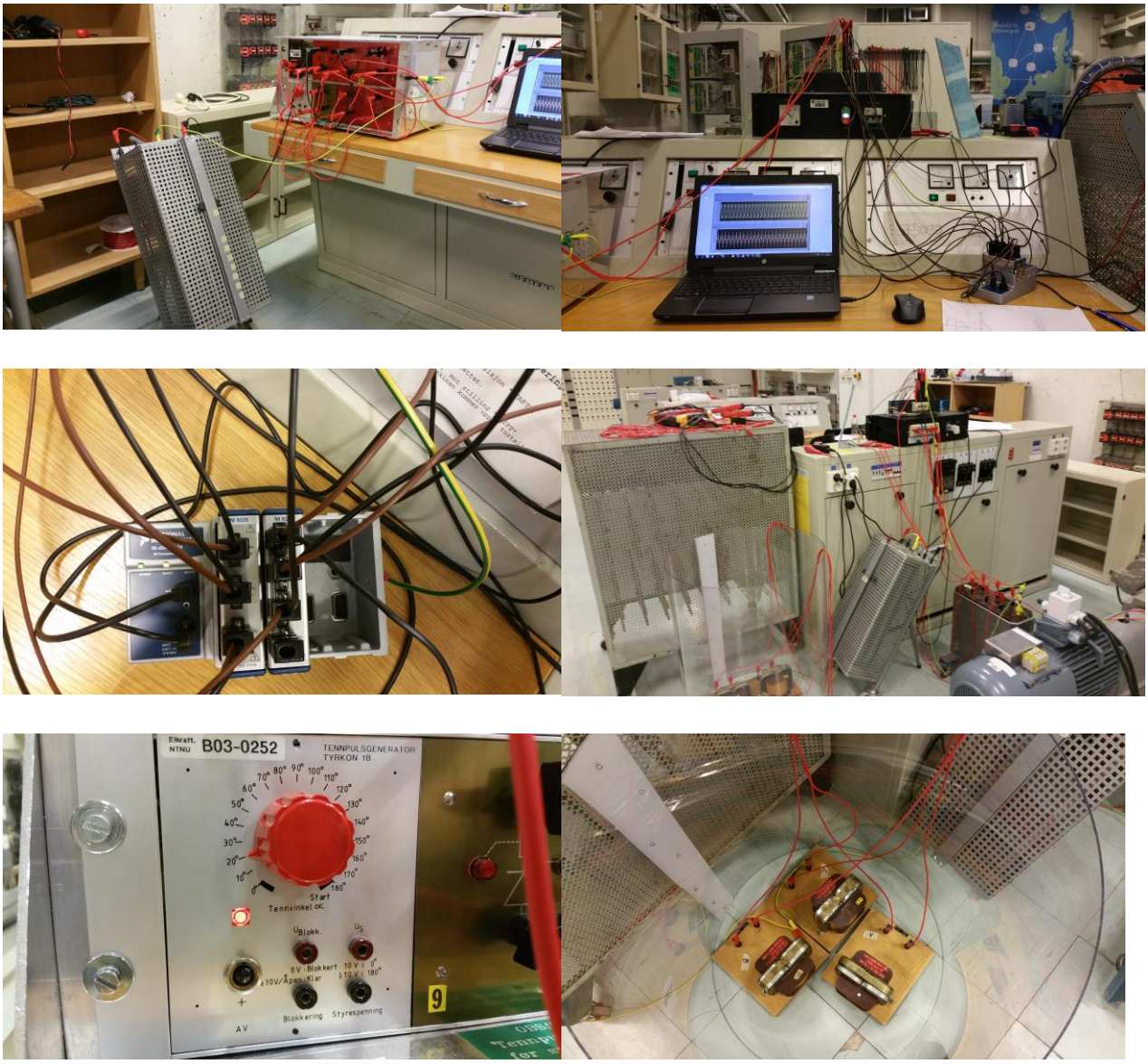

Figure 7.11 - Pictures from the laboratory set-up

The active harmonic filter used for this project is the same as used in [36]. The control system and the theory used for control of the filter will not be rendered for simplicity. For further information on the applied filter the reader is referred to [36].

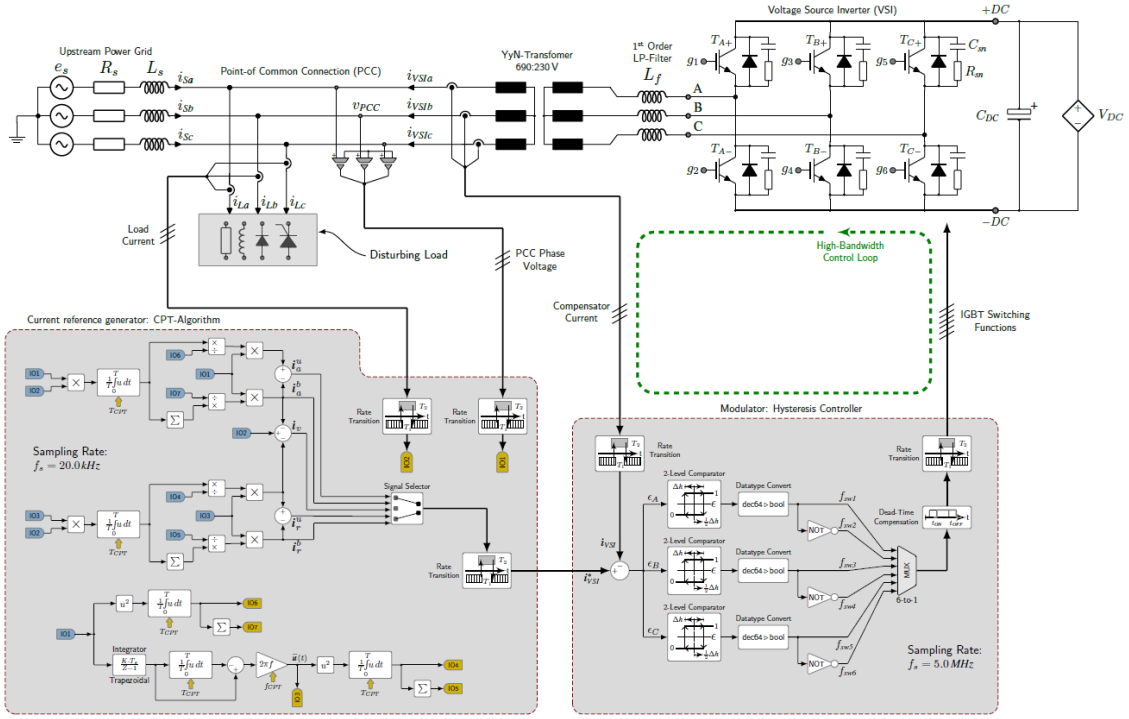

Figure 7.12 - Parallel AHF arrangement [36]

Table 7.2 - AHF technical details [36]

Equipment	Specifications
Converter system	P_n = 20 kW; V_{DC} = 500 V; L_f = 2.0mH R_f = 0:1, IGBTs: SKM 400GB 123D
Voltage source	230 VAC_{RMS} stiff 3-phase 50 Hz network
DC regulator parameters	K_p = 0.05 and T_i = 1.05 (PI-type)
Current transducers	Hall effect device LEM LA 55-P
Voltage transducers	Hall effect device LEM LV25-800
Real-time controller	OPAL-RT OP5600 simulator (CPU) Xilinx Virtex-6 ML605 kit (FPGA)
Data sampling	50.0 kHz, 64-bit floating-point format (CPU) 0.50 MHz, 16-bit fixed-point format (FPGA)

8 Measurement results

The measurements made according to the four different configurations listed in 7.4 gave the results given in the following tables. The values gives is the peak value of the given harmonic component in the left column of the tables. The measurements were made with both the NI compactDAQ system designed for this project purpose and a ELSPEC G4500 BLACKBOX PQA measurements device for comparison of the measurements.

For the voltage measurements following harmonic magnitudes were measured:

Table 8.1 - IHDv magnitudes for configuration 1

Configuration 1: All loads running						
	NI compactDAQ			ELSPEC G4500 BLACKBOX PQA		
Phase:	**AB**	**BC**	**CA**	**AB**	**BC**	**CA**
V(h=3)	0,1522	0,4942	0,3740	0,055	0,307	0,337
V(h=5)	1,8600	1,5700	1,9200	0,722	0,326	0,460
V(h=7)	1,2500	1,0700	1,0900	1,316	1,141	1,178
V(h=9)	0,5262	0,1739	0,3587	0,109	0,040	0,091
V(h=11)	0,9179	0,8955	0,7592	0,356	0,354	0,368
V(h=13)	0,8378	0,7765	0,8110	0,498	0,554	0,573
V(h=15)	0,4375	0,1153	0,3488	0,055	0,000	0,000
V(h=17)	0,3509	0,1885	0,2006	0,276	0,235	0,247

Table 8.2 - IHDv magnitudes for configuration 2

Configuration 2: Disconnected RL load						
	NI compactDAQ			ELSPEC G4500 BLACKBOX PQA		
Phase:	**AB**	**BC**	**CA**	**AB**	**BC**	**CA**
V(h=3)	0,1522	0,4942	0,3740	0,280	0,337	0,022
V(h=5)	1,8600	1,5700	1,9200	0,902	0,494	0,643
V(h=7)	1,2500	1,0700	1,0900	0,110	0,000	0,078
V(h=9)	0,5262	0,1739	0,3587	1,149	0,994	10,12
V(h=11)	0,9179	0,8955	0,7592	0,360	0,280	0,354
V(h=13)	0,8378	0,7765	0,8110	0,727	0,729	0,692
V(h=15)	0,4375	0,1153	0,3488	0,301	0,091	0,274
V(h=17)	0,3509	0,1885	0,2006	0,280	0,129	0,230

Table 8.3 - IHDv magnitudes for configuration 3

Configuration 3: Disconnected diode bridge load						
	NI compactDAQ			ELSPEC G4500 BLACKBOX PQA		
Phase:	**AB**	**BC**	**CA**	**AB**	**BC**	**CA**
V(h=3)	0,1561	0,3958	0,2453	0,361	0,398	0,101
V(h=5)	1,4200	1,1000	1,5300	0,652	0,277	0,519
V(h=7)	1,5900	1,4400	1,3700	1,331	1,167	1,207
V(h=9)	0,5516	0,1971	0,3558	0,315	0,099	0,212
V(h=11)	0,8961	0,9348	0,7607	0,291	0,198	0,270
V(h=13)	0,7678	0,6990	0,7271	0,782	0,713	0,754
V(h=15)	0,4391	0,1345	0,3354	0,320	0,088	0,282
V(h=17)	0,0884	0,2933	0,2368	0,099	0,088	0,077

Table 8.4 - IHDv magnitudes for configuration 4

Configuration 4: Disconnected thyristor bridge load						
	NI compactDAQ			ELSPEC G4500 BLACKBOX PQA		
Phase:	**AB**	**BC**	**CA**	**AB**	**BC**	**CA**
V(h=3)	0,3239	0,3035	0,6226	0,074	0,360	0,398
V(h=5)	1,5200	1,2200	1,4700	0,744	0,376	0,539
V(h=7)	1,2300	0,9965	1,0500	10182	0,992	0,973
V(h=9)	0,2669	0,1888	0,0447	0,151	0,094	0,091
V(h=11)	1,0100	1,1500	1,0600	0,392	0,429	0,406
V(h=13)	0,7463	0,7929	0,7830	0,576	0,580	0,626
V(h=15)	0,0540	0,0526	0,0115	0,040	0,022	0,022
V(h=17)	0,3385	0,3525	0,3247	0,247	0,200	0,190

For the current measurements following harmonic components magnitudes were measured for given configurations by the NI compactDAQ system:

Table 8.5 - IHDi magnitudes for configuration 1

Configuration 1: All loads running			
Phase:	**A**	**B**	C
I(h=3)	0,5474	0,3405	0,2542
I(h=5)	0,4451	0,4036	0,4678
I(h=7)	0,1767	0,1731	0,1379
I(h=9)	0,1736	0,1053	0,0741
I(h=11)	0,1843	0,1266	0,1777
I(h=13)	0,5294	0,0520	0,0249
I(h=15)	0,1164	0,0724	0,0542
I(h=17)	0,1059	0,0586	0,0721

Table 8.6 - IHDi magnitudes for configuration 2

Configuration 2: Disconnected RL load			
Phase:	**A**	**B**	C
I(h=3)	0,5444	0,3457	0,2471
I(h=5)	0,4624	0,4100	0,4779
I(h=7)	0,1606	0,1598	0,1248
I(h=9)	0,1740	0,1050	0,0756
I(h=11)	0,1826	0,1204	0,1655
I(h=13)	0,0297	0,0319	0,0065
I(h=15)	0,1172	0,0704	0,0551
I(h=17)	0,0932	0,0571	0,0508

Table 8.7 - IHDi magnitudes for configuration 3

Configuration 3: Disconnected diode bridge load			
Phase:	**A**	**B**	C
I(h=3)	0,5476	0,3620	0,2304
I(h=5)	0,1730	0,1277	0,2001
I(h=7)	0,1091	0,1513	0,1206
I(h=9)	0,1753	0,1065	0,0756
I(h=11)	0,0757	0,0394	0,0989
I(h=13)	0,0797	0,0103	0,0874
I(h=15)	0,1186	0,0722	0,0537
I(h=17)	0,0578	0,0159	0,0665

Table 8.8 - IHDi magnitudes for configuration 4

Configuration 4: Disconnected thyristor bridge load			
Phase:	**A**	**B**	C
I(h=3)	0,0079	0,0099	0,0030
I(h=5)	0,2713	0,2740	0,2739
I(h=7)	0,1418	0,1389	0,1385
I(h=9)	0,0012	0,0012	0,0003
I(h=11)	0,1154	0,1165	0,1172
I(h=13)	0,0753	0,0740	0,0737
I(h=15)	0,0011	0,0006	0,0007
I(h=17)	0,0694	0,0704	0,0707

The THDv for the four configurations were as seen in Table 8.9:

Table 8.9 - THDv for the configurations

THDv [%]						
	NI compactDAQ			ELSPEC G4500 BLACKBOX PQA		
Phase:	**AB**	**BC**	**CA**	**AB**	**BC**	**CA**
Configuration 1	0,8864	0,1686	0,8471	1,0998	0,7866	0,9356
Configuration 2	0,8475	0,7027	0,7419	1,0900	0,7875	0,9078
Configuration 3	0,8431	0,7416	0,7915	1,0906	0,7696	0,8897
Configuration 4	0,7934	0,7186	0,7791	0,7752	0,6666	0,6853

The THDi for the four configurations were as given in following Table 8.10:

Table 8.10 - THDi for the configurations

THDi [%]						
	NI compactDAQ			ELSPEC G4500 BLACKBOX PQA		
Phase:	**A**	**B**	**C**	**A**	**B**	**C**
Configuration 1	22,2038	15,3923	13,6766	23,262	16,680	14,227
Configuration 2	40,5082	25,6035	21,6018	42,697	27,567	22,742
Configuration 3	26,8902	17,5580	12,0970	28,255	18,525	12,869
Configuration 4	12,2891	12,1402	12,2387	12,749	12,901	12,672

The output waveforms for the four configurations analysed shown on the LabVIEW VI front panel can be found in appendices together with the output of the harmonic component levels given on the front panel. Harmonic component spectrums are found in the appendices.

For the measurements made with an AHF coupled to the test systems PCC following THD levels were measured for configuration 1:

Table 8.11 - THD measurements with an AHF at PCC

AHF measurement THD levels for configuration 1			
	NI compactDAQ		
THDv [%]	0,7206	0,7802	0,8069
THDi [%]	6,0562	7,4569	8,8209

9 Analysis

9.1 Harmonic voltage component method

The informative parameters obtained from the VI designed in LabVIEW are enough information to test the harmonic voltage component method. As the current harmonic components also are measured these will be analysed as well in the same way, with the same method to check for any compliance or difference between current and voltage harmonic results.

The following tables are the results of the harmonic voltage (and current) component method given by (Eq. 6.1). The given values of the voltage and current changes are in percentage, referred to the PCC voltage before load disconnection, measured in configuration 1.

Table 9.1 - Voltage and current components change for configuration 2

Configuration 2: Disconnected RL load							
Phase:	**AB**	**BC**	**CA**		**A**	**B**	**C**
ΔV(h=3)	0,00 %	0,00 %	0,00 %	**ΔI(h=3)**	0,53 %	-1,52 %	2,82 %
ΔV(h=5)	0,00 %	0,00 %	0,00 %	**ΔI(h=5)**	-3,88 %	-1,60 %	-2,16 %
ΔV(h=7)	0,00 %	0,00 %	0,00 %	**ΔI(h=7)**	9,12 %	7,64 %	9,49 %
ΔV(h=9)	0,00 %	0,00 %	0,00 %	**ΔI(h=9)**	-0,25 %	0,29 %	-2,01 %
ΔV(h=11)	0,00 %	0,00 %	0,00 %	**ΔI(h=11)**	0,94 %	4,89 %	6,86 %
ΔV(h=13)	0,00 %	0,00 %	0,00 %	**ΔI(h=13)**	94,39 %	38,65 %	73,78 %
ΔV(h=15)	0,00 %	0,00 %	0,00 %	**ΔI(h=15)**	-0,66 %	2,75 %	-1,62 %
ΔV(h=17)	0,00 %	0,00 %	0,00 %	**ΔI(h=17)**	12,04 %	2,64 %	29,57 %

For configuration 2, where the RL load is disconnected from the test system the obtained voltage and current components changes are listed in Table 9.1. Based on the harmonic voltage components method which in this case also is applied for the current harmonic components as well, the table shows that there is no change in the harmonic voltage component levels. This indicates that the RL load has no effect on the voltage harmonic distortion in the system.

Looking at the change in the current components the only changes worth mentioning are for the 13^{th} and 17^{th} harmonic components. The indications from the table are that the RL load

injects 13th harmonic current to the test system as well as some 7th and 17th harmonic current. The other components are of such small magnitude that with some uncertainty taken into account no conclusion can be made in a certain manner.

Comparing the levels in the table with the levels when the RL load is measured by itself found in Table 9.5, it can be seen that the current component changes are quite similar to the obtained results. The big difference is the 13th harmonic component. The voltage harmonic components are hard to say something about as the changes obtained by the harmonic voltage component method are zero and the voltage harmonic components are completely supplied by the source in this case, according to the results from the tested method.

Table 9.2 - Voltage and current components change for configuration 3

Configuration 3: Disconnected diode bridge load							
Phase:	**AB**	**BC**	**CA**		**A**	**B**	**C**
ΔV(h=3)	-2,56 %	19,91 %	34,43 %	**ΔI(h=3)**	-0,05 %	-6,32 %	9,36 %
ΔV(h=5)	23,66 %	29,94 %	20,31 %	**ΔI(h=5)**	61,14 %	68,36 %	57,22 %
ΔV(h=7)	-27,20 %	-34,58 %	-25,69 %	**ΔI(h=7)**	38,24 %	12,60 %	12,55 %
ΔV(h=9)	-4,83 %	-13,34 %	0,83 %	**ΔI(h=9)**	-1,01 %	-1,17 %	-2,05 %
ΔV(h=11)	2,37 %	-4,39 %	-0,20 %	**ΔI(h=11)**	58,96 %	68,86 %	44,38 %
ΔV(h=13)	8,36 %	9,98 %	10,34 %	**ΔI(h=13)**	84,94 %	80,19 %	-251,43%
ΔV(h=15)	-0,35 %	-16,63 %	3,84 %	**ΔI(h=15)**	-1,92 %	0,23 %	0,90 %
ΔV(h=17)	74,81 %	-55,61 %	-18,06 %	**ΔI(h=17)**	45,43 %	72,91 %	7,77 %

For configuration 2 where the diode bridge load is disconnected from the test system the obtained voltage and current components changes are listed in Table 9.2. For the 6-pulse diode bridge it would be expected that the harmonic injection is of the 5th, 7th, 11th, 13th and 17th harmonic components. According to the obtained results the diode bridge injects some 5th harmonic distortion to the system voltage. It could also appear that there is some injection of the 3rd harmonic. The rest of the values vary much between the phases, and the triplen harmonic components are quite low except from the 3rd harmonic.

Looking at the change in the current components the results are more as expected. Here the typical harmonic components produced by a 6-pulse diode bridge are clearly indicated as

injected by the load. An exception to this is the C phase for the 13th harmonic component. Other than that the triplen harmonic components are very low, indicating that the diode bridge load draws only the characteristic harmonic components, as to be expected for a 6-pulse diode bridge.

Comparing the obtained results in Table 9.2 with the measured harmonic components for the diode bridge load alone in Table 9.5 the results seem to be quite accurate for the current harmonic components. When the load is measured by itself it can be seen that the characteristic components stick out from the others, especially for the current components. For the voltage components it can seem that the load injects more 3rd harmonics and lower levels of 5th and 11th harmonics than would be expected. The unclear results obtained for the voltage component can be explained by the low levels of harmonic voltage components injected by the load compared to the components injected by the voltage supply itself. These are also measured, representing the majority of the measured voltage harmonics making it hard to see the impact from the load due to uncertainty and varying, low harmonic levels.

Table 9.3 - Voltage and current components change for configuration 4

Configuration 4: Disconnected thyristor bridge load							
Phase:	**AB**	**BC**	**CA**		**A**	**B**	**C**
ΔV(h=3)	-112,75%	38,58 %	-66,45 %	**ΔI(h=3)**	98,55 %	97,10 %	98,84 %
ΔV(h=5)	18,28 %	22,29 %	23,44 %	**ΔI(h=5)**	39,06 %	32,12 %	41,45 %
ΔV(h=7)	1,60 %	6,87 %	3,67 %	**ΔI(h=7)**	19,74 %	19,75 %	-0,44 %
ΔV(h=9)	49,27 %	-8,57 %	87,55 %	**ΔI(h=9)**	99,30 %	98,89 %	99,65 %
ΔV(h=11)	-10,04 %	-28,42 %	-39,62 %	**ΔI(h=11)**	37,38 %	7,98 %	34,07 %
ΔV(h=13)	10,92 %	-2,10 %	3,45 %	**ΔI(h=13)**	85,78 %	-42,21 %	-196,38%
ΔV(h=15)	87,67 %	54,35 %	96,71 %	**ΔI(h=15)**	99,03 %	99,11 %	98,76 %
ΔV(h=17)	3,51 %	-87,01 %	-61,84 %	**ΔI(h=17)**	34,51 %	-19,99 %	1,96 %

For configuration 4, where the thyristor bridge load is disconnected from the test system, the results from the harmonic voltage components method are listed in Table 9.3 for both voltage and current. By looking at the voltage component changes it would seem that the thyristor bridge load is injecting triplen harmonics into the test system except from the 3rd harmonic. Further is appears that the load consumes some 3rd, 11th and 17th harmonic components.

The harmonic current component changes obtained by the method indicate that the thyristor bridge load injects most of the harmonic components taken into account. For the triplen harmonic current components it seems that the load injects almost all the triplen harmonics found in the PCC in configuration 1. For the other harmonic current components it is hard to draw any conclusions as the contribution seems to be unbalanced between the phases, except from for the 5^{th} harmonic which is indicated to be injected. The best way to analyse the results would be to say that all the components are injected into phase A. The 5^{th}, 7^{th} and the triplen harmonics are injected into phase B. For phase C it is the same as for phase B except for the injection of the 7^{th} harmonic. The 13^{th} harmonic is consumed by phase B and especially by phase C.

When the results from Table 9.3 are compared to the measurements in **Error! Reference source not found.** it can be concluded that the results are very accurate for the triplen harmonic current components. The remarkable difference between the tables is the 7^{th} and 13^{th} harmonic current components. Comparing the voltage components it is seen that the triplen harmonics except for the 3^{rd} harmonic stick out as quite similar here as well. This can be taken as a clear indication on the accuracy of these results obtained for the voltage components. For the other components it is yet again hard to say something due to the relative small magnitude of voltage harmonics injected by the load compared to the harmonics already found in the test system's voltage source.

For further comparison and analysis of the results the THD for current and voltage is also listed and analysed. The following tables present the current and voltage THD for the different configurations and for each load individually.

Table 9.4 - Voltage and current THD for each load individually

Voltage and current THD for each load individually			
THDv [%]	**AB**	**BC**	**CA**
RL load	0,8298	0,7194	0,7542
Diode bridge load	0,7476	0,6690	0,7245
Thyristor bridge load	0,8686	0,7715	0,7937
THDi [%]	**A**	**B**	**C**
RL load	1,0631	1,1318	1,2505
Diode bridge load	28,4761	28,5552	28,4854
Thyristor bridge load	83,1157	40,9614	25,4902

By comparing the current and voltage THD levels presented in Table 8.9 and Table 8.10 it is seen that the voltage distortion is very low for the test system. This makes the analysis based on the voltage components hard to use as the uncertainty increases with low harmonic levels. An observation from the THDv levels is the unbalance in the THD that is present when the thyristor bridge load is connected to the system and running showing an unbalanced harmonic distortion injection from the thyristor bridge load.

When looking at the current THD levels for the different configurations it is much clearer how the thyristor bridge load affects the THD levels in an unbalanced way, contributing more to phase A, and less to phase C. It can also be seen that when the RL load is connected, the THD decreases due to the increased current level without much harmonic components. Linear loads connected to the system clearly lower the THDi of the system as expected due to the increased fundamental component magnitude compared to the other harmonic components (see (Eq. 2.10)).

Table 9.5 - Voltage and current components for each load related to configuration 1

Voltage and current harmonic magnitudes for each load individually									
Load:	**RL**			**Diode**			**Thyristor**		
				Voltage					
Phase:	**AB**	**BC**	**CA**	**AB**	**BC**	**CA**	**AB**	**BC**	**CA**
V(h=3)	307,52 %	105,46 %	14,36 %	164,90 %	71,45 %	160,55 %	309,64 %	87,93 %	38,97 %
V(h=5)	58,06 %	43,29 %	49,41 %	50,14 %	36,33 %	44,31 %	42,73 %	20,22 %	37,16 %
V(h=7)	136,80 %	150,47 %	147,71 %	137,60 %	141,12 %	142,20 %	163,20 %	180,37 %	176,15 %
V(h=9)	86,14 %	46,24 %	105,23 %	35,59 %	52,29 %	29,49 %	92,51 %	54,99 %	109,74 %
V(h=11)	71,30 %	69,25 %	77,90 %	69,81 %	83,53 %	90,74 %	57,30 %	63,59 %	64,95 %
V(h=13)	121,75 %	124,54 %	120,68 %	98,39 %	108,30 %	104,91 %	131,30 %	131,36 %	128,24 %
V(h=15)	99,67 %	96,82 %	100,36 %	11,36 %	31,47 %	6,53 %	98,20 %	100,29 %	99,35 %
V(h=17)	102,09 %	82,11 %	169,05 %	83,68 %	158,01 %	150,40 %	11,74 %	88,27 %	76,91 %
				Current					
Phase:	**A**	**B**	**C**	**A**	**B**	**C**	**A**	**B**	**C**
I(h=3)	1,53 %	1,00 %	4,48 %	0,44 %	0,17 %	0,70 %	100,13 %	102,57 %	97,91 %
I(h=5)	2,97 %	4,01 %	3,10 %	63,93 %	70,57 %	60,82 %	40,12 %	32,82 %	42,84 %
I(h=7)	2,73 %	2,82 %	4,06 %	82,73 %	84,87 %	106,66 %	61,30 %	81,36 %	77,94 %
I(h=9)	0,34 %	0,90 %	1,78 %	0,65 %	0,36 %	1,98 %	102,00 %	102,63 %	101,44 %
I(h=11)	2,63 %	3,97 %	3,36 %	64,19 %	93,49 %	66,33 %	40,11 %	26,50 %	52,24 %
I(h=13)	0,62 %	5,40 %	13,95 %	14,75 %	151,07 %	318,66 %	15,31 %	201,54 %	333,53 %
I(h=15)	0,21 %	0,45 %	1,29 %	0,71 %	0,50 %	2,07 %	102,36 %	101,84 %	99,91 %
I(h=17)	2,04 %	4,01 %	3,59 %	67,28 %	121,42 %	97,67 %	50,42 %	22,77 %	89,43 %

9.2 Measurements accuracy

This purpose of this project is not only to identify the harmonic injection sources in a power system. A big part is also setting together a measurement system for harmonics, both THD and IHD, and testing the results from the measurements. As a reference for the measurement results obtained by the designed system in this project an ELSPEC G4500 BLACKBOX PQA measurement system, categorised as Class A according to IEC 61000-4-30, is also used for measurements on the same test system.

The results from the two sets of measurements are listed in the tables for harmonic voltage components measurements and both current and voltage THD measurements in the results chapter (Ch. 8).

The two measurements show that there are differences in the harmonic voltage component magnitudes obtained from the two measurement systems. On the other hand, if the measurement results are presented as IHDv values the measurements are quite similar in magnitude.

For the THD levels measured by the two measurement systems the results are presented in percent, according to (Eq. 2.10). These results clearly present very similar results for the two systems with a difference of nothing more than a few percent. The changes and balance between the phases is the same for the two sets of measurements for both current and voltage.

9.3 Harmonic filtering

With the AHF connected to the PCC the current THD levels is clearly reduces, compared to the measurement for THDi for configuration 1. The unbalance in the current distortion between the phases is eliminated.

For the voltage distortion levels there are some improvements to see, though they are limited. Phase BC measurements for THDv measurements for configuration 1 seems to be wrong, but comparing the two other phase-to-phase measurements the filter has its effect, though it is limited for the already low THDv before the filter is connected.

10 Discussion

10.1 Harmonic voltage component method

The analysis of the harmonic voltage component method shows that the voltage component results are hard to analyse with the measured voltage components. As mentioned in 6.1 the uncertainty of the method increases with low harmonic levels. As seen by the THDv measurements in Table 8.9 and **Error! Reference source not found.** the levels are very rarely exceeding 1% and in general approximately 0.8%. For the test system it is then hard to draw any conclusions regarding the sources for the harmonic voltage components, as most of the harmonic distortion seems to be coming from the test system's voltage source in all the configurations. The effect on the voltage distortion caused by the loads are then very hard to identify and with the uncertainty regarding measurements and varying harmonic levels from the voltage source it is hard to conclude anything for certain from the results obtained for the harmonic voltage components method.

For Table 9.5 which is meant as a reference measurement the voltage measurements are also here hard to analyse. The measured harmonic levels are given in percentage relative to configuration 1. As the voltage source harmonics are included in all the measurements and the voltage harmonic levels from the loads are as low as they are the harmonics from the source are dominating most of the measurements.

10.1.1 Configuration 2

For configuration 2, where the results from the harmonic voltage component method are presented in Table 9.1, it is expected that the harmonic voltage component injection is either non-existing or very low. Looking at the table, the results say that there is no injection or consumption of any of the considered harmonics in this project. This is what would be expected of a linear load such as the RL load.

10.1.2 Configuration 3

The results for configuration 3, given in Table 9.2 are not as precise as for configuration 2. The diode bridge is expected to produce certain harmonics. Looking at the results for the expected harmonic components there is little compliance. The only components matching the expected results are the 5^{th}, 13^{th} and 17^{th} harmonics. The other components are once again

hard to say something about, and the low harmonic voltage levels injected by the loads are yet again to blame.

10.1.3 Configuration 4

The voltage components for configuration 4, where the thyristor bridge is disconnected, are presented in Table 9.3. Based on the numbers it can seem that the load injects 9^{th} and 15^{th} harmonic voltage components. Again, if the levels of the harmonics are taken into account and the magnitude of the voltage source harmonics this are very uncertain values and hard to draw any conclusion from.

10.2 Harmonic current component method

Taking a look at the results for the harmonic current component levels it is much easier to see the differences between the components. If the THDi levels from Table 8.10 and **Error! Reference source not found.** are compared one can clearly read changes in the distortion level for the different configurations related to the distortion measurements for each load individually found in **Error! Reference source not found.**.

10.2.1 Configuration 2

For configuration 2 where the RL load is disconnected from the test system an increase in the THDi is observed. This is to be expected, as the THDi for the RL load alone is very low, meaning it draws a very sinusoidal current almost without and distortion at all. Removing this current from the test system results in a lower total current in the PCC where the fundamental harmonic is greatly reduced compared the other harmonic components injected by the other loads remains connected. From (Eq. 2.10) it is then expected that the THDi levels will increase, which it also does. Common for configuration 1 and configuration 2 is the unbalance in harmonic levels between the phases indicating that the unbalanced harmonic injection is still injected by the loads remaining connected to the test system.

For the IHDi levels under configuration 2, seen in Table 9.1, the results imply that the RL load has very little effect on all harmonic current components except from the 13^{th} harmonic component which seems to be injected in some degree by the load. The reason for the injection of the 13^{th} harmonic current component is unknown, but it can be that the inductances in the load inject this harmonic current.

Taking a look at the current drawn by the RL load alone in Table 9.5 the indication is that practically none of the harmonic current components in the PCC under configuration 1 is injected by the RL load. The 13^{th} harmonic injection indication from the harmonic current component method can then maybe be the result of resonance with the 13^{th} harmonic current.

10.2.2 Configuration 3

For configuration 3, the change in THDi compared to configuration 1 (see Table 8.10) increases by a few percentages on average. As for configuration 2, the total current naturally decreases as the load is disconnected, making the THDi calculations for the remaining harmonic components increase due to a lower magnitude of the fundamental component. What can be read from the table is that the harmonic distortion unbalance between the phases still is unchanged, indicating that the unbalanced harmonic injection is coming from another load.

The IHDi levels for configuration 3 seen in Table 9.2 indicate a typical 6-pulse diode bridge current component injection. The remaining harmonic components are very low, basically zero if a uncertainty margin is taken into account. This indicates that the results for the harmonic current component methods are very successful for this configuration. The exception for these results is the 13^{th} harmonic at phase C which seems to be consuming a great level of the component. The reason for this can possibly be explained by other reasons found in the system components not operating ideally.

Comparison between the obtained results in Table 9.2 and the current measured for the diode bridge load alone in Table 9.5 strengthens the validity of the measured results. The harmonic current injection verifies that the load injects the typical harmonics expected from a 6-pulse diode bridge.

10.2.3 Configuration 4

The results for configuration 4 from the measurements indicate according to the THDi seen in Table 8.10 that the unbalance between the phases is eliminated when the thyristor bridge load is disconnected from the test system. By these results it is safe to say that the load injects unbalanced harmonic distortion to the phases, where phase A suffers the most and phase C suffers the least distortion injection. Compared to the other configurations where the load in connected to the system and running it can be seen that the THDi level is at the lowest for configuration 4. This indicates that the majority of the harmonic current distortion is injected

by the thyristor bridge load. Compared to the measured harmonic current components for the load alone, presented in Table 9.5 this can be confirmed by these measurements as well. It can be seen that for the triplen harmonic components, the thyristor bridge load is injecting practically all of the triplen harmonics present under configuration 1.

Based on the IHDi results from the harmonic current component method in Table 9.3 it is indicated here as well that the triplen harmonic components are almost completely injected by the thyristor bridge load. Further, these results indicate some unbalance between the phases for the remaining components, confirming what is seen in the THDi measurements. As the IHDi injection is indicated as positive for almost all the harmonic components it can be concluded that the load injects almost all the analysed harmonics and in a significant magnitude as well.

10.3 Measurement accuracy

The comparison between the measurements systems used in this project show compliance between the measured values, especially for the current measurements. For the voltage measurements the obtained IHDv magnitudes vary in a greater manner, but it must be kept in mind the IHDv levels for the voltage components which are very low. The testing conditions also has its impact on the results measured, increasing the uncertainty in the obtained levels where the voltage source characteristics can have changed in the time between the measurements conducted by the two measurement systems (see 10.4).

According to the requirements in the standards given in chapter 5 the specifications for the NI compactDAQ system put together in this project matches the requirements for Class I instrumentation according to IEC 61000-4-7 and Class A according to IEC 61000-4-30. Based on this information the measurement results from the two measurement system should give the same results. Due to the uncertainty caused by the testing conditions this project does not give well enough testing conditions for obtaining these results.

10.4 Testing conditions

For this project and the measurements done in the laboratory it has to be pointed out that there are great differences between the test system and a real operating maritime power system. The rating of the test system is small compared to a real maritime power system. The voltage

levels, power rating of the loads and the impedance in the power system are some of the greatest differences.

In a maritime power system the largest loads will consume large currents, at least 100 times the current measured in the laboratory testing. Combining this with the system's impedance in the power system the current distortion will in much greater extent affect the voltage. The impedance present in a maritime power system is also much greater than the impedance in the test system. Large and long power cables as well as large switchboards, transformers etc. all represent impedance in the power system. As the maritime power systems are isolated systems the network is not as stiff as the laboratory testing system. This allows greater affect from the harmonic injection from the loads on the voltage. All this results in much larger harmonic levels than the ones measured in the laboratory.

The harmonic spectrum produced in a typical maritime power system can be quite varying. For the different loads there can be different frequency converters. 6-pulse diode rectifiers are typical front ends for many VFDs, and the 12-pulse diode bridge is also quite common. Some loads can utilize the AFE which generates high order harmonic components. All these are harmonic sources that need to be considered when the harmonic levels are measured.

For the accuracy comparison of the measurement systems there are some sources of error in the testing procedure. Firstly the measurements are made at different occasions with some days in between the measurements. The measurement of the voltage harmonic distortion levels can have changed, depending on the voltage source which contains a large quantity of the total harmonic distortion. The comparison of these measurements must therefore be seen in a sceptical way where small differences in the harmonic component levels can't be taken as any indications of measurement deviation between the two measurement systems.

For the current measurements the levels of distortion is provided by almost completely by the loads. Some harmonic distortion must be expected from the source, but these levels are quite small compared to the injected harmonic distortion from the loads. Due to the higher levels of harmonic components and distortion in the current measurements the comparison between the current measurements are more valid that for the voltage measurement comparison. Still, as for the voltage comparison, the harmonic levels may have changed in the time between the measurements were made, both due to possible changes in the source distortion levels and the

fact that the loads may be operating slightly different due to temperature of the components in the test system.

10.5 Harmonic filtering

The AHF seems to work as an AHF is expected to, mitigating the harmonic distortion levels in the test system, even though the changes are very small for the voltage. This is due to the limited injection of harmonic distortion from the loads. As the filter is coupled to filter out the harmonic components from the loads the effect of this is naturally enough limited. The measurement inaccuracy and uncertainty also affects the result for the low THDv levels measured. For the current harmonic distortion level, the filter has a remarkable effect.

11 Conclusion

11.1 Harmonic source detection method

From the analysis based on the harmonic voltage/current component method used in this project the result is different regarding current and voltage measurements. For the harmonic voltage component method the testing conditions was not good enough for obtaining accurate results. The uncertainty introduced by low harmonic levels mixed with low current and impedance in the test system giving very little effect on the voltage did not give good enough results for making any accurate conclusions regarding harmonic voltage component injection from the different loads. The measurements for each load individually were also too inaccurate due to the domination of harmonic components found in the systems voltage source and the low levels of harmonic distortion. For verification of this method the measurements would have to be done on a larger system with much larger currents and higher impedance, making the affect from the current components higher on the voltage.

For the harmonic current component method analysis the results are giving much better results than for the voltage components. The measurements from the loads alone and the analysis results are complying in a great degree. However, some unbalances on some of the phases give unclear results for the phase in matter. For this reason the recommendation by the author is to measure all three phases. In this way, an unbalance for one phase will be seen when compared to the other phases and a conclusion can be made on basis of all three phases instead of one unbalance phase.

The use of the harmonic current component method is on the other hand not necessary for other reasons other than verification of the harmonic currents injected or consumed by loads. There are no limits on the harmonic voltage distortion levels in maritime power systems. In this project the this method in used due to the testing conditions where the harmonic distortion is very low in general injected by the voltage source and not so much by the loads. For a real maritime power system where only the voltage distortion levels are regulated and with high voltage distortion levels, currents and system impedance the measurements of current components are unnecessary for measurements of the voltage distortion levels.

Based on these factors mentioned the conclusion for the harmonic source detection is that the harmonic voltage component method should be tested in a real maritime power system with known levels of harmonic components for comparing obtained results with the known values.

11.2 Measurement accuracy

The measurement system used in this project, the NI compactDAQ is a good solution with together with LabVIEW to analyse all parameters found in the maritime power system. For the harmonic measurements the NI compactDAQ hardware (NI 9225 and NI 9227) is satisfying the IEC 61000-4-7 and 61000-4-30 standards, rated as Class I and Class A according to the standards.

The DAQ system can be used for most voltage levels. For high voltage levels (greater than $400V_{RMS}$ phase-to-phase/$800V_{RMS}$ phase-to-neutral) a voltage transformer can be used for adjusting the systems input voltage. For currents there are no modules measuring more than $5A_{RMS}$ directly, but with the use of current transducers the current measurement range is limited by the transducer ratings.

The test system is compact and portable. It is easy to install for measurements and is very user friendly.

The LabVIEW programming opportunities allows a great variety of measurement analysis outputs. The blocks designed on advance performing the calculations necessary makes the programming intuitive and versatile. With LabVIEW's power suite, the analysis made in the blocks are done according to the IEC standards mentioned in this project, and if other calculations are necessary there are several blocks giving same outputs, calculated on other premises.

To conclude, the NI with the compactDAQ hardware and LabVIEW software solution is considered as a very precise, easy to use and versatile measurement system.

11.3 Harmonic filtering

The effect of the harmonic filter can be seen for both voltage and current distortion levels. This indicates that the filter work as it is intended to, but should be tested under more demanding conditions in term of system ratings and distortion levels to document the filters capacity and especially the effect on harmonic voltages.

12 Further work

Due to the limited time available for this project some further work is recommended. For the harmonic source detection methods mentioned the FIS method briefly described in chapter 0 was not tested and analysed any further in this project. The method can be tested and compared to the voltage harmonic component method used in this project, analysing the use of the methods and versatility.

The whole project with testing of the measurement system and the harmonic source detection method should be tested for a real maritime power system, giving proper measurements according to the specifications it is intended for.

For measurement accuracy verification the measurement system should be tested under known, stabile circumstances and compared up against another Class A and Class I measurement system, according to the IEC 91000-4-7 and IEC 61000-4-30 standards.

The measurement system can be designed for measurements of even more parameters in the maritime power system and tested as a complete solution for measurements of power quality parameters in maritime power systems for testing according to international standards and verification of compliance with these.

The active harmonic filter can be studied further in term of power factor correction and general design and use for maritime power systems.

13 Bibliography

[1] American Bureau of Shipping, “Guidance Notes on Control of Harmonics in Electrical Power Systems,” American Bureau of Shipping, Houston, TX 77060 USA, 2006.

[2] E. F. Fuchs and M. A. S. Masoum, Power quality in power systems and electrical machines, Amsterdam: Academic Press/Elsevier, 2008.

[3] [Online]. Available: http://www.learnabout-electronics.org/Amplifiers/amplifiers34.php. [Accessed December 2014].

[4] “Fourier Series,” Wolfram MathWorld, [Online]. Available: http://mathworld.wolfram.com/FourierSeries.html. [Accessed May 2015].

[5] C. Sankaran, Power quality, The electric power engineering series, Boca Raton: CRC Press, 2002.

[6] [Online]. Available: http://www.vias.org/matsch_capmag/matsch_caps_magnetics_chap5_02.html. [Accessed December 2014].

[7] [Online]. Available: http://www.vias.org/matsch_capmag/matsch_caps_magnetics_chap5_03.html. [Accessed December 2014].

[8] H. Akagi, “Active Harmonic Filters,” September 2005.

[9] S. N. Kalaschnikow, “High Efficient Low Harmonic Drives with Integrated Active Filters,” 2013.

[10] “Measurement category,” Wikipedia, [Online]. Available: http://en.wikipedia.org/wiki/Measurement_category. [Accessed May 2015].

[11] “Isolation Technologies for Reliable Industrial Measurements,” National Instruments, [Online]. Available: http://www.ni.com/white-paper/3546/en/. [Accessed May 2015].

[12] “Isolation Types and Considerations when Taking a Measurement,” National Instruments, [Online]. Available: http://www.ni.com/white-paper/3410/en/. [Accessed May 2015].

[13] “Isolation Technologies for Reliable Industrial Measurements,” National Instruments, [Online]. Available: http://www.ni.com/white-paper/3546/en/. [Accessed May 2015].

[14] “Sampling (signal processing),” Wikipedia, [Online]. Available: http://en.wikipedia.org/wiki/Sampling_(signal_processing). [Accessed May 2015].

[15] “Discrete-time signal,” Wikipedia, [Online]. Available: http://en.wikipedia.org/wiki/Discrete-time_signal. [Accessed May 2015].

[16] “How to Choose the Right DAQ Hardware for Your Measurement System,” National Instruments, 2015.

[17] “Aliasing,” National Instruments, [Online]. Available: http://zone.ni.com/reference/en-XX/help/371361L-01/lvanlsconcepts/aliasing/. [Accessed May 2015].

[18] “Sampling Rate,” National Instruments, [Online]. Available: http://zone.ni.com/reference/en-XX/help/371361L-01/lvanlsconcepts/sampling_rate_df/. [Accessed May 2015].

[19] “Anti-aliasing filter,” Wikipedia, [Online]. Available: http://en.wikipedia.org/wiki/Anti-aliasing_filter. [Accessed May 2015].

[20] “Introduction to Data Acquisition,” National Instruments, [Online]. Available: http://www.ni.com/white-paper/3536/en/. [Accessed May 2015].

[21] “How to Measure Current and Make Power Measurements,” National Instruments, [Online]. Available: http://www.ni.com/white-paper/8198/en/. [Accessed May 2015].

[22] A. Ferrero, M. Priolo and S. Salicone, “A metrological comparison between different methods for harmonic pollution metering,” 2012.

[23] A. Ferrero, M. Prioli and S. Salicone, “Fuzzy metrology-sound approach to the

identification of sources injecting periodic disturbances in electric networks," 2011.

[24] "Datainnsamling (DAQ) og datalogging," National Instruments, [Online]. Available: http://norway.ni.com/datainnsamling. [Accessed May 2015].

[25] "NI cDAQ-9174," National Instruments, [Online]. Available: http://sine.ni.com/nips/cds/view/p/lang/no/nid/207535. [Accessed May 2015].

[26] "NI 9227," National Instruments, [Online]. Available: http://sine.ni.com/nips/cds/view/p/lang/no/nid/208794. [Accessed May 2015].

[27] "NI 9225," National Instruments, [Online]. Available: http://sine.ni.com/nips/cds/view/p/lang/no/nid/208795. [Accessed May 2015].

[28] "NI 9244," National Instruments, [Online]. Available: http://sine.ni.com/nips/cds/view/p/lang/no/nid/212307. [Accessed May 2015].

[29] "NI 9239," National Instruments, [Online]. Available: http://sine.ni.com/nips/cds/view/p/lang/no/nid/208797. [Accessed May 2015].

[30] "LabVIEW," National Instruments, [Online]. Available: http://www.ni.com/labview/. [Accessed May 2015].

[31] "Using the DAQ Assistant to Automatically Generate LabVIEW Code," National Instruments, [Online]. Available: http://www.ni.com/tutorial/4656/en/. [Accessed May 2015].

[32] "Write To Measurement File Express VI," National Instruments, [Online]. Available: http://zone.ni.com/reference/en-XX/help/371361L-01/lvexpress/write_lv_measurement_file/. [Accessed May 2015].

[33] "Harmonic Distortion Analyzer VI," National Instruments, [Online]. Available: http://zone.ni.com/reference/en-XX/help/371361L-01/lvwave/harmonic_distort_analyzer/. [Accessed May 2015].

[34] "Power Measurement VIs," National Instruments, [Online]. Available:

http://zone.ni.com/reference/en-XX/help/373375D-01/lvept/ep_mea_pal/. [Accessed May 2015].

[35] “Read From Measurement File Express VI,” National Instruments, [Online]. Available: http://zone.ni.com/reference/en-XX/help/371361L-01/lvexpress/read_lv_measurement_file/. [Accessed May 2015].

[36] T. S. Haugan and E. Tedeschi, “Reactive and Harmonic Compensation,” 2015.

[37] Veritas, Bureau, “Rules for the Classification of Steel Ships, Part C - Machinery, Electricity, Automation and Fire Protection,” Veristar, Neuilly-sur-Seine Cedex, France, 2014.

[38] N. Mohan, T. M. Undeland and W. P. Robbins, Power electronics: converters, applications, and design, New York: Wiley, 1995.

[39] D. N. Veritas, “Rules for classification of ships,” DNV, Høvik, 2013.

Appendix A – VI front panel for configuration 1

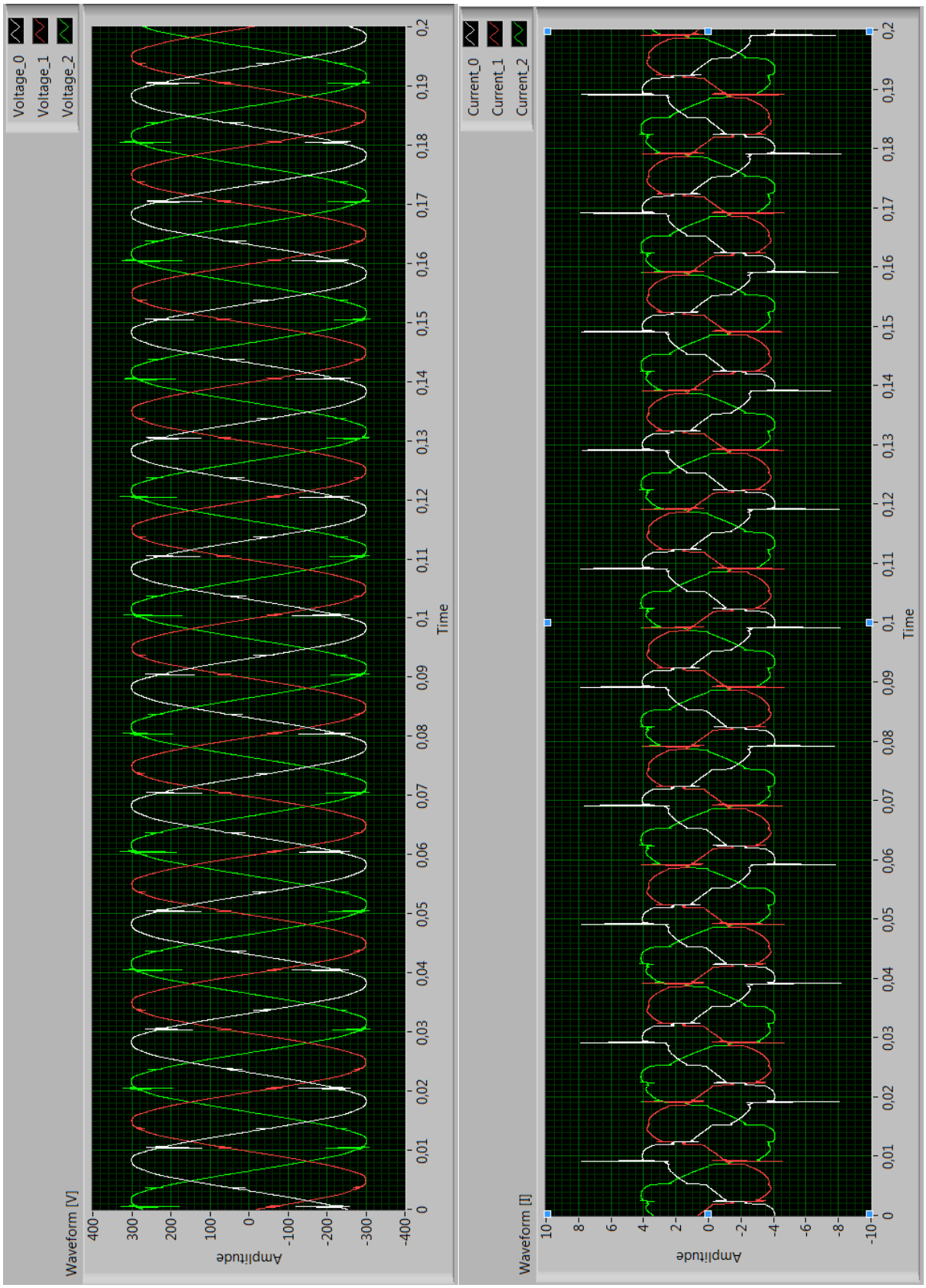

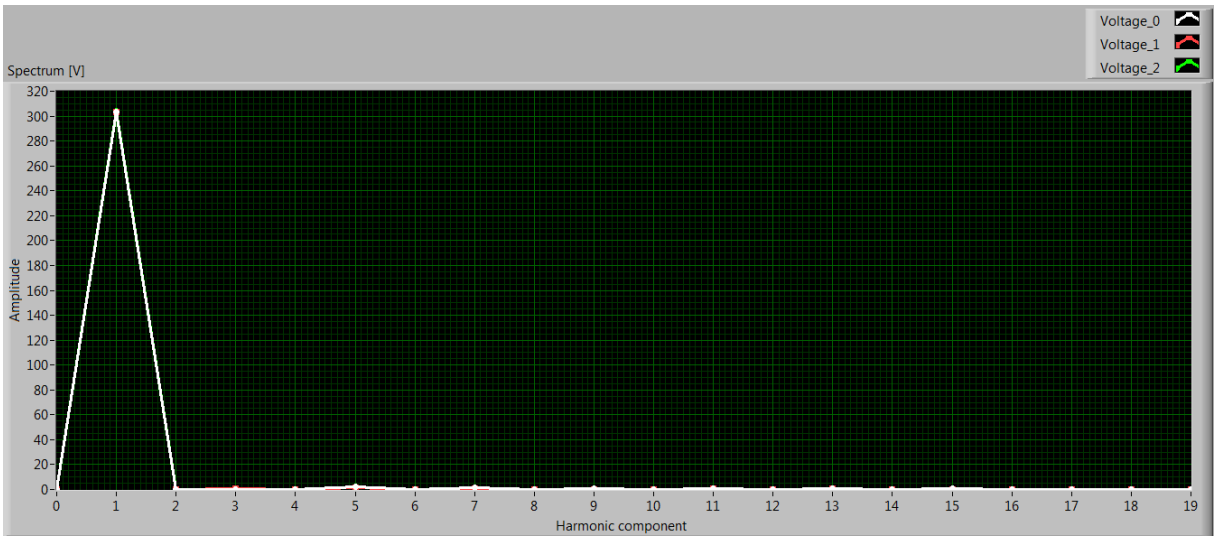

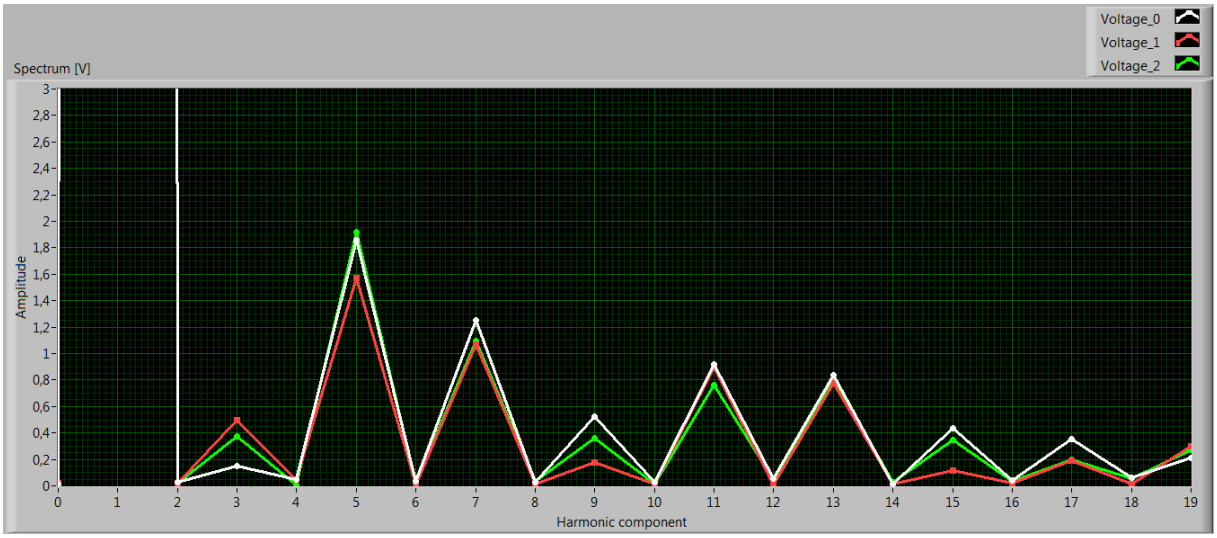

THD [V]

0	0,8864	0,7686	0,8471

THD [I]

0	22,2038	15,3923	13,6766

Voltage RMS

0	214,767	214,409	214,808

Current RMS

0	2,59718	2,76097	3,09059

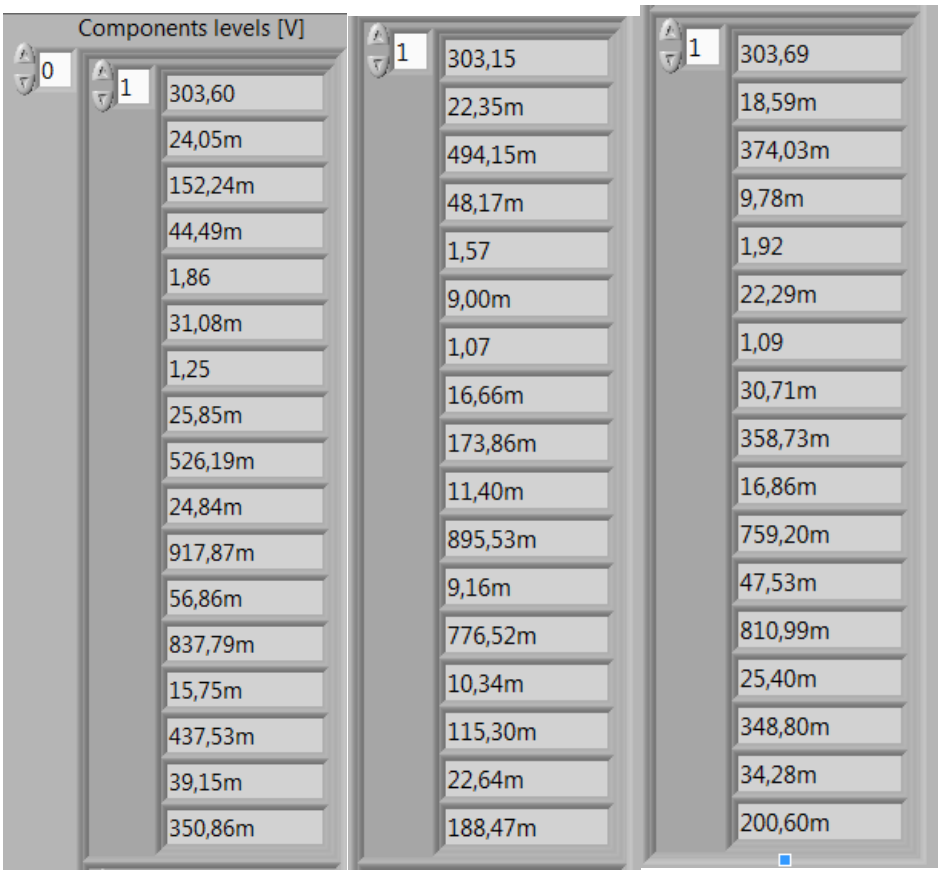
Components levels [V]
0
1
303,60
24,05m
152,24m
44,49m
1,86
31,08m
1,25
25,85m
526,19m
24,84m
917,87m
56,86m
837,79m
15,75m
437,53m
39,15m
350,86m
1
303,15
22,35m
494,15m
48,17m
1,57
9,00m
1,07
16,66m
173,86m
11,40m
895,53m
9,16m
776,52m
10,34m
115,30m
22,64m
188,47m
1
303,69
18,59m
374,03m
9,78m
1,92
22,29m
1,09
30,71m
358,73m
16,86m
759,20m
47,53m
810,99m
25,40m
348,80m
34,28m
200,60m

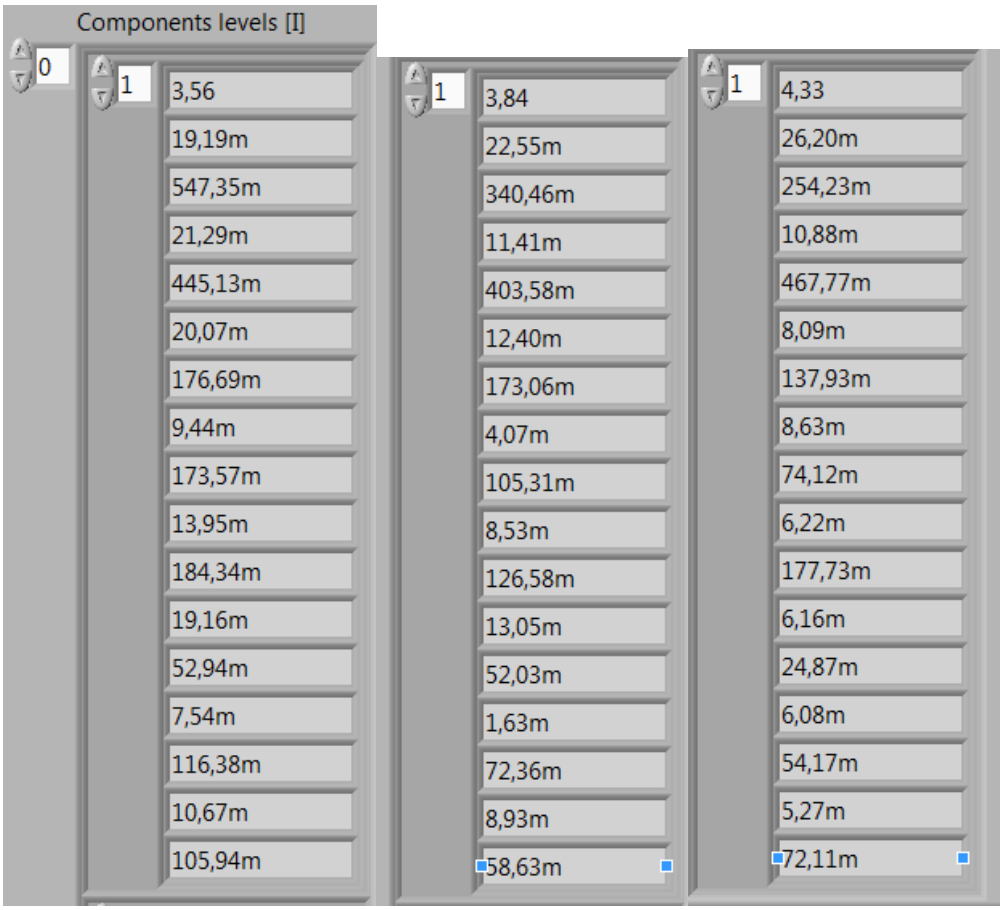
Components levels [I]
0
1
3,56
19,19m
547,35m
21,29m
445,13m
20,07m
176,69m
9,44m
173,57m
13,95m
184,34m
19,16m
52,94m
7,54m
116,38m
10,67m
105,94m
1
3,84
22,55m
340,46m
11,41m
403,58m
12,40m
173,06m
4,07m
105,31m
8,53m
126,58m
13,05m
52,03m
1,63m
72,36m
8,93m
58,63m
1
4,33
26,20m
254,23m
10,88m
467,77m
8,09m
137,93m
8,63m
74,12m
6,22m
177,73m
6,16m
24,87m
6,08m
54,17m
5,27m
72,11m

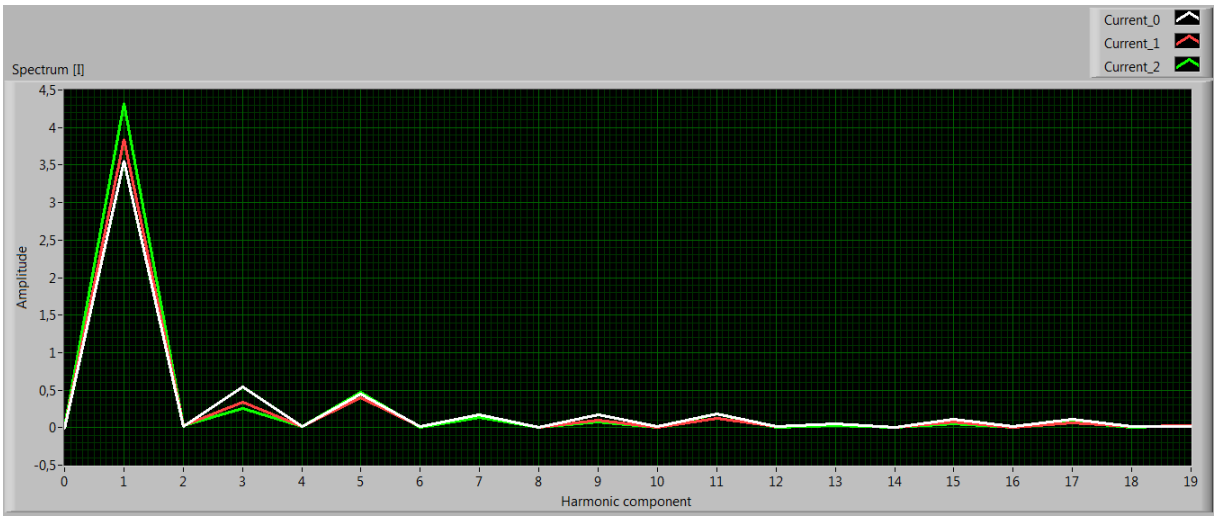
Current_0
Current_1
Current_2
Spectrum [I]
Amplitude
Harmonic component

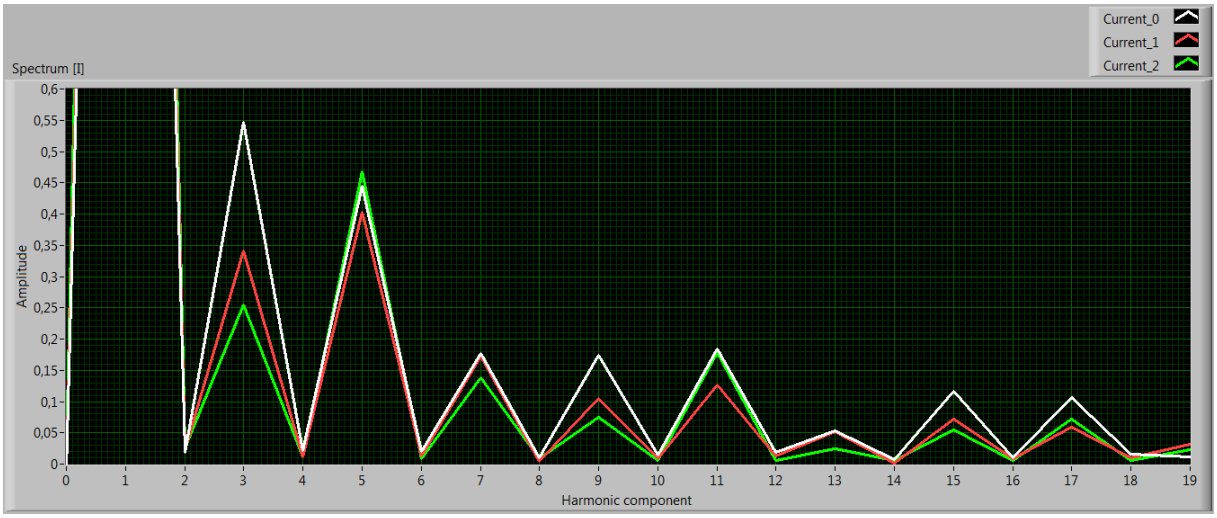
Current_0
Current_1
Current_2
Spectrum [I]
Amplitude
Harmonic component

Appendix B – VI front panel for configuration 2

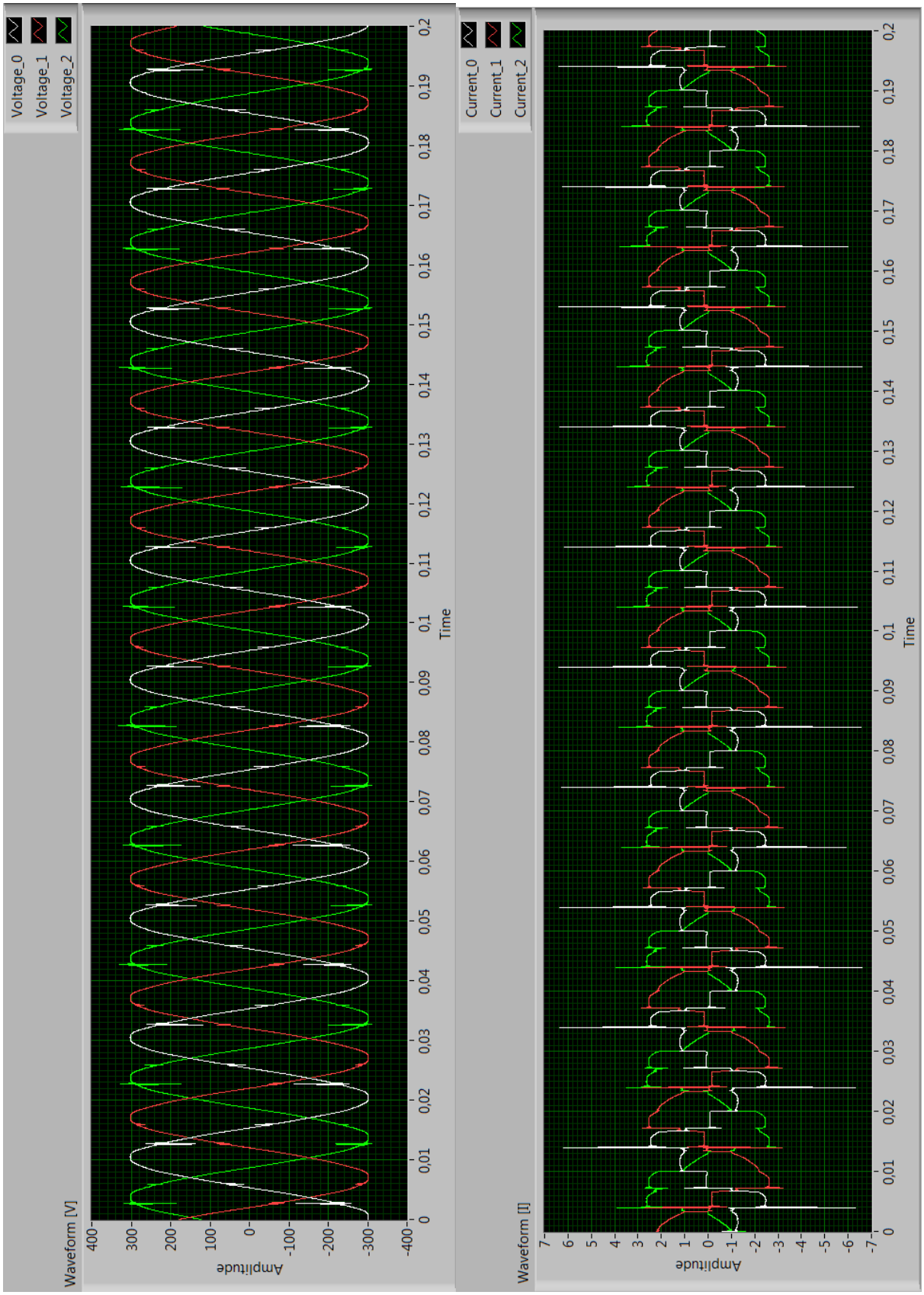

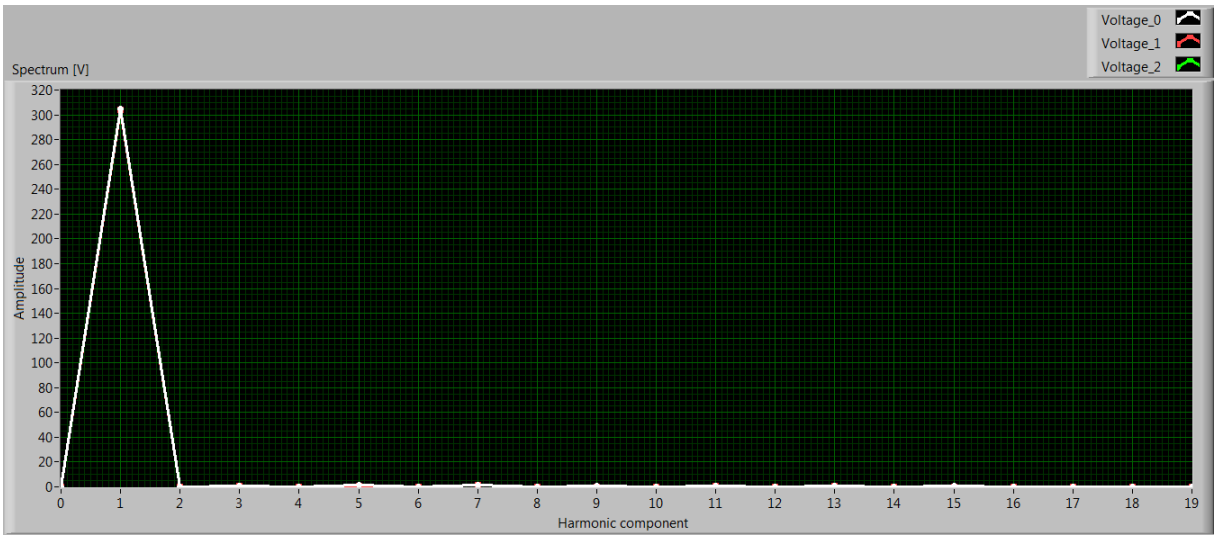

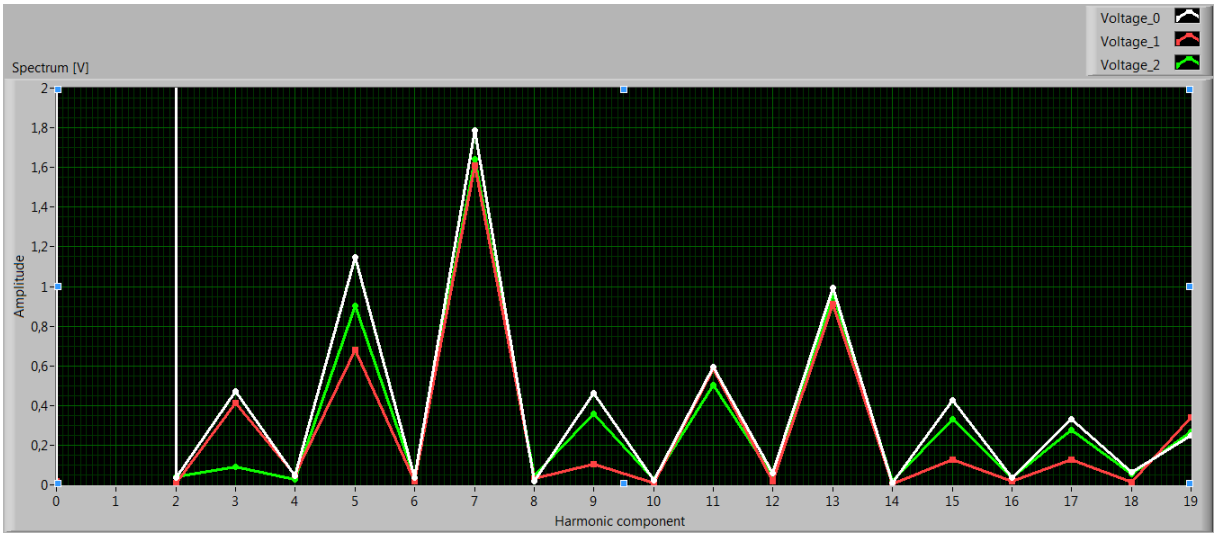

THD [V]

0	0,8475	0,7027	0,7419

THD [I]

0	40,5082	25,6035	21,6018

Voltage RMS

0	215,356	215,131	215,341

Current RMS

0	1,52928	1,71326	1,97924

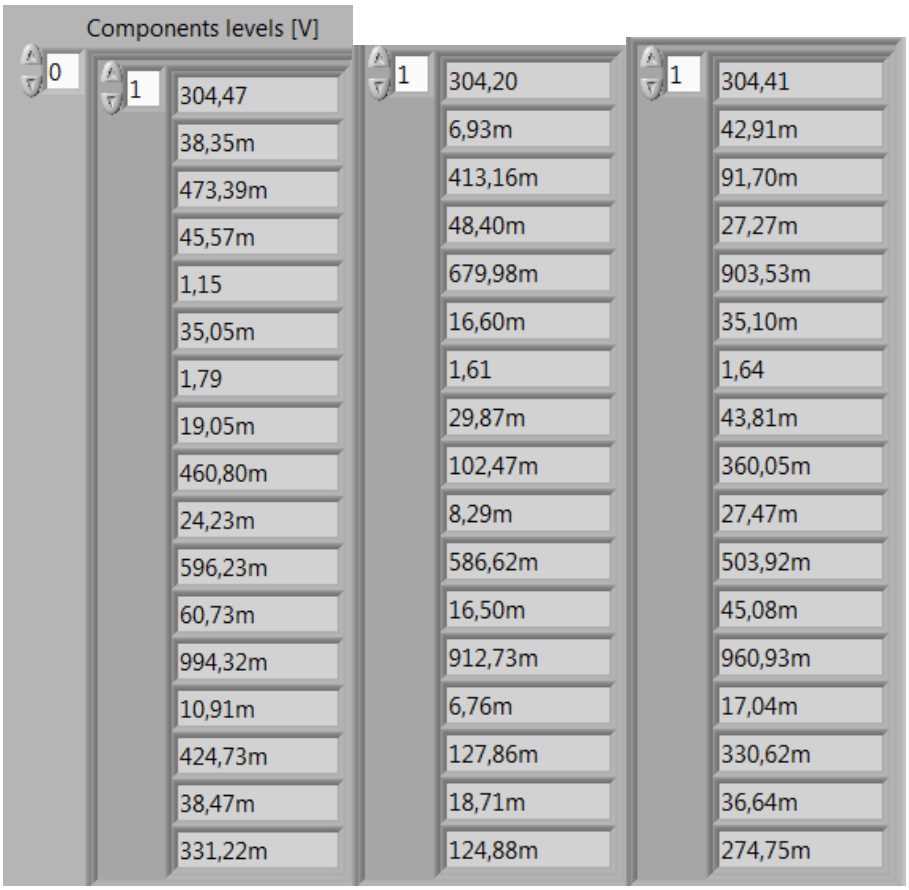
Components levels [V]
0
1
304,47
38,35m
473,39m
45,57m
1,15
35,05m
1,79
19,05m
460,80m
24,23m
596,23m
60,73m
994,32m
10,91m
424,73m
38,47m
331,22m
1
304,20
6,93m
413,16m
48,40m
679,98m
16,60m
1,61
29,87m
102,47m
8,29m
586,62m
16,50m
912,73m
6,76m
127,86m
18,71m
124,88m
1
304,41
42,91m
91,70m
27,27m
903,53m
35,10m
1,64
43,81m
360,05m
27,47m
503,92m
45,08m
960,93m
17,04m
330,62m
36,64m
274,75m

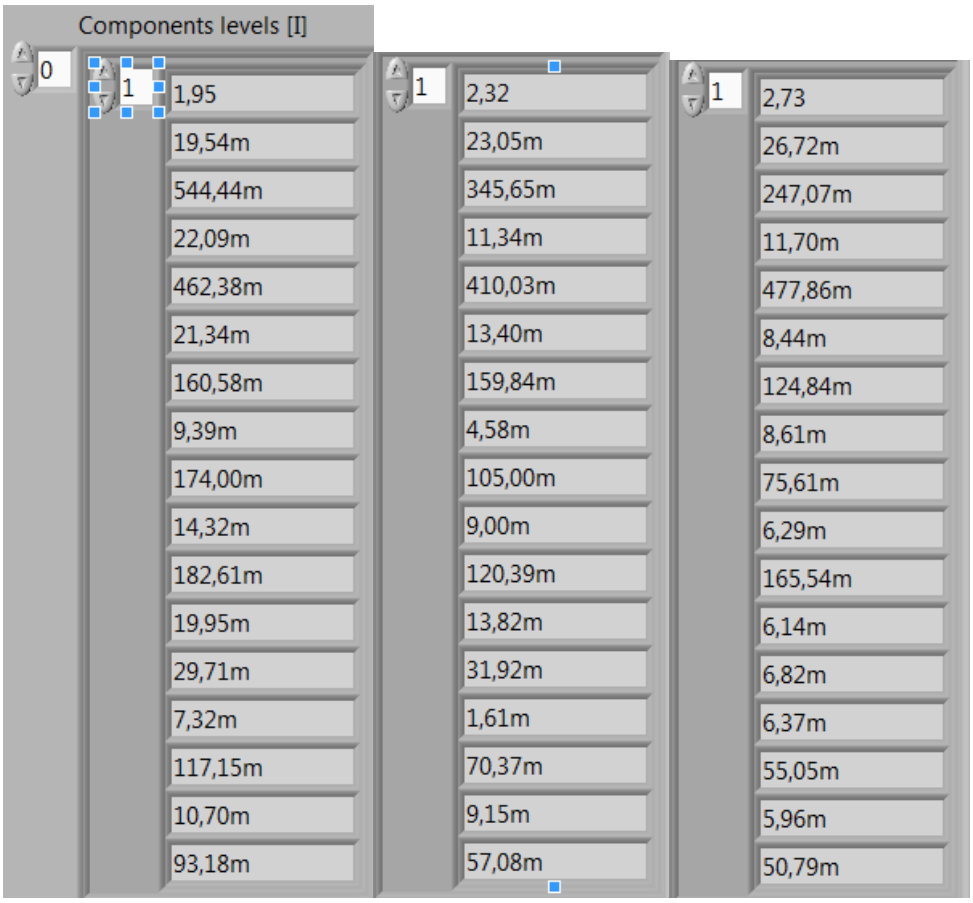
Components levels [I]
0
1
1,95
19,54m
544,44m
22,09m
462,38m
21,34m
160,58m
9,39m
174,00m
14,32m
182,61m
19,95m
29,71m
7,32m
117,15m
10,70m
93,18m
1
2,32
23,05m
345,65m
11,34m
410,03m
13,40m
159,84m
4,58m
105,00m
9,00m
120,39m
13,82m
31,92m
1,61m
70,37m
9,15m
57,08m
1
2,73
26,72m
247,07m
11,70m
477,86m
8,44m
124,84m
8,61m
75,61m
6,29m
165,54m
6,14m
6,82m
6,37m
55,05m
5,96m
50,79m

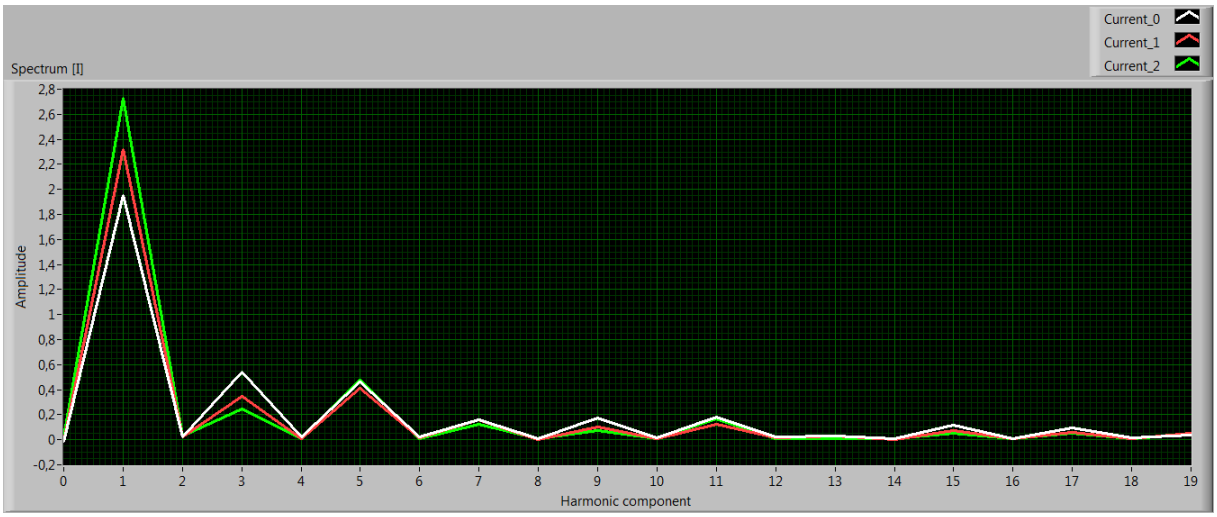
Spectrum [I]
Current_0
Current_1
Current_2
Amplitude
Harmonic component

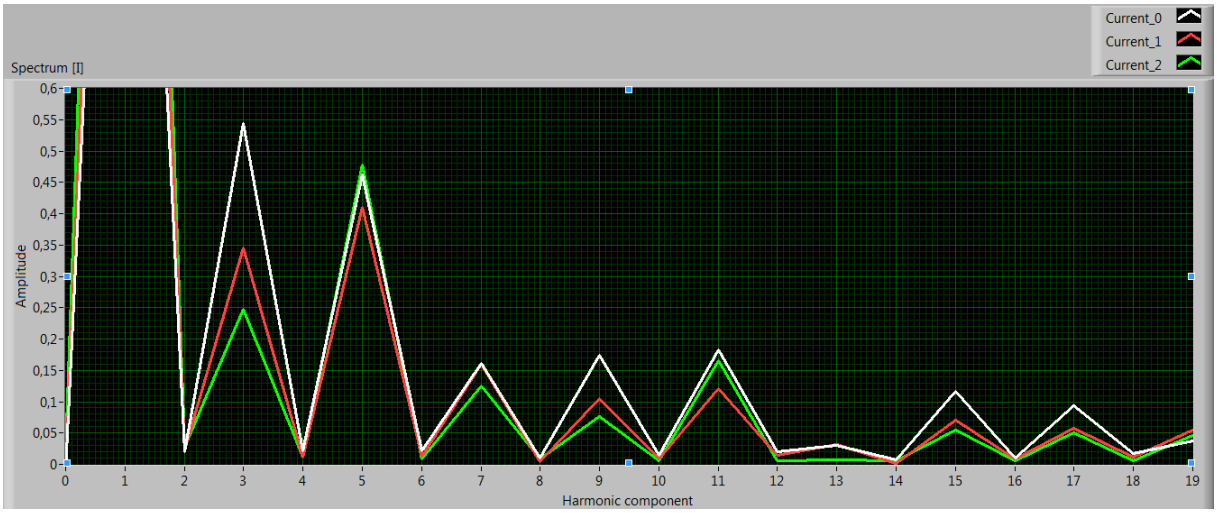
Spectrum [I]
Current_0
Current_1
Current_2
Amplitude
Harmonic component

Appendix C – VI front panel for configuration 3

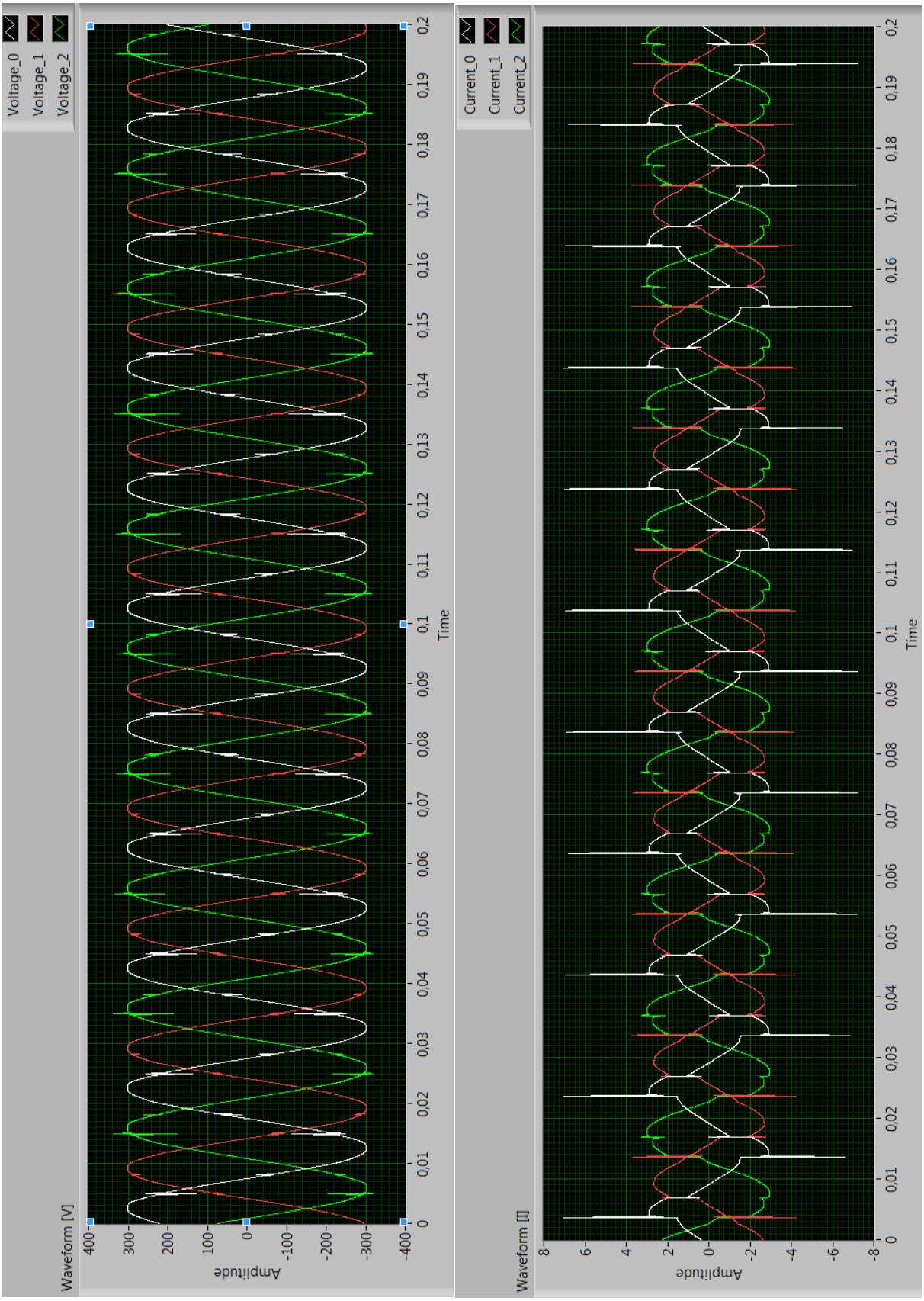

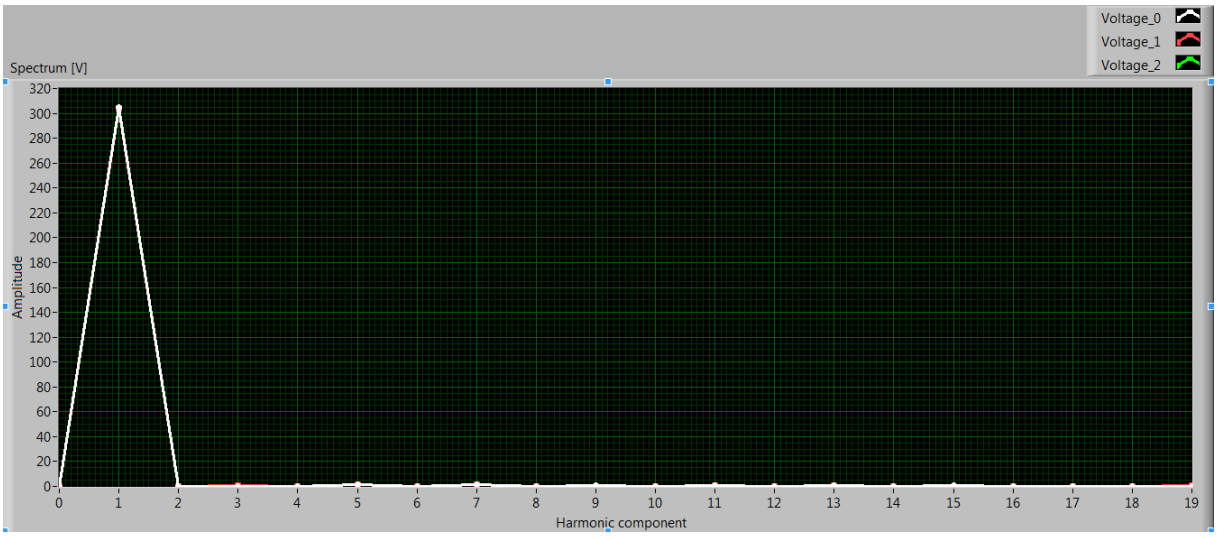

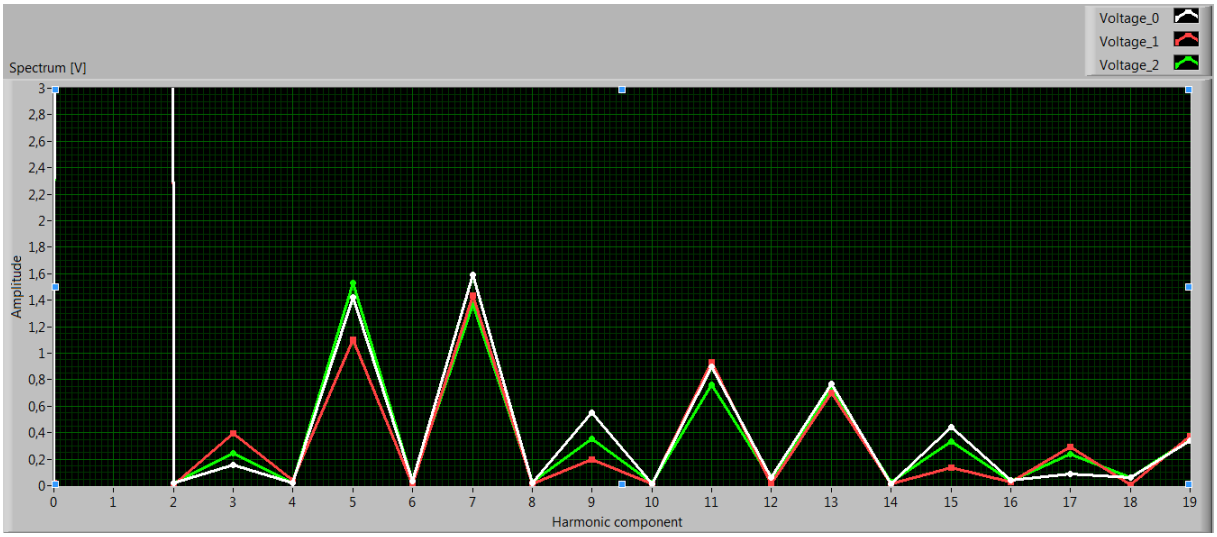

THD [V]

0	0,8431	0,7416	0,7915

THD [I]

0	26,8902	17,5580	12,0970

Voltage RMS

0	215,497	214,982	215,645

Current RMS

0	1,77411	1,86647	2,22562

Components levels [V]

0	1	1	1
	304,59	304,18	304,73
	20,72m	8,70m	22,46m
	156,13m	395,75m	245,26m
	17,25m	37,58m	22,53m
	1,42	1,10	1,53
	34,62m	6,99m	35,00m
	1,59	1,44	1,37
	19,35m	13,48m	26,14m
	551,59m	197,05m	355,77m
	15,49m	11,92m	18,07m
	896,10m	934,83m	760,71m
	59,62m	12,76m	46,64m
	767,75m	699,04m	727,14m
	16,88m	16,05m	26,93m
	439,07m	134,48m	335,42m
	38,93m	24,28m	37,16m
	88,39m	293,28m	236,82m

Components levels [I]

0	1	1	1
	2,38	2,58	3,12
	20,01m	23,22m	26,68m
	547,61m	361,97m	230,44m
	22,81m	11,85m	12,45m
	172,99m	127,70m	200,09m
	22,35m	14,37m	8,77m
	109,12m	151,26m	120,62m
	8,79m	4,57m	7,88m
	175,32m	106,54m	75,64m
	13,87m	9,07m	6,18m
	78,66m	39,42m	98,85m
	20,05m	13,81m	6,25m
	79,74m	103,06m	87,40m
	7,91m	2,50m	7,28m
	118,62m	72,19m	53,68m
	10,60m	8,89m	7,21m
	57,81m	15,88m	66,51m

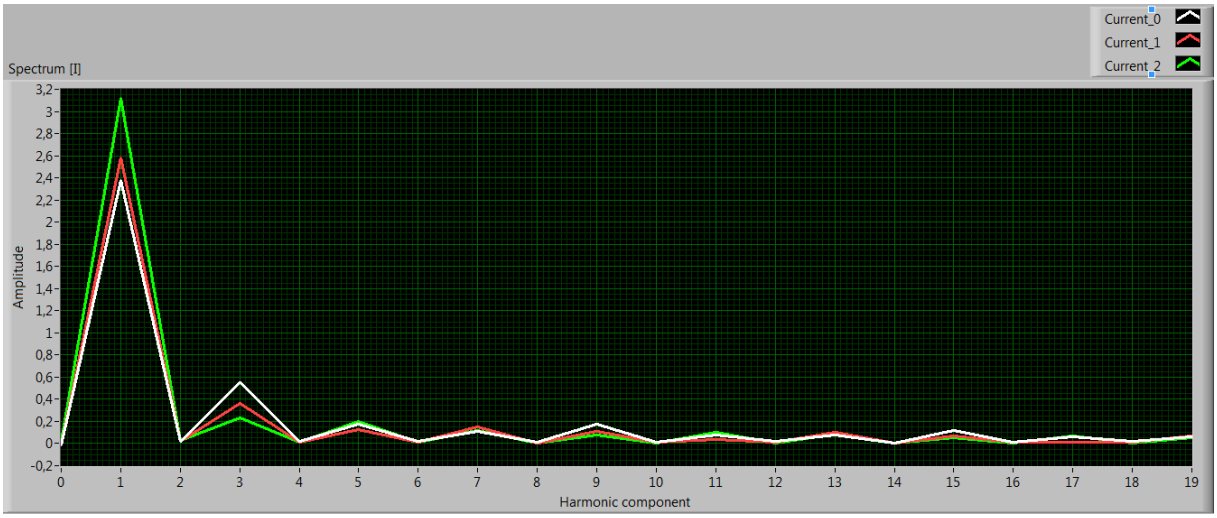
Current_0
Current_1
Current_2
Spectrum [I]
Amplitude
Harmonic component

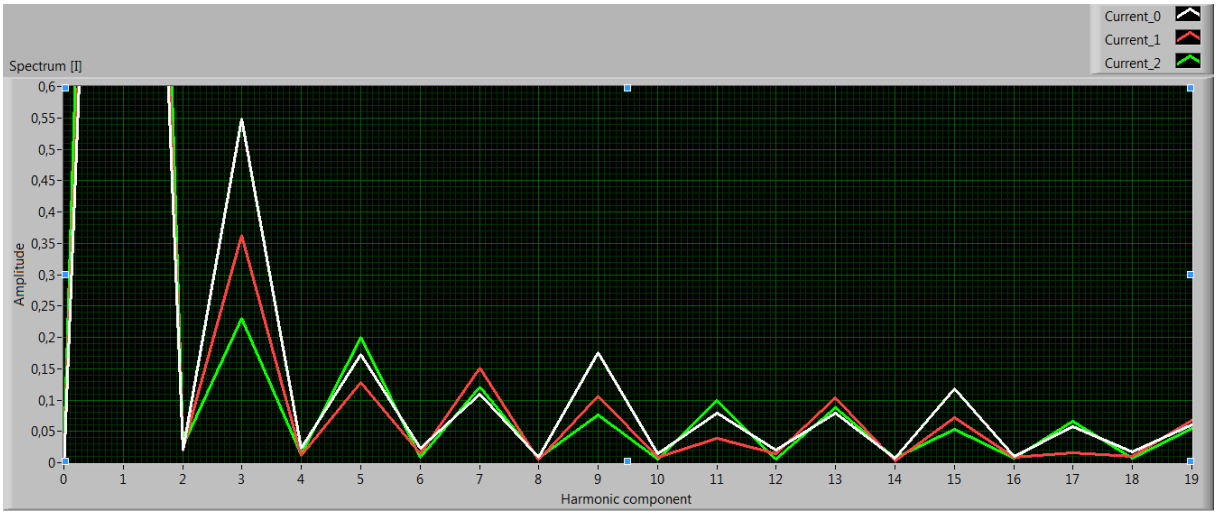
Current_0
Current_1
Current_2
Spectrum [I]
Amplitude
Harmonic component

Appendix D – VI front panel for configuration 4

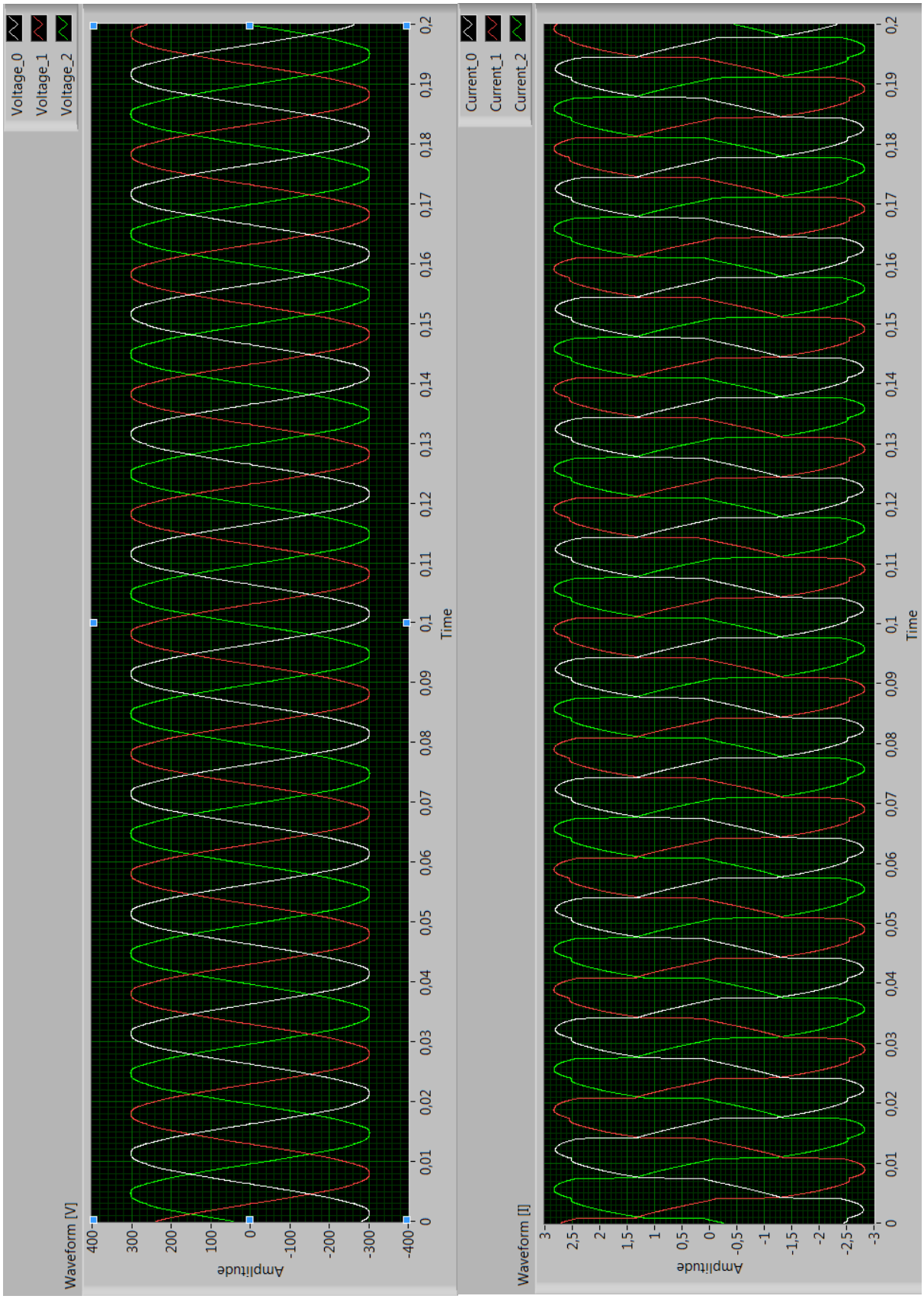

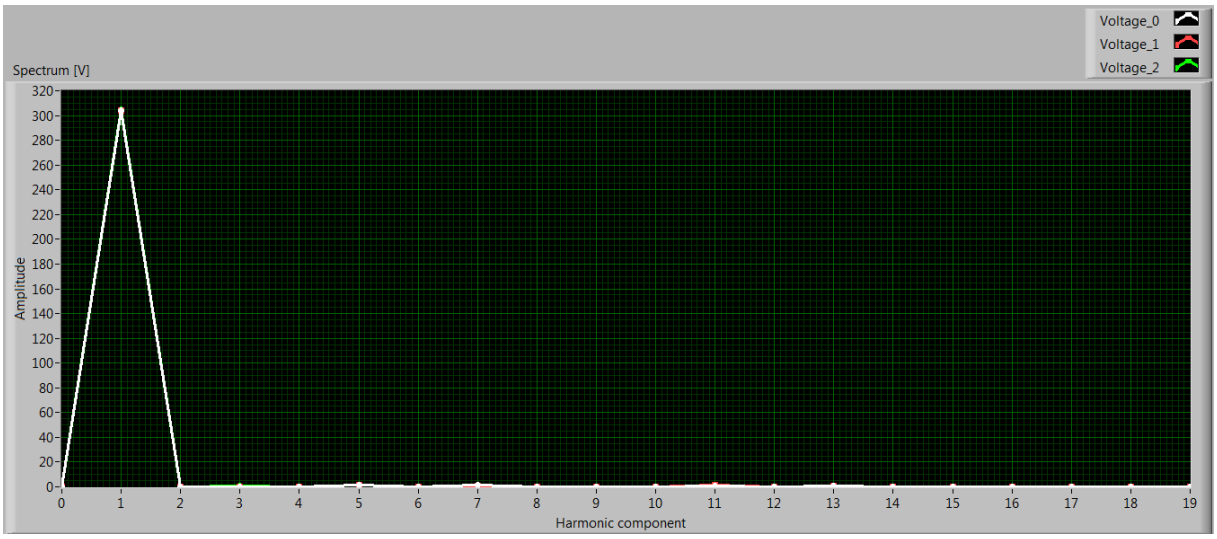
Voltage_0
Voltage_1
Voltage_2
Spectrum [V]
Amplitude
Harmonic component

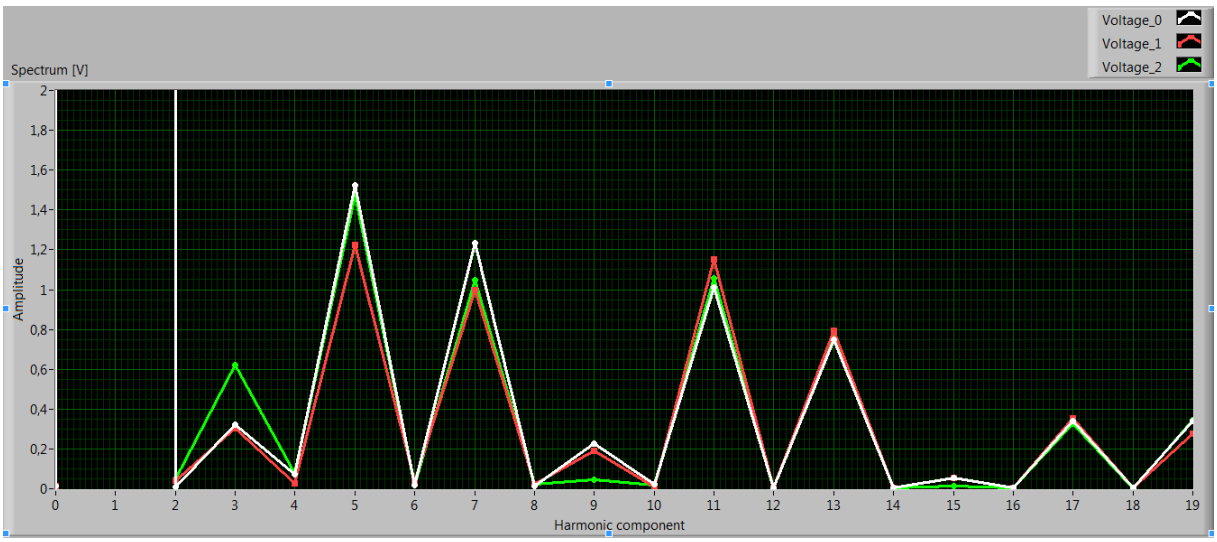
Voltage_0
Voltage_1
Voltage_2
Spectrum [V]
Amplitude
Harmonic component

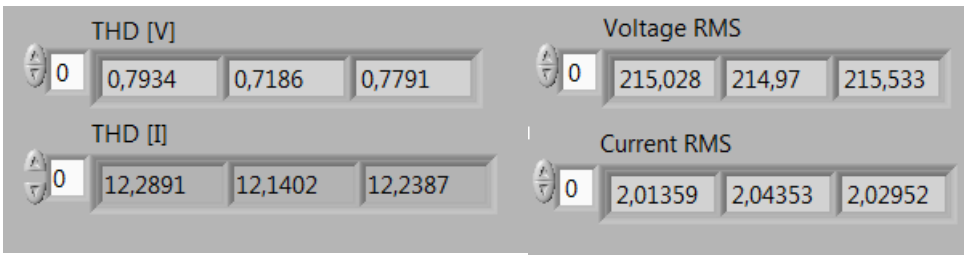
THD [V]
0
0,7934
0,7186
0,7791
THD [I]
0
12,2891
12,1402
12,2387
Voltage RMS
0
215,028
214,97
215,533
Current RMS
0
2,01359
2,04353
2,02952

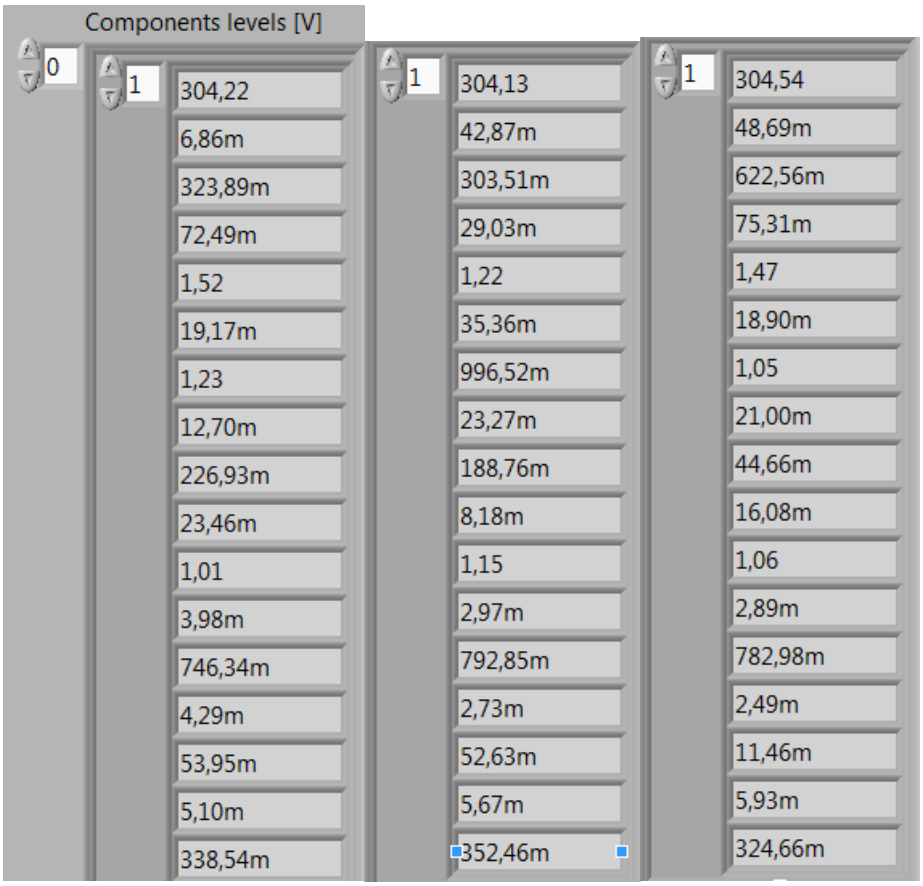
Components levels [V]
0
1
304,22
6,86m
323,89m
72,49m
1,52
19,17m
1,23
12,70m
226,93m
23,46m
1,01
3,98m
746,34m
4,29m
53,95m
5,10m
338,54m
1
304,13
42,87m
303,51m
29,03m
1,22
35,36m
996,52m
23,27m
188,76m
8,18m
1,15
2,97m
792,85m
2,73m
52,63m
5,67m
352,46m
1
304,54
48,69m
622,56m
75,31m
1,47
18,90m
1,05
21,00m
44,66m
16,08m
1,06
2,89m
782,98m
2,49m
11,46m
5,93m
324,66m

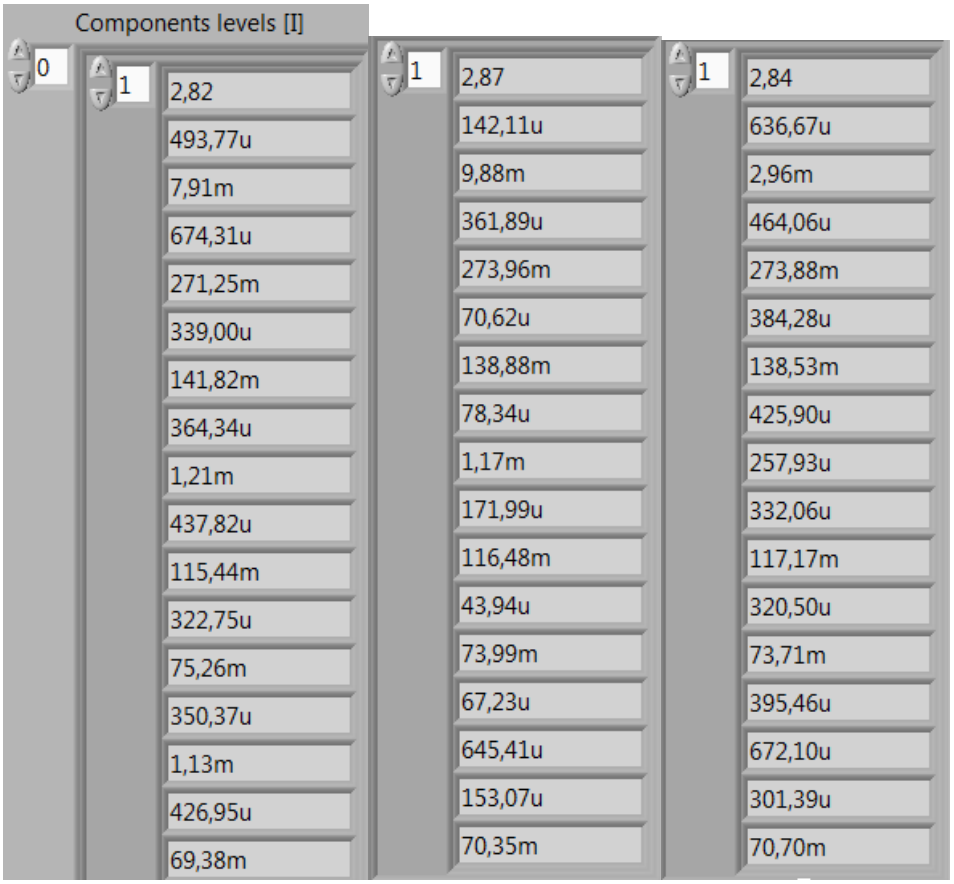
Components levels [I]
0
1
2,82
493,77u
7,91m
674,31u
271,25m
339,00u
141,82m
364,34u
1,21m
437,82u
115,44m
322,75u
75,26m
350,37u
1,13m
426,95u
69,38m
1
2,87
142,11u
9,88m
361,89u
273,96m
70,62u
138,88m
78,34u
1,17m
171,99u
116,48m
43,94u
73,99m
67,23u
645,41u
153,07u
70,35m
1
2,84
636,67u
2,96m
464,06u
273,88m
384,28u
138,53m
425,90u
257,93u
332,06u
117,17m
320,50u
73,71m
395,46u
672,10u
301,39u
70,70m

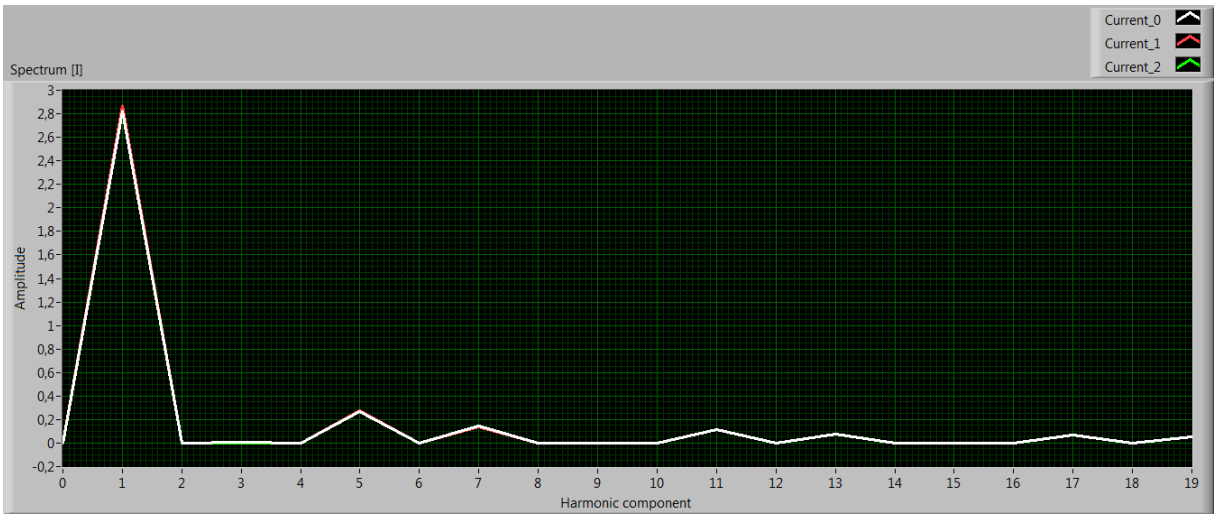
Spectrum [I]
Current_0
Current_1
Current_2
Amplitude
Harmonic component

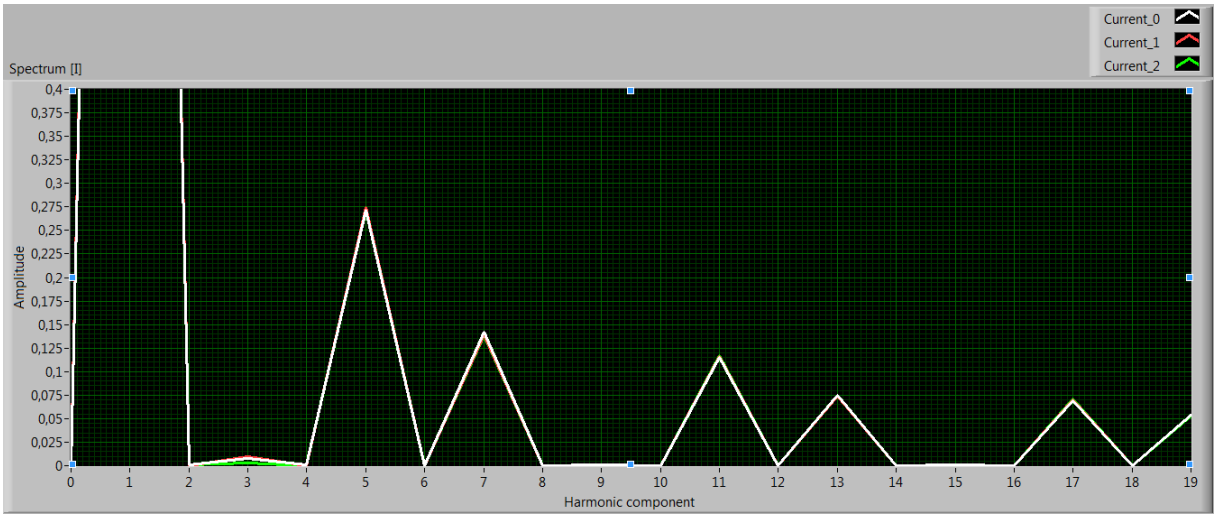
Spectrum [I]
Current_0
Current_1
Current_2
Amplitude
Harmonic component